ACTA BIOMEDICA LOVANIENSIA

Sofie JANSSEN

EFFECTS OF IL-6 AND IL-8 ON RESPIRATORY AND PERIPHERAL SKELETAL MUSCLE FUNCTION: CONSEQUENCES FOR SYSTEMIC INFLAMMATION IN COPD

LEUVEN UNIVERSITY PRESS

ACTA BIOMEDICA LOVANIENSIA
Katholieke Universiteit Leuven
Faculteit Geneeskunde
Departement Inwendige 1
Afdeling Pneumologie
Laboratorium Ademspieren

Sofie JANSSEN

EFFECTS OF IL-6 AND IL-8 ON RESPIRATORY AND PERIPHERAL SKELETAL MUSCLE FUNCTION: CONSEQUENCES FOR SYSTEMIC INFLAMMATION IN COPD

LEUVEN UNIVERSITY PRESS

Thesis submitted in partial fulfillment of the requirements for the degree of «Doctor in de Medische Wetenschappen»

© 2006 by Leuven University Press / Presses Universitaires de Louvain / Universitaire Pers Leuven.
Blijde-Inkomststraat 5, B-3000 Leuven (Belgium)

All rights reserved. Except in those cases expressly determined by law, no part of this publication may be multiplied, saved in an automated data file or made public in any way whatsoever without the express prior written consent of the publishers.
ISBN
ISBN

D/
NUR:

Quidquid agis, prudentar agas, et respice finem!

Als sterren konden spreken,
Als sterren konden zien,
Zou je dan heel eventjes willen zwaaien
En twinkelen als groet
Zodat ik hier beneden weet,
Dat het goed met je gaat.

Voor Karen Vanduren, Suzanne Mees, Cyrille Vaesen, Maria Vanschoonbeek, Pieter Janssen en Christine Doomen

TABLE OF CONTENTS

DANKWOORD

LIST OF ABBREVIATIONS

CHAPTER 1: INTRODUCTION **1**
1.1 Characterization of COPD 1
1.1.1 COPD as a chronic pulmonary disease 1
1.1.1.1 Pulmonary inflammation 3
1.1.1.1.1 Changes in central and small airways 6
1.1.1.1.2 Changes in lung parenchyma 6
1.1.2 COPD as a chronic systemic disease 6
1.1.2.1 Systemic inflammation 7
1.1.2.1.1 Weight loss 10
1.1.2.1.2 Skeletal muscle dysfunction 10
1.1.2.1.3 Cardiovascular effects 17
1.1.2.1.4 Nervous system effects 18
1.1.2.1.5 Osteoskeletal effects 19
1.1.2.1.6 Bone marrow effects 19
1.2 Inflammation and skeletal muscle function in COPD 20
1.2.1 Effects of TNF-α on diaphragm and peripheral skeletal muscles 21
1.2.2 Effects of IL-6 on peripheral skeletal muscles 22
1.2.2.1 Transgenic animal models overexpressing IL-6 22
1.2.2.2 *In vivo* administration of IL-6 23
1.2.2.3 *In vitro* experiments or cell culture 25
1.2.3 Effects of IL-8 on diaphragm and peripheral skeletal muscles 26
1.2.4 Proteolytic pathways in skeletal muscles 28
1.2.4.1 Cytokines and signaling pathways in skeletal muscles 29
1.2.4.1.1 Intracellular skeletal muscle signaling pathway induced by TNF-α 29
1.2.4.1.2 Intracellular skeletal muscle signaling pathway induced by IL-6 31
1.3 Systemic inflammation and other diseases 33
1.3.1 Effects of cytokines on the myocardium 34

CHAPTER 2: AIMS OF THE STUDY **39**

CHAPTER 3: MATERIALS AND METHODS **41**
3.1 Animal experiments 41
3.1.1 Study design 41
3.1.1.1 rhIL-6 administration to rats 41
3.1.1.1.1 *In vivo* experiments 41
3.1.1.1.2 *In vitro* experiments 42
3.1.1.2 rhIL-8 administration to rats 42
3.1.2 Experimental methodology 43
3.1.2.1 Pump implantation 43
3.1.2.2 *In vitro* contractile properties of the diaphragm 43
3.1.2.3 Histochemical and histological examination 46

3.1.2.3.1 Diaphragm and gastrocnemius 46
3.1.2.3.2 Heart 47
3.1.2.3.3 Lungs 48
3.1.2.4 Measurement of cytokine, albumin and IGF-I plasma levels 49
3.1.2.5 Invasive haemodynamic measurements 49
3.1.2.6 Blood flow measurements 52
3.1.2.7 Food intake 53
3.1.2.8 Activity level 53
3.1.2.9 Statistical analysis 53
3.2 Patient experiments 54
3.2.1 Patient characteristics 54
3.2.2 Experimental methodology 55
3.2.2.1 Clinical and haemodynamic variables 55
3.2.2.2 Measurement of cytokine and troponin-I plasma levels 56
3.2.2.3 Statistical analysis 56

CHAPTER 4: EFFECTS OF IL-6 ON SKELETAL AND CARDIAC MUSCLE FUNCTION 59
4.1 *In vivo* experiments 59
4.1.1 Body and tissue weight 59
4.1.2 Diaphragm *in vitro* contractile properties 60
4.1.3 Morphometry of diaphragm and gastrocnemius 62
4.1.4 Plasma levels 63
4.1.5 Invasive haemodynamic analysis 63
4.1.6 Correlations: muscle weight - cardiovascular functional parameters 66
4.1.7 Blood flow analysis 66
4.1.8 Heart histology 66
4.1.9 Lung histology and water content 67
4.1.10 Food intake 68
4.1.11 Activity level 69
4.2 *In vitro* experiments 69

CHAPTER 5: EFFECTS OF IL-8 ON SKELETAL MUSCLE FUNCTION 71
5.1 Body and tissue weight 71
5.2 Diaphragm *in vitro* contractile properties 72
5.3 Morphometry of diaphragm and gastrocnemius 73
5.4 Plasma levels 75
5.5 Lung histology and water content 75

CHAPTER 6: CLINICAL RELEVANCE OF PERI-OPERATIVE CYTOKINE LEVELS IN HEART VALVE SURGERY 77
6.1 Clinical variables 77
6.2 Haemodynamic variables 78
6.3 Cytokine and troponin-I plasma levels 79
6.4 Correlates of preoperative cytokine plasma levels 80
6.5 Correlates of cytokine plasma levels at the end of surgery 81
6.6 Correlates of cytokine and troponin-I plasma levels 12 hrs after the end of surgery 83

CHAPTER 7: GENERAL DISCUSSION **85**
7.1 Effects of IL-6 on skeletal muscle function 85
7.2 Effects of IL-8 on skeletal muscle function 93
7.3 Clinical relevance of peri-operative cytokine levels in heart valve surgery 94
7.4 Summary and general conclusion 100

REFERENCES **103**

SUMMARY **121**

SAMENVATTING **123**

CURRICULUM VITAE

LIST OF PUBLICATIONS

DANKWOORD

Een dankwoord, gericht tot oneindig veel mensen... Mensen die me hebben bijgestaan met raad en daad betreffende mijn onderzoeksproject, maar ook mensen, die ik gewoon zou willen bedanken om hun persoonlijkheid, hun bezorgdheid en hun liefde, want zonder hen zou dit alles niet mogelijk zijn geweest.

Eerst en vooral zou ik graag Prof M. Vervenne, Rector van de Katholieke Universiteit Leuven, en Prof B. Himpens, Decaan van de Faculteit Geneeskunde, willen bedanken omdat ze mij de kans gegeven hebben een doctoraatsthesis aan deze universiteit voor te bereiden.

Vervolgens zou ik ook mijn gemeende appreciatie willen uitdrukken ten opzichte van de voorzitter en de leden van de jury voor hun waardevolle opmerkingen en suggesties: Prof G. Opdenakker, Prof F. Wuytack, Prof P. Proost, Prof R. Dekhuijzen, Prof E. Derom and Prof L. Delaunois. Ook Prof J. Tack, departementsvoorzitter Inwendige 1, zou ik graag in de bloemetjes willen zetten omwille van zijn souplesse.

De allerbelangrijkste personen die ik zou willen bedanken, zijn zonder twijfel Prof Dr M. Decramer, mijn promotor, en Prof G. Gayan-Ramirez, mijn co-promotor. Beiden hebben me altijd met raad en daad bijgestaan, en hebben daar dan ook vele uren tijd ingestoken. Zonder overdracht van hun wetenschappelijke kennis zou ik waarschijnlijk nooit zover geraakt zijn. Naast dit wetenschappelijk aspect, zou ik hen beiden ook willen bedanken voor de fijne momenten die we deelden in onze vrije tijd: Prof Decramer in het bijzonder voor de plezante tennismatchen, en Prof Gayan-Ramirez voor de luidruchtige en gezellige uitstapjes op congressen. Tevens wil ik hen ook bedanken voor hun luisterend oor op momenten dat ik het moeilijk had.

Ik wil ook mijn collega's van het labo Ademspieren bedanken voor de fijne momenten en alle hulpvaardigheid. Bedankt Karen, Tim, Dries, Daniel, Didier, Nadège, Fabio, Vanessa, Eline, Anita, Thierry en Rik. Sommige zijn ondertussen reeds uitgegroeid tot echte vrienden, en met spijt in het hart neem ik dan ook

afscheid van hen. Eline en Anita, de praatjes die wij bijna dagelijks hielden, zal ik heel zeker missen. Jullie waren een echte steun en toeverlaat. Maar geen nood, het einde van mijn doctoraat betekent echter niet het einde van onze vriendschap!

Natuurlijk mag ik ook mijn vrienden en collega's van de omringende labo's niet vergeten: Rozenn, Sophie, Leifu, Bart, Tim, Peter, Hade, en Ben (labo Pneumologie), Nele, Nicole, Caroline en Arne (labo Thoraxheelkunde), Kasran (labo Immunologie), An, Veerle, Paul en Patrick (labo Experimentele Heelkunde en Anesthesie), en Elke (labo Experimentele Cardiologie). Bart, jou wil ik toch nog eventjes speciaal in de bloemetjes zetten! Je zal zelf nog wel weten waarom... An, jou zou ik daarentegen - na waarschijnlijk al honderd keren - nog een laatste maal willen bedanken voor de moeilijke en tijdslopende experimenten die je voor mij hebt uitgevoerd. Ik zal onze plezierige tijd samen in het provisorium niet snel vergeten. Ook jij Paul, heel fel bedankt voor het geduld dat je hebt opgebracht om de hartcatheterizatie bij onze ratten op punt te stellen, en voor al de energie die je in onze patiënten studie hebt gestoken.

Graag zou ik ook de mensen van het operatiekwartier (E-kern) en de verpleging van de intensieve zorgen willen bedanken omdat zij bereid waren mee te werken aan onze klinische studie.

Een neergeschreven dankwoord om mijn appreciatie ten opzichte van mijn ouders, Jan Janssen en Ghislaine Vaesen, uit te drukken, schiet woorden te kort. Toch wil ik dat jullie weten dat ik ontzettend veel van jullie beiden houd en dat ik me geen betere ouders kan voorstellen. Jullie hebben me zoveel kansen gegeven. Jullie zijn alles en tegelijkertijd nog zoveel meer voor mij!

Ook mijn familieleden, goede vrienden van het thuisfront, en tennisfanaten zou ik graag willen bedanken voor hun onvoorwaardelijke steun en interesse in mijn onderzoek.

Tot slot de laatste paragraaf, gericht aan mijn verdere toekomst, mijn wederhelft. Tom, bedankt om mijn geklaag te aanhoren tijdens moeilijke momenten, om mij te steunen en op te vangen. Jouw liefde gaf me moed, en heeft er heel zeker toe bijgedragen dat ik dit project tot een goed eind heb kunnen brengen! Het idee om

ons gezinnetje verder uit te breiden lijkt nu, na het beëindigen van dit proefschrift, ineens niet meer zover weg...

LIST OF ABBREVIATIONS

ABP	arterial blood pressure
ANOVA	analysis of variance
ATP	adenosine triphosphate
ATPase	adenosine triphosphatase
CK	creatine kinase
CO	cardiac output
COPD	Chronic Obstructive Pulmonary Disease
CRP	C-reactive protein
CSA	cross-sectional area
CVP	central venous pressure
DOB	dobutamine
DOPA	dopamine
+ dP/dt	positive first derivate of pressure to time
- dP/dt	negative first derivate of pressure to time
Ea	arterial elastance
EDL	extensor digitorum longus
EDP	end-diastolic pressure
EDPVR	end-diastolic pressure-volume relation
EDV	end-diastolic volume
Ees	end-systolic elastance
EF	ejection fraction
ESV	end-systolic volume
ESP	end-systolic pressure
FEV_1	forced expiratory volume in one second
GOLD	Global Initiative for Obstructive Lung Disease
HR	heart rate
H&E	hematoxylin-eosin
ICAM-1	intercellular adhesion molecule-1
IGF-I	insulin-like growth factor-1
IL	interleukin
IL-6R	interleukin-6 receptor
IκB	inhibitory κB
JAK1	janus kinase-1
JAK2	janus kinase-2
KC	keratinocyte-derived chemokine
LAP	left atrial pressure
LBP	lipopolysaccharide binding protein
L_o	optimal length
LV	left ventricle
LVEF	left ventricular ejection fraction
Mac-1	macrophage antigen-1
MAFbx	Muscle Atrophy F-box
MAPK	mitogen-activated protein kinase
MHC	myosin heavy chain
MIP-2	macrophage inflammatory protein-2
mRNA	messenger ribonucleic acid
MURF	Muscle Ring Finger
NA	norepinephrine
NAD^+	nicotinamide adenine dinucleotide
NF-κB	nuclear factor-κB
NO	nitric oxide
NOS	nitric oxide synthase
PaO_2	partial oxygen pressure
PAP	pulmonary artery pressure
PARP-1	poly(ADP-ribose) polymerase-1
PBS	phosphate buffered saline
PDE	phosphodiesterase

P_o	tetanic tension
PRSW	preload recruitable stroke work
P_t	twitch tension
P_t/P_o	twitch-to-tetanus ratio
PVR	pulmonary vascular resistance
REE	resting energy expenditure
rh	recombinant human
RIS	residual interstitial space
RNS	reactive nitrogen species
ROS	reactive oxygen species
1/2 RT	half-relaxation time
SERCA2	sarcoendoplasmic reticulum Ca^{2+} adenosine triphosphatase 2
SHP2	SH2-domain-containing tyrosine phosphatase
SOCS	suppressor of cytokine signaling
STAT	signal transducer activator of transcription
sTNF-R1	soluble tumour necrosis factor-α receptor 1
sTNF-R2	soluble tumour necrosis factor-α receptor 2
sTNF-Rs	soluble tumour necrosis factor-α receptors 1and 2
SV	stroke volume
SVR	systemic vascular resistance
SW	stroke work
S6K1	p70-S6 kinase
TDE	total daily energy expenditure
TNF-α	tumour necrosis factor-α
TNF-R1	tumour necrosis factor-α receptor 1
TNF-R2	tumour necrosis factor-α receptor 2
TPT	time to peak tension
TYK2	tyrosine kinase-2

CHAPTER 1: INTRODUCTION

1.1 Characterization of COPD

Chronic Obstructive Pulmonary Disease (COPD) is a major public health problem. Although it is currently ranked as the fourth leading cause of mortality and the twelfth leading cause of disability, by the year 2020 it is estimated to become the third leading cause of death and the fifth leading cause of disability worldwide[1]. Moreover, the economic costs are alarming, as direct and indirect medical costs keep on rising yearly and are most likely underestimated[2].

1.1.1 COPD as a chronic pulmonary disease

For years, COPD has been described as a serious respiratory disorder characterized by airflow obstruction that is not fully reversible[2]. A ratio of post-bronchodilator forced expiratory volume in one second (FEV_1) over forced vital capacity ≤ 0.7 is used to confirm the presence of this irreversible airflow obstruction. In addition with FEV_1 % predicted, COPD might be classified by its severity into mild, moderate, severe and very severe clinically advanced disease stages[3]. Moreover, the airflow limitation is usually progressive, secondary to chronic central and peripheral airway inflammation, changes in the pulmonary vasculature and emphysema[4]. All these features are known to occur predominantly in response to noxious particles and gases, with tobacco smoking as the most significantly contributing risk factor when compared to air pollution, occupational exposure to dust, gases or fumes and α-1-antitrypsin deficiency[2]. However, it should be noted that only 15-20% of smokers develop COPD while globally 80% of this disease is directly attributable to smoking[1].

The underlying pathology is somewhat complex, including chronic bronchitis, emphysema and small airway obstruction. Chronic bronchitis is histologically characterized by hypertrophy and hyperplasia of the submucosal glands in the proximal airways and by increased numbers of mucus-secreting goblet cells in the peripheral airways. Both airways also contain inflammatory infiltrates and some areas with squamous epithelium. By way of contrast, emphysema is defined pathologically by distention and destruction of gas-exchanging portions of the lungs, leading to centrilobular or panlobular emphysema. COPD patients may also suffer from small airway obstruction as a result of a bronchiolitis, having distinctive pathologies including distortion, fibrosis, and smooth muscle hyperplasia of the small airways (Figure 1.1). Due to all these pathological changes, COPD is clinically characterized by complaints such as chronic cough, sputum production and dyspnea. So far, no treatment for COPD itself is known; only treatments for the amelioration of its symptoms are available. At present, smoking cessation is thought to be the single most important intervention to attenuate lung function impairment as it significantly reduces the age-related decline in FEV_1[3].

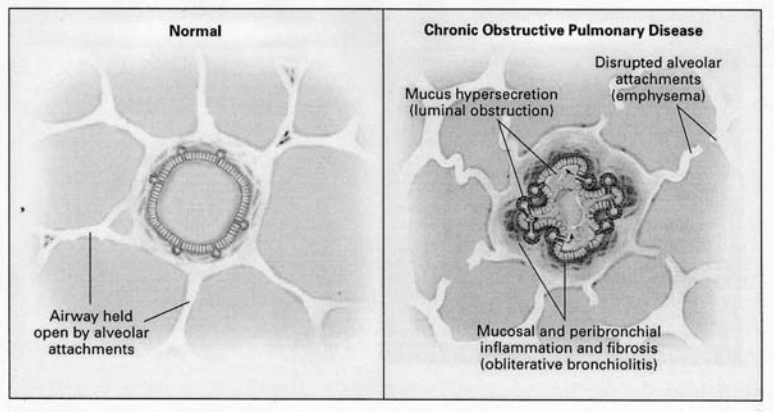


Figure 1.1. Pathologic changes in the airways of COPD patients. (Adapted from Barnes PJ. New Engl J Med. 2000; 343: 269-280)

1.1.1.1 Pulmonary inflammation

Inflammation is characterized as a localized protective response in vascularized tissues induced by microbial infection, cell or tissue injury. Inflammatory cells and mediators involved in the expiratory airflow obstruction that predominantly defines COPD are mainly situated both at the level of the membranous bronchiole, devoid of cartilage and submucosal glands, and in the lung tissue itself. In contrast, the inflammatory process involved in cough and sputum production is situated in the epithelium of the central airways, extending into the mucus-producing glands[5]. Although the inflammation in COPD occurs predominantly in the peripheral airways and lung parenchyma, the inflammatory processes occurring in the central and peripheral airways are rarely different[6].

In general, cigarette smoke and other noxious gases or particles are known to activate macrophages and epithelial cells in the lower respiratory tract, which in turn release inflammatory and chemotactic cytokines, lipid mediators and reactive oxygen (ROS) and nitrogen species (RNS). Subsequently, mainly monocytes, neutrophils and $CD8^+$ T-lymphocytes extravasate to the site of inflammation and release different mediators such as proteases that break down connective tissue components in the lung parenchyma, resulting in emphysema, or stimulate mucus hypersecretion in the airways[7] (Figure 1.2).

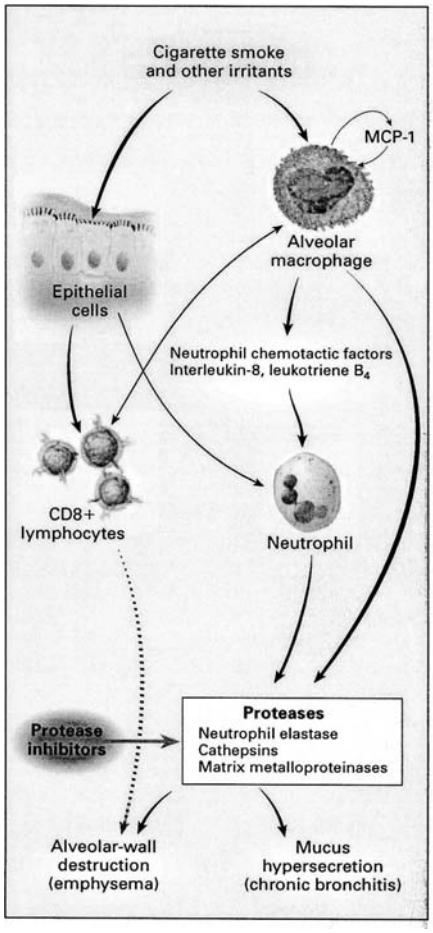


Figure 1.2. Inflammatory mechanisms in COPD. (Adapted from Barnes PJ. New Engl J Med. 2000; 343: 269-280)

In normal circumstances, all the proteolytic enzymes released by activated inflammatory cells are counteracted by antiproteases, however in patients with COPD, the production of antiproteases may be inadequate to neutralize the effects of multiple proteases[8].

During the course of COPD, monocytes, $CD8^+$ T-lymphocytes and neutrophils all migrate from the bloodstream to the site of injury using similar sequential mechanisms, although they differ in their responses to chemotactic and inflammatory stimuli, as well as in the expression of adhesion molecules. The latter are needed for tethering and migration of inflammatory cells into injured sites. Neutrophils have shown to be the primary cell type that is recruited to the airways in response to the earlier released chemotactic and inflammatory mediators which regulate the expression of L- and E-selectins on leucocytes and vascular endothelium cells, respectively. These selectins are known to be responsible for the initial attachment and movement of leucocytes along vessel walls by reversible binding to their ligands. Firm adhesion of these leucocytes to the vessel wall involves the activation of the integrin expression pathway in leucocytes. On neutrophils in particular, increased expression levels of macrophage antigen (Mac)-1 adhesion molecules, which interact strongly with endothelial intercellular adhesion molecule (ICAM)-1, have been observed after activation. Furthermore, not only the degree of neutrophilic activation is elevated in COPD patients, but also their number is increased[7].

Lipid mediators, ROS, RNS, and cytokines derived from activated inflammatory or epithelial cells do not solely activate and attract inflammatory cells to the site of inflammation, they may also further exacerbate COPD. Indeed, lipid mediators like platelet-activating factor, leukotriene B_4 and prostaglandin E_2 have been shown to stimulate the release of pro-inflammatory cytokines from inflammatory cells. ROS

and RNS might not only directly injure microbes or airway epithelium cells, and therefore amplify the inflammatory cell influx, they may also activate nuclear factor-κB (NF-κB), a transcription factor for inflammatory cytokines, decrease the levels of antiproteases, increase the production of isoprostanes and mucus secretion, and exert bronchoconstriction. Cytokines are furthermore known to enhance the expression of adhesion molecules and trigger the secretion of substantial amounts of other cytokines[7;8]. All these features thus represent perpetuating mechanisms that maintain the chronic inflammatory process in COPD.

The pattern of bronchial inflammation is known to change when COPD becomes more severe. It has been shown that there exists a prominent increase in the number of macrophages and $CD8^+$ T-lymphocytes in the airway wall and of neutrophils in the airway lumen of smokers with severe COPD, when compared to smokers with normal lung function. Moreover, these increased neutrophil and T-lymphocyte levels are correlated with the annual decline in lung function and with the degree of airflow limitation, suggesting a role for these cells in the progression of the disease[7].

Acute exacerbations of COPD mostly occur after bacterial or viral infection and are generally characterized by an enhanced airway inflammation, accompanied by a worsening of respiratory symptoms. Both elevated neutrophilic and eosinophilic inflammation have been described during acute exacerbations, with a clear association between neutrophilic inflammation and bacterial etiology. Increased mediators implicated in inflammatory cell recruitment and activation have also been observed, and the activation process may in turn further elevate the levels of inflammatory mediators[9].

1.1.1.1.1 Changes in central and small airways

A prolonged time constant for lung emptying, resulting from airflow limitation, is known to be caused predominantly by an increased resistance of the small conducting airways. Not only inflammatory cell infiltration, but also structural changes such as epithelial metaplasia, increased smooth muscle mass, goblet cell hyperplasia, submucosal gland hypertrophy, defective mucociliary clearance, disruption of the epithelial barrier, deposition of connective tissue, increased smooth muscle force generation and consequently bronchial hyperresponsiveness may all contribute to this increased airway resistance through airway wall thickening[5].

1.1.1.1.2 Changes in lung parenchyma

In emphysematous lungs, maximum expiratory flow is reduced due to decreases in elastic recoil force available to drive air out of the lung. Both centrilobular and panlobular emphysema have been described, the former most closely associated with tobacco smoking and characterized by separate lesions in the upper lobes, the latter usually correlated with α-1-antitrypsin deficiency and characterized by destruction of the whole lower lobes[5]. Neutrophil retention in the pulmonary vasculature is likely to be ultimately important in inducing these emphysematic patterns, as neutrophils are known to be the major source of elastase in the lungs. The importance of neutrophil sequestration might be further supported by the inverse correlation between the decline in FEV_1 and the peripheral blood white cell count[10].

1.1.2 COPD as a chronic systemic disease

COPD is nowadays not only known as a respiratory disorder, but also as a multi-organ system disease with several extra-pulmonary components, for which systemic

inflammation might partly be responsible. However, the origin of this systemic inflammation still remains poorly understood.

1.1.2.1 Systemic inflammation

The global systemic inflammatory process in COPD, following similar pathways as those observed during pulmonary inflammation (Figure 1.2), consists of several components, with the most important being changes in the number and activation level of circulating neutrophils, $CD8^+$ lymphocytes and monocytes, oxidative stress, and altered circulating levels of pro-inflammatory or anti-inflammatory mediators and acute-phase proteins. However, the pathological implications of most of these findings are still unclear, and need confirmation in well characterized patient groups and in different phases of the disease process.

Not only increased numbers but also the activation of peripheral blood neutrophils, resulting in potentiation of migratory and cytotoxic responses as shown by elevated expression levels of Mac-1 adhesion molecules and an increased production of neutrophil elastase and ROS, have been extensively described in stable COPD patients[11-14]. Plasma levels of soluble ICAM-1 and E-selectin, used as surrogates of their expression on the endothelium, are dependent on the severity of the disease[11;15]. However, during acute exacerbations, the expression of neutrophilic Mac-1 and lymphocyte function associated antigen-1 adhesion molecules has been shown to be reduced when compared to stable patients, likely because the most activated cells are sequestered in the pulmonary microcirculation, leaving in turn a subpopulation of circulating cells which do not show such increased expression[11]. Although peripheral blood lymphocytes have been less well studied, recent findings indicate an abnormal function in COPD. In particular, activation of nuclear enzyme

poly(ADP-ribose) polymerase-1 (PARP-1) in peripheral blood lymphocytes of patients with COPD was found to be more prevalent than in lymphocytes of healthy, age-matched control subjects, supporting a role for PARP-1 in the pathophysiology of COPD. Its activation process was indeed associated with a reduction of the nicotinamide adenine dinucleotide (NAD^+) status, leading to a reduced glycolysis rate, mitochondrial respiration and impaired production of high-energy phosphates, and finally to necrotic cell death[16]. Futhermore, circulating monocytes of COPD patients have been shown to release more matrix metalloproteinase-9 and interleukin (IL)-6 than those obtained from healthy subjects[17].

As a consequence of the activation of circulating inflammatory cells, changes in the oxidant/anti-oxidant balance likely occur. Indeed, increases in oxidative stress markers have been observed in patients with severe COPD by enhanced levels of lipid peroxidation products like malondialdehyde, or by a reduced antioxidant capacity such as erythrocyte glutathione peroxidase or vitamin C, when compared to patients with moderate COPD[17-19]. Moreover, both oxidative and anti-oxidative factors were related to the severity of the disease[18]. During exacerbations of the disease, plasma levels of malondialdehyde were further increased, while those of erythrocyte glutathione peroxidase and vitamin C were further decreased[19], indicating that the oxidant/anti-oxidant imbalance is more severe in patients suffering from an acute exacerbation.

Increased levels of acute-phase reactants, which are liver-derived key players in reduction of inflammatory reactions, and cytokines have also been reported as a systemic manifestation of COPD. Enhanced levels of C-reactive protein (CRP) and lipopolysaccharide binding protein (LBP) have been found in patients with stable COPD, and were more pronounced in a subset of patients with an increased resting

energy expenditure and decreased fat-free mass[14;20]. It has moreover been revealed that increased plasma levels of fibrinogen, another acute-phase reactant, are associated with a reduced lung function and an increased risk of COPD hospitalization, independent of smoking status[21]. The formation of these acute-phase reactants is strongly induced by IL-6 and tumour necrosis factor (TNF)-α, which are generally elevated in stable COPD. Increased circulating levels of IL-8 and both soluble TNF-receptor 1 (TNF-R1) and 2 (TNF-R2) have also been described in these patients[14;16;20;22-26], while anti-inflammatory cytokine levels remain unchanged[14]. Conflicting results regarding a link between TNF-α and leptin, a hormone involved in body weight control and energy homeostasis, have been provided[26-28]. In general, increased leptin levels are thought to induce excessive metabolic effects underlying anorexia and loss of body weight. However, plasma leptin levels have been shown to be decreased in patients with stable COPD and weight loss[24], while remaining unchanged in patients with normal body weight[26], therefore likely suggesting a compensatory mechanism to preserve body fat content. The positive correlation between plasma leptin levels and body mass index in weight-losing COPD patients moreover confirms that circulating leptin levels remain regulated even in the cachexic status seen in COPD[28]. Most circulating pro-inflammatory cytokines, acute-phase reactants and leptin are known to be further upregulated during acute exacerbations, suggesting a more pronounced imbalance between pro- and anti-inflammatory mediators. In particular, increased levels of circulating IL-6, IL-8, TNF-α, fibrinogen and leptin have been reported during exacerbations when compared to stable COPD patients[26;27;29;30], and are therefore thought to be involved in the worsening of patient's clinical symptoms.

1.1.2.1.1 Weight loss

The incidence of weight loss in COPD is known to correlate with the severity of disease, and together with muscle wasting, it acts as an independent predictor of increased mortality[31]. Cachexia might rather be a more appropriate term as there is a preferential loss of fat-free mass in patients with COPD[32].

After adjusting for fat-free mass, hypermetabolism is thought to be responsible for weight loss as resting energy expenditure (REE) was found to be elevated in 26% of patients with clinically stable severe COPD[33]. In some patients, this increased REE was furthermore accompanied by elevated systemic levels of CRP and LBP, and of inflammatory mediators such as IL-8 and soluble TNF-R1 and 2, suggesting a link between hypermetabolism and the hepatic acute phase response[33]. Moreover, free living total daily energy expenditure (TDE) is also known to be increased in clinically stable patients, but the causes are not directly related to an elevated REE. The increased TDE in patients with COPD appears to reflect most likely differences in energy expenditure for activities[34].

A reduced dietary intake is also known to affect 15% of COPD patients with mild-to-moderate disease and 50% of patients with advanced-stage disease[35].

1.1.2.1.2 Skeletal muscle dysfunction

Dysfunction or weakness of respiratory and peripheral skeletal muscles is another extra-pulmonary effect frequently occurring in patients with COPD[36]. When compared to peripheral muscles, respiratory muscles are subjected to a mechanical disadvantage, especially the diaphragm, as airflow obstruction and emphysematous changes in the lung parenchyma of COPD patients lead to incomplete emptying of the lungs during expiration and therefore resulting in dynamic hyperinflation.

Respiratory muscles are thus working against an increased mechanical load and adapt to cope with this chronic load[37]. Consequently, different adaptations might occur in both respiratory and peripheral muscles, likely due to the different conditions under which both work, and these adaptations are moreover correlated with disease severity.

Most of the diaphragmatic adaptations have been reported in patients with advanced COPD. In particular, in order to maintain adequate ventilation, an increased neural drive to the diaphragm has been observed in patients with severe COPD[38]. Data concerning diaphragm dimensions are scarce and rather controversial. While some reported muscle fiber hypertrophy in emphysematous patients[39], others found reductions in volume and thickness in chronic bronchitis[40] or even no changes at all in severe COPD[41]. Maximal inspiratory and transdiaphragmatic pressures, which are measurements for global inspiratory muscle or diaphragmatic strength, have been found to be reduced in severe COPD while the functioning of the expiratory muscles seems to be well preserved[42;43]. The decrease in diaphragm force might be related to a shortened sarcomere length, such that the diaphragm is contracting on the ascending branch of its length-tension relationship[44]. Moreover, a decreased force-generating capacity, concomitant with loss of myosin heavy chains has even been observed in single diaphragm type I and IIa fibers of patients with mild to moderate COPD, in which the remaining cross-bridge cycling and Ca^{2+} sensitivity were dysfunctional[45]. In patients with severe COPD, the diaphragm further adapts to the chronically increased workload by shifting from type II to type I fibers[46] and by atrophy of type II fibers[47]. Moreover, an inverse relation between the proportion of type I fibers and FEV_1 has been found in the diaphragm of mild to severe COPD patients[48]. The diaphragm also increases its oxidative

enzymes such as 3-hydroxyacylCoA-dehydrogenase, citrate synthase, and succinate dehydrogenase, and this consistent with an increase in mitochondrial density and enhanced adenosine triphosphate (ATP) generating capacity in mild to severe COPD[49-51]. Moreover, the increase in citrate synthase activity in the diaphragm correlated negatively with FEV_1 % predicted in patients with severe COPD[52]. Decreases in the glycolytic enzyme capacity of hexokinase and lactate dehydrogenase have been observed in the diaphragm of patients with mild to moderate COPD while phosphofructokinase activity has been shown to be decreased in severe COPD only[53]. Moreover, the phosphofructokinase activity was inversely related to the static lung volume[53]. The number of capillaries in the diaphragm is furthermore known to increase proportionally with disease severity, as shown by the negative relationship with FEV_1 % predicted[54]. This might be in line with its enhanced oxidative enzyme capacity. Consequently, all these adaptations might increase endurance capacity and resistance to fatigue of the diaphragm.

Most of the adaptations in peripheral muscles have been examined in the vastus lateralis and quadriceps muscle. For this latter, an impaired excitability propagation has been observed in patients with mild to severe COPD, as increases in M-wave duration and decreases in its amplitude occurred after the onset of exercise when compared to healthy subjects[55]. However, this finding was in contradiction with a post-exercise unchanged M-wave amplitude, excluding transmission failure in the quadriceps of patients with moderate COPD[56]. Using indirect evaluations for measuring peripheral muscle mass, it has been shown that fat-free mass and creatinine height index were decreased in COPD patients in relation to disease severity[32]. When using tomography, thigh muscle cross-sectional area (CSA) was also found to be reduced in severe COPD patients when compared to healthy

controls[57]. In addition, quadriceps force is known to be strongly reduced by about 30% in severe COPD[57-59]. Nevertheless, reductions in the peripheral muscle mass and strength are of similar magnitude in these patients, suggesting that the remaining contractile apparatus is functionally preserved[57]. Furthermore, quadriceps strength and muscle CSA are positively correlated with FEV_1 % predicted [57] (Figure 1.3) and quadriceps force itself is known to decrease further during exacerbations[29;60;61]. Both reductions in the endurance of the quadriceps or unchanged endurance properties have been reported in moderate to severe COPD, and might reflect the heterogeneity in skeletal muscle function[62;63]. Recently, quadriceps endurance capacity was found to be inversely correlated with oxidative stress in the vastus lateralis of severe COPD patients[64]. Furthermore, decreases in quadriceps twitch force have been reported after cycling exercise both in moderate and severe COPD, leading to an increased fatigability[56;65]. Most of the previously described adaptations depend on disease severity and might be the result of changes in muscle fiber type and size. Indeed, in patients with moderate COPD, the quadriceps fiber proportion did not change while type II fibers were significantly atrophied[47]. In contrast, in the vastus lateralis of severe COPD patients, decreases in the proportion of type I fibers together with increases in fiber type II proportion were reported, while both fiber types were atrophied[66]. Lower activities of citrate synthase and 3-hydroxyacylCoA-dehydrogenase have been found in the vastus lateralis of patients with moderate to severe COPD[67], and were furthermore related to the proportion of type I fibers[68]. Glycolytic enzymes have been found to be unchanged in moderate to severe COPD patients, except for phosphofructokinase some controversy is present, being increased or unchanged[69;70]. These oxidative and glycolytic capacity data might be in line with depletion of energy-rich phosphates in the quadriceps muscle of severe

COPD patients, such as ATP, creatine phosphate, and creatine[71]. Reductions in the number of capillaries per unit CSA have also been observed in the vastus lateralis muscle of patients with severe COPD[72]. Furthermore, fibrosis, fat cell replacement and apoptosis might also contribute to malfunctioning of the quadriceps muscle in severe COPD[73;74].

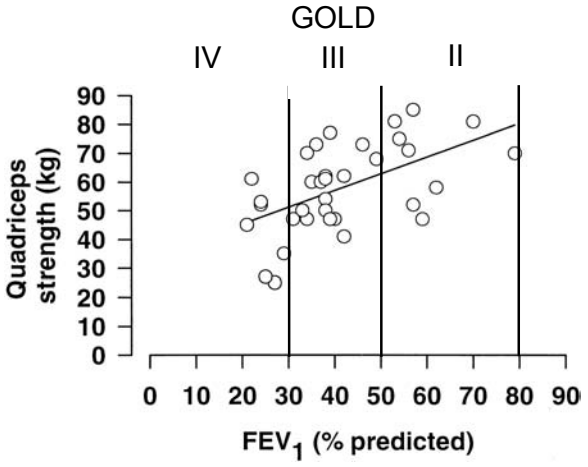


Figure 1.3. Relationship between FEV_1 (percentage of predicted) and quadriceps strength (kg) in GOLD stage II-IV COPD patients. A significant positive relationship was found ($r=0.55$, $p<0.0005$). (Adapted from Bernard et al. Am J Respir Crit Care Med. 1998; 158: 629-634)

The importance of peripheral muscle dysfunction in COPD might not be underestimated as it has been shown to exert a negative impact on different outcomes, upon the reduced pulmonary function. Indeed, midthigh muscle CSA was found to be a better predictor of mortality than body mass index, and had moreover a stronger impact on mortality in patients with FEV_1 <50% predicted[75]. Peripheral muscle weakness has also been related to an enhanced utilization of health care resources[76] as patients with high medical consumption showed a clearly reduced quadriceps peak torque when compared to patients with low medical consumption. In addition, the number of hospital admissions, the number of hospital days, the number of out-patient visits, and the average daily dose of corticosteroids were related to quadriceps force[76]. Furthermore, 6-minutes walking distance in COPD patients admitted to a pulmonary rehabilitation program was found to be positively

correlated to quadriceps force, indicating peripheral muscle force as an important determinant of exercise capacity[58]. A reduced quality of life is also believed to be a clinical outcome of peripheral muscle dysfunction as the score of activity of daily living was found to be a significant determinant of quality of life in stable COPD patients[77]. Moreover, it should be strengthened that the degree of peripheral muscle dysfunction was found to be strongly related to patients' GOLD stage (classification according to the Global Initiative for Chronic Obstructive Lung Disease), and therefore it most likely influences all of the above-mentioned outcomes negatively[57] (Figure 1.3). The frequency of peripheral muscle weakness might also not be underestimated, as quadriceps weakness is observed in 62% of patients with very severe COPD, in 58% of patients with severe COPD and in 67% in patients with moderate disease (data from the REVALIS study in Leuven).

Although the pathophysiological mechanisms underlying respiratory and peripheral skeletal muscle dysfunction in COPD have not been fully elucidated yet, muscle dysfunction is thought to be multi-factorial in these patients (Figure 1.4).

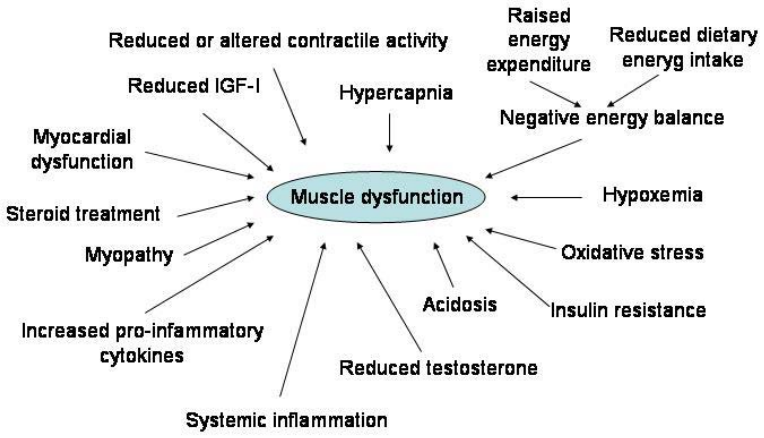


Figure 1.4. Most important factors involved in skeletal muscle dysfunction in COPD.

Deconditioning might be a very important contributor to peripheral skeletal muscle weakness[35], as disuse has been shown to reduce the proportion of type I fibers in the

quadriceps muscle[78]. These changes were paralleled by a decline in mitochondrial enzyme activity levels and an increase in glycolytic enzyme activity[79]. Corticosteroids are used as treatment procedures in COPD, and as steroid-induced myopathy has been well described, these medications might contribute to both respiratory and peripheral skeletal muscle weakness[80]. Moreover, reductions in maximal force and endurance have been reported in the diaphragm and vastus lateralis of chronic hypoxemic COPD patients[63]. A positive correlation was even described between arterial oxygen pressure and the percentage of type I fibers in the vastus lateralis of COPD patients[71]. Oxidative stress, resulting in extensive cell and tissue damage, has also been reported in both the diaphragm and quadriceps muscle of patients with COPD and was moreover correlated with the degree of airflow obstruction[81;82]. Furthermore, the influence of hypercapnia might not be excluded as a decrease in inspiratory muscle strength was described in COPD patients with chronic hypercapnia when compared with normocapnic COPD patients[83]. The nutritional imbalance, often occurring in COPD, might also contribute to muscle dysfunction as seen by marked reductions in ATP and creatine phosphate in the quadriceps muscle, while lactate concentrations were increased[84]. Recently, it has been shown that alternative splicing of the titin gene, resulting in an increased length of the elastic segment, is involved in the reduced passive tension generation of the diaphragm of patients with mild to moderate COPD[85]. These changes might in turn be detrimental for the diaphragm as normal passive-elastic properties of titin are essential for maintaining structural and mechanical stability of the sarcomere during calcium activation. Moreover, an increased activity of proteasome subunits together with elevated mRNA levels of muscle-specific ubiquitin-ligase MAFbx and increased ubiquitin-protein conjugation have been observed in the diaphragm of the previous

mentioned patient group, demonstrating the activation of the ubiquitin-proteasome protein degradation pathway in the COPD diaphragm[45;86]. As increases in TDE and REE are frequent in COPD patients, they may also contribute to muscle mass loss[34;87]. Furthermore, anabolic hormone levels such as insulin-like growth factor (IGF)-I and testosterone, which are known to induce muscle growth and development under normal circumstances, are known to be declined with aging, and decrease further in patients suffering from COPD[88]. Moreover, a positive correlation has recently been described between quadriceps peak torque and circulating insulin-like growth factor (IGF)-I levels in these patients[29], and testosterone levels were found to be correlated with the severity of arterial hypoxemia and hypercapnia in acutely ill and hospitalized COPD patients[89]. Although no data are available on the effects of pulmonary heart disease (cor pulmonale) on muscle function in COPD, cardiac failure is already known for years to exert deleterious effects on both respiratory and peripheral skeletal muscle performance[90]. Finally, increased plasma levels of pro-inflammatory cytokines such as TNF-α and IL-6 have been observed in patients with clinically stable COPD following acute moderate-intensity constant-work-rate exercise and might negatively affect patient's skeletal muscles through activation of protein degradation pathways or through amplification of the inflammatory cascade[91;92]. Along the same lines, the chronic systemic inflammatory response as occurring in COPD has also been postulated to be involved in skeletal muscle dysfunction. This issue will be discussed in detail later.

1.1.2.1.3 Cardiovascular effects

COPD is known to increase the risk of cardiovascular diseases by two- to threefold, which might subsequently account for about 50% of the total number of

deaths among COPD patients[93]. Cardiovascular diseases in COPD mostly comprise cardiac arrhythmias, angina pectoris, acute myocardial infarction, congestive heart failure, stroke, pulmonary hypertension and atherosclerotic peripheral vascular diseases[94].

Different mechanisms underlying these cardiovascular events in COPD patients have been proposed. The onset is likely due to the persistent low-grade systemic inflammation, with smoking as the initiating factor[95], as systemic inflammation is known to be linked to atherosclerosis, ischemic heart disease, strokes, and coronary deaths[93]. Indeed, increases in CRP, for example, represent a major risk factor for atherosclerosis[96]. However, reductions in expiratory flow volumes, as occurring in COPD, are now also known to elevate the risk of coronary events, independent of the well-known risk factors such as cigarette smoking, obesity, serum total cholesterol and hypertension[97-99].

1.1.2.1.4 Nervous system effects

Various aspects of the nervous system may be abnormal in patients with COPD. As normal cerebral cell function is critically dependent on intracellular energy metabolism via oxidative phosphorylation and the production of ATP, and especially as severe COPD is known to be associated with chronic hypoxia, an increasing dependence on glycolytic pathways to maintain accurate cellular high-energy phosphate levels has been observed in the brains of stable COPD using nuclear magnetic resonance spectroscopy[100]. Furthermore, the prevalence of anxiety disorders and depression in patients with COPD might be attributed to their respiratory symptomatology[101] and might further complicate their quality of life, progression of illness and success of treatment and rehabilitation[102;103]. However, it

is equally possible that depression may bear some relationship to systemic inflammation[104]. Indeed, negative changes in patient's mood following injection with Salmonella typhi vaccine were significantly correlated with increases in IL-6 production[105]. Finally, general cognitive and neuropsychological functioning such as attention, information processing and memory tasks are also known to be significantly impaired both in hypoxemic and non-hypoxemic COPD patients[102;106;107]. The physiologic events impairing this cognitive performance have not been elucidated yet.

1.1.2.1.5 Osteoskeletal effects

Baseline rates of co-morbidities such as osteoporosis and bone fractures are extremely high in COPD patients[108]. Osteoporosis is characterized by net loss of bone tissue mass and can have multiple causes, single or in combination, including worse nutritional status[109], decreased exercise capacity[110], corticosteroid treatment[111], age, smoking and systemic inflammation[112]. Besides predisposing to painful vertebral fractures, osteoporosis itself may further impact lung function negatively by altering the configuration of the chest wall, as has been observed by a decrease in forced vital capacity in women suffering from osteoporosis[113].

1.1.2.1.6 Bone marrow effects

Recently, several reports have challenged the view that anemia is a frequently occurring condition in COPD patients hospitalized for an acute exacerbation or worsening of their disease[114;115]. Systemic cytokines and chemokines are thought to be responsible as it has been shown that they might shorten the survival of red blood cells, dysregulate iron homeostasis and impair bone marrow erythropoietic

responses as seen in many chronic diseases[115]. Particularly, in COPD patients, anemia was found to be related to the degree of systemic inflammation and is likely to be caused by erythropoietin resistance as erythropoietin levels itself are increased[116].

1.2 Inflammation and skeletal muscle function in COPD

As mentioned before, circulating cytokines are chronically upregulated in patients with stable COPD suffering from skeletal muscle weakness[14;20;22-25], and are known to increase more during an acute exacerbation[26;27;29;30], while muscle force is further decreased[29;60;61].

Starting from these observations, it is not surprising that cytokines are thought to contribute to skeletal muscle dysfunction. This hypothesis might moreover be strengthened by several data. First of all, elevated levels of circulating IL-6, IL-8 and CRP have been associated with an increased REE and unresponsiveness to nutritional interventions in stable COPD, giving support to the concept that these cytokines may play a role in COPD-associated cachexia[20]. Furthermore, an inverse relationship between an indirect estimation of skeletal muscle mass as assessed by the creatinine height index and circulating levels of IL-6, TNF-α and both soluble TNF-receptors (TNF-Rs) has been found in patients with clinically stable COPD[23]. Moreover, the IL-6/dehydroepiandrosterone ratio, which is a marker for the catabolic/anabolic balance, was reported to be significantly correlated with midthigh muscle CSA in patients with severe COPD[117]. Finally, quadriceps peak torque was found to be highly inversely associated with both IL-6 and IL-8 plasma levels in patients during an acute COPD exacerbation. In contrast, in clinically stable patients, the relationship with IL-8 still remained significant, while there was no

correlation between IL-6 and peripheral muscle force in these patients[29]. However, this was contradictory with the findings of others who reported that elevated plasma levels of IL-6 correlated significantly with reduced quadriceps strength even in stable patients with mild to severe COPD[118]. We have no explanation for this apparent discrepancy. It might be related to the difference in sample size, which was twenty times higher in the latter study, as muscle force and cytokine levels were quite similar in both studies.

Recently, an endogenous production of TNF-α by skeletal muscles has also been observed in stable COPD patients[91;119], although its precise role still needs to be elucidated.

As described below, the potential role of some cytokines in inducing skeletal muscle dysfunction is known, while that of others is still questionable.

1.2.1 Effects of TNF-α on diaphragm and peripheral muscles

The detrimental effects of TNF-α on skeletal muscle have already been extensively described. Therefore only a brief non-detailed overview will be presented here.

Decreases in global diaphragm force, but not in soleus or extensor digitorum longus (EDL) muscles have been reported in transgenic mice with cardiac-specific overexpression of TNF-α when measured *in vitro*. These changes were likely caused through endogenous production of oxidative stress with plasma levels of TNF-α of more than 300 pg/mL[120].

In vivo administration of TNF-α at rather low doses for several consecutive days resulted not only in decreases in respiratory muscle force production but even in breakdown of skeletal muscle proteins. Indeed, a decreased synthesis of myofibrillar

proteins has been observed both in the diaphragm and peripheral muscles of rats[121-123], together with increases in skeletal muscle proteolysis[124]. This is in line with the increase in free and conjugated ubiquitin concentration of skeletal muscle proteins observed in rats after TNF-α administration[125]. Moreover, a depressed *in vivo* diaphragm pressure generation and costal shortening has been observed in dogs post TNF-α infusion[126].

Diaphragm contractile properties have also been shown to decrease after *in vitro* TNF-α administration to mice, rats or hamsters[120;127;128], although only when huge amounts of TNF-α were used[128;129]. Also in the soleus muscle of rats treated with low doses of TNF-α, no proteolysis was observed[130].

Treatment of murine or rat myocyte cell cultures with TNF-α was found to be rather biphasic, with both decreasing and increasing protein expression depending on the dose used[131-134].

In summary, the effects of TNF-α on skeletal muscles are rather contradictory and likely dependent on the setting as *in vivo* deleterious effects could already be seen at low doses, while direct effects of TNF-α on skeletal muscles itself or on muscle cell cultures rather depended on the dose used. It is therefore likely that other mediators are involved in inducing detrimental effects on skeletal muscles *in vivo*.

1.2.2 Effects of IL-6 on peripheral skeletal muscles

1.2.2.1 Transgenic animal models overexpressing IL-6

The weight of the gastrocnemius muscle of 16 weeks old IL-6 transgenic mice of C57BL/6 origin with IL-6 overexpression in their spleen, lymph nodes, thymus, heart, lungs, liver, kidneys and intestine decreased significantly when compared to control

mice, while body weight increased due to hepatosplenomegaly. In relation to the decreased muscle weight, cathepsin B and B+L levels and activities and also messenger ribonucleic acid (mRNA) levels of mono- and poly-ubiquitins were increased in the gastrocnemius while muscle specific calpain 3 mRNA levels were decreased, suggesting a role for these proteolytic systems in IL-6-induced muscle proteolysis. Plasma concentrations of human IL-6 in these mice were above 600 pg/mL after 12 weeks[135-137]. Furthermore, all these changes could be completely blocked by administration of an anti-mouse IL-6 receptor (IL-6R) antibody when administered twice weekly starting from week 5 on[137]. Data on muscle performance were absent in this setting.

1.2.2.2 *In vivo* administration of IL-6

It has been shown that two intraperitoneal injections of 115 µg/kg recombinant human (rh)IL-6 with 3 hours in between led to a rise in protein breakdown in isolated EDL muscles, as measured by the release of tyrosine and 3-methylhistidine in male Sprague-Dawley rats, whereas one intraperitoneal or intravenous injection was not efficient in inducing protein breakdown 12 hours later[138]. Similar results were obtained in the soleus and EDL muscle when Sprague-Dawley rats were injected intraperitoneally twice with 1000 µg/kg of rhIL-6 with an interval of 4 hours, as no changes in the weight of the soleus or EDL muscle were found 8 hours after the first injection, which was in accordance with unchanged cathepsin B+L activities[135]. Moreover, normal adult A/J mice treated with 3 intraperitoneal injections of 100 µg/kg rhIL-6 with 8-hours intervals, also did not influence total and myofibrillar protein breakdown rates of EDL muscles[139]. In summary, these data suggest that the inability of one or more intraperitoneal injections of IL-6 to augment muscle protein

breakdown might be related either to the low dose used in these settings or most likely to the very short half-life of IL-6. Indeed, the plasma half-life time of intravenously injected rhIL-6 in rats is about 3 minutes and circulating IL-6 distributes predominantly to the liver[140]. Moreover, as seen in the previously mentioned normal adult A/J mice treated with 3 intraperitoneal injections, IL-6 plasma levels reached peak values of about 30 ng/mL only directly after injection while they were already decreased to baseline values one hour before the next injection[139].

The importance of maintaining continuously relevant plasma levels might be supported by the observed gastrocnemius atrophy, together with increases in cathepsin B and B+L activities, in mice 3-5 days after intramuscular injection of turpentine oil in the opposite gastrocnemius muscle. This intramuscular injection immediately increased circulating IL-6 levels, reaching its highest value of about 400 pg/mL 3 days after injection. The involvement of locally produced IL-6 in the activation of both cathepsins was moreover confirmed using a rat IL-6 receptor antibody[141]. Furthermore, when female Sprague-Dawley rats received modest continuous infusions of rhIL-6 directly into the tibialis anterior muscle during 14 days (each hour administered at doses of 22 pg/mL daily), reaching plasma levels comparable to those present after intense exercise, both total and myofibrillar protein content decreased with 9% and 17%, respectively[142]. However, whether this protein breakdown was due to a direct effect of IL-6 or to the damage caused by the intramuscular injections might be disputed.

A reduced loss of gastrocnemius weight, together with decreased IL-6 plasma levels after 16 days of treatment of male tumor-bearing Balb/c mice with an anti-IL-6-antibody also seemed to support a role of IL-6 in the regulation of muscle protein breakdown in cancer cachexia[143].

However, in contrast to the earlier described detrimental actions of IL-6 on skeletal muscles, an anabolic response of endogenously produced IL-6 has also been reported. Indeed, it has been shown that contracting skeletal muscles may produce IL-6, likely in order to repair the exercise-induced tissue injury and consequently to restore muscle function. Furthermore, IL-6 is known to stimulate glucose output from the liver or adipose tissue and might therefore contribute to maintain glucose homeostasis during exercise[144].

1.2.2.3 *In vitro* experiments or cell culture

In vitro or cell culture data concerning the direct effects of IL-6 on skeletal muscles are rather controversial and difficult to interpret, likely due to the different activities of the IL-6 used.

The *in vitro* addition of 2000 U/mL of rhIL-6 to soleus or EDL muscles of female Wistar rats for 90 minutes ruled out the involvement of IL-6 in muscle protein breakdown as measured by the rate of tyrosine release to the incubation medium. In addition, no changes in the rate of protein synthesis or amino acid uptake were detected[145]. Identical results were obtained when EDL muscles were incubated for 6 hours in the presence of 750 ng/mL rhIL-6[138]. Moreover, in cultured L6 rat myotubes, different concentrations of rhIL-6 ranging up to 2000 ng/mL were unable to cause protein degradation when treated for 6, 24, or 48 hours[139].

All these findings are in contrast with the fact that rhIL-6 at a dose of 100 U/mL shortened the half-life of long-lived proteins in mice C2C12 myotubes after 2 days, together with increases in the transcription levels and activities of the 26S proteasome and both cathepsins B and B+L[146]. Furthermore, palmitate-induced IL-6 production has been shown to downregulate the expression of glucose transporter 4

in mice C2C12 skeletal muscle cells after 16 hours exposure, suggesting that IL-6 is likely to be involved in insulin resistance[147] and might thus be involved in skeletal muscle wasting due to an imbalanced metabolic energy uptake. On the contrary, other authors showed that the addition of 100 U/mL of recombinant murine IL-6 to mice C2C12 myotubes for 48 hours resulted in an increase in total protein, with an even more pronounced increase in the rate of protein synthesis. Regarding the proteolytic system components, this murine IL-6 caused decreases in ubiquitin transcripts, cathepsin mRNA and m-calpain mRNA[148]. These latter data might be strengthened by the fact that proliferation of human myoblast cultures was provoked by autocrine secretion of IL-6 after stimulation with activated monocytes for 7 days[149;150].

1.2.3 Effects of IL-8 on diaphragm and peripheral skeletal muscles

The effects of IL-8 on skeletal muscle function have never been tested in animals or in *in vitro* or cell culture experiments. Only indirect evidence suggesting a catabolic role for IL-8 in patients has been published.

An inverse correlation between quadriceps peak torque and circulating IL-8 levels has been found in clinically stable COPD patients, but was more significant in patients suffering from an acute exacerbation. Handgrip force was also negatively associated with IL-8 plasma levels during acute exacerbations. Stepwise multiple regression analysis showed that IL-8 was the only independent determinant of quadriceps peak torque in patients suffering from an acute exacerbation. Corticosteroid treatment could be ruled out as a contributor to skeletal muscle weakness as all exacerbated patients received a similar dose, and no relationship

was found between the dose of oral methylprednisolone and the changes in muscle force[29].

Along the same lines, a significant positive correlation was found between creatine kinase (CK) skeletal muscle enzyme and circulating IL-8 levels measured at hospital admission in children with meningococcal disease. Myositis is a frequently occurring phenomenon in these patients and high systemic concentrations of CK are known to be indicative of muscle damage due to a variety of causes including acute myositis, febrile illness, and bacterial, viral, fungal, and parasitic infections[151]. These findings might therefore support the hypothesis that IL-8 plasma levels are involved in muscle wasting and hence, muscle weakness.

Finally, recent data suggest that neutralization of IL-8 with a monoclonal antibody therapy once monthly during 3 months may improve dyspnea in patients with stable severe COPD, when this primary outcome variable was measured by the transition dyspnea index (Figure 1.5). It is moreover worthwhile mentioning that anti-IL-8 treatment did not alter lung function, perhaps suggesting that IL-8 may be involved in respiratory muscle weakness[152]. This might be strengthened by an improved inspiratory muscle strength together with a reduced dyspnea in stable COPD patients after targeted inspiratory muscle training[153]. However, it should be considered that a decrease in inflammatory mediators after IL-8-antibody therapy might be responsible for the observed reduced dyspnea.

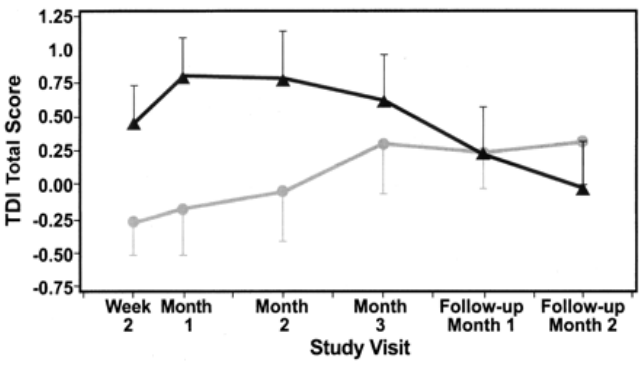


Figure 1.5. Transition dyspnea index total scores (mean ± SEM) during treatment (week 2, month 1, month 2, and month 3) and follow-up periods. Anti-IL-8 (closed triangles) vs placebo (closed circles). At week 2, p = 0.046; at month 1, p = 0.05. (Adapted from Mahler et al. Chest. 2004; 126: 926-934)

1.2.4 Proteolytic pathways in skeletal muscles

Proteolytic pathways involved in skeletal muscle protein degradation remain somewhat obscure. In general, protein degradation takes place by four major pathways[154]. The lysosomal system relies on the activity of four acidic proteases (cathepsin B, H, L, and D) with poor selectivity and seems to be responsible for basal degradation of mainly extracellular proteins. In contrast, the three cytosolic proteolytic pathways show high specificity for intracellular proteins[125]. Muscle-specific calpain 3 is thought to be the most important Ca^{2+}-dependent cysteine protease in muscle catabolism. In the second degradative cytosolic pathway, the protein ubiquitin seems to be involved in targeting particularly contractile proteins undergoing ATP-dependent degradation by the 26S proteasome through the formation of covalent ubiquitin conjugates, with ulterior regeneration of free, functional ubiquitin[125]. The conjugation of ubiquitin to proteins mostly involves the activation of three E3 ubiquitin ligases: Muscle Atrophy F-box (MAFbx)/atrogin-1, Muscle Ring Finger (MuRF)-1, and E3α-II[155] (Figure 1.6). Finally, caspases are a family of cytosolic cysteine proteases mostly known for their role in the execution of the apoptotic process[154].

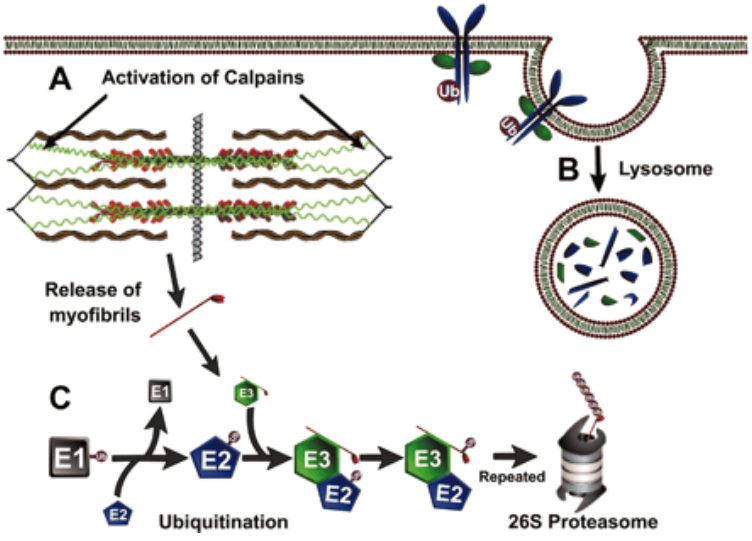


Figure 1.6. Three known proteolytic systems implicated in muscle atrophy: the calcium-dependent calpain system (*A*), the lysosomal protease system (cathepsins; *B*), and the ubiquitin (Ub; *C*)-proteasome system. Recent evidence points toward interactive involvement of these systems in proteolysis. (Adapted from Jackman and Kandarian. Am J Physiol Cell Physiol. 2004; 287: C834-C843)

1.2.4.1 Cytokines and signaling pathways in skeletal muscles

TNF-α and IL-6 may be implicated in the mechanism leading to protein breakdown in cultured myoblasts or to cachexia in small animals, as described in detail in paragraphs 1.2.1 and 1.2.2. However, the precise intracellular skeletal muscle signaling pathways activated by these cytokines are not clear yet.

1.2.4.1.1 Intracellular skeletal muscle signaling pathway induced by TNF-α

The responses of skeletal muscle cells to TNF-α are mediated by either TNF-R1 (55 kDa) or TNF-R2 (75 kDa). When shed, the extracellular domain fragments of both receptors can be detected as soluble forms, and may be able to stabilize the TNF-α molecule, thereby potentiating its long-term actions[156].

Catabolic intracellular signaling cascades have been widely described in skeletal muscles. The most important catabolic action of the TNF-α pathway seems to be mediated by NF-κB, which is a ubiquitous transcription factor present in the cytosol in an inactive form when coupled to its natural inhibitor, inhibitory κB (IκB). After TNF-α stimulation, which induces an increased production of ROS, IκB is degraded by proteasomes, resulting in the active NF-κB. Free of its inhibitor, it might translocate into the nucleus and regulate the transcription of genes encoding immune and inflammatory responses, cell growth control, and apoptosis[157]. However, the list of target genes for NF-κB during cachexia is scarce. For instance, MyoD expression, a transcription factor essential and specific for skeletal muscle differentiation and repair, is known to be inhibited by NF-κB[158]. TNF-α-induced NF-κB activation also appears to interfere with the ubiquitin-proteasome pathway by increasing the ubiquitin-conjugating activity together with an upregulation of the ubiquitin-conjugating E2 enzyme[159] and by suppressing the transcription of the C3 proteasome

subunit. Several mechanisms independent of NF-κB activation are also known to induce a catabolic state in skeletal muscles. Indeed, it has been shown that TNF-α might exert catabolic effects on skeletal muscles by suppressing the growth related bioactivity of circulating IGF-I through upregulation of the expression of its inhibitory IGF-I binding protein 1[160] (Figure 1.7).

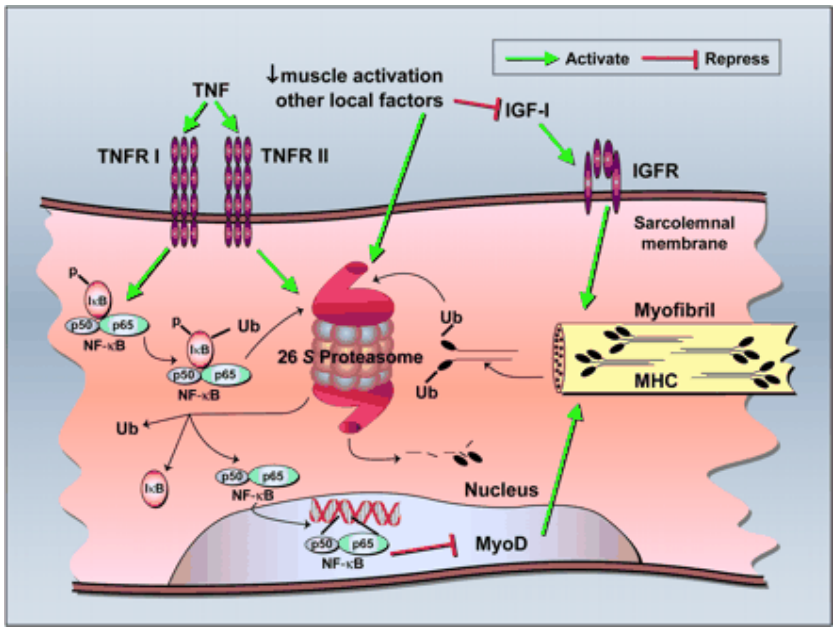


Figure 1.7. Possible mechanisms of cachexia in COPD. (Adapted from Debigare et al. Am J Resp Crit Care Med. 2001; 164(9): 1712-7)

Mitogen-activated protein kinases (MAPK) have been demonstrated to act as second messengers, as activation of p38 MAPK increased the expression of the atrogin1/MAFbx ubiquitin ligase gene[161]. TNF-α-induced insulin resistance in skeletal muscles also involved the activation of p38 MAPK, which impaired the tyrosine phosphorylation of insulin receptor components and the corresponding activation of its signaling pathway[162]. Moreover, TNF-α has been shown to recruit components of the caspase pathway, and might therefore mediate cell death[163].

1.2.4.1.2 Intracellular skeletal muscle signaling pathway induced by IL-6

The IL-6R complex in skeletal muscles consists of two distinct membrane-bound glycoproteins, a cognate IL-6R itself and a transmembrane signal-transducing element, gp130[164]. In addition to this membrane-bound IL-6R, a soluble form has been purified, which acts together with IL-6 as an agonist for cell types that although they express gp130, would not inherently respond to IL-6 alone[165]. Moreover, soluble gp130 has also been demonstrated to be present in human plasma, and is thought to act as a buffer to modulate systemic responses to circulating IL-6 in combination with the soluble IL-6R. IL-6 signaling is in turn facilitated through the homodimerization of gp130 to the ligand-receptor complex.

Data on intracellular pathways of IL-6 after activation of its receptor are predominantly described in hepatic and immune systems. One intracellular signaling pathway is triggered via activation of gp130-associated cytoplasmic tyrosine kinase family members (janus kinase-1 - JAK1, janus kinase-2 - JAK2, and tyrosine kinase-2 - TYK2), leading to the activation of transcription factors by phosphorylation of signal transducer activators of transcription (STATs). Another major signaling pathway for IL-6 is the Ras-Raf signaling cascade, which regulates the phosphorylation of MAPKs. Both phosphorylated STATs and MAPKs ultimately lead to gene expression (Figure 1.8).

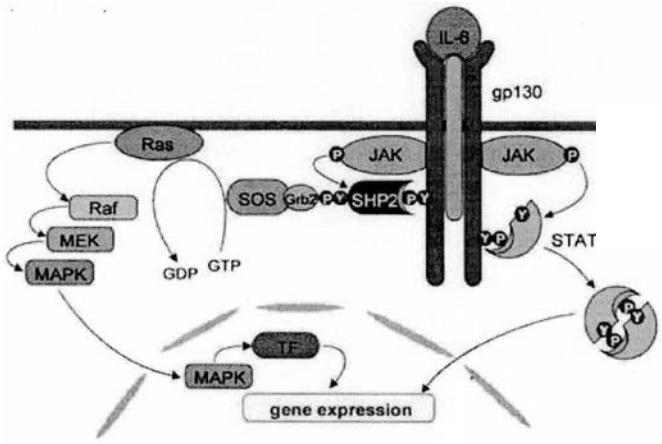


Figure 1.8. IL-6-induced JAK/STAT and Ras-Raf signaling pathways. (Adapted from Heinrich et al. Biochem J. 2003; 374: 1-20)

Several inhibitory mechanisms have also been described. SH-2-domain-containing tyrosine phosphatase (SHP2) is thought to act as a negative regulatory mechanism stopping IL-6 signaling by causing dephosphorylation of JAK/STAT proteins (Figure 1.6). Furthermore, protein inhibitors of activated STAT proteins interact with phosphorylated STAT transcription factors, and consequently inhibit STAT-mediated gene induction. Finally, a classical feedback mechanism has also been discovered. Suppressors of cytokine signaling (SOCS) proteins are known to be upregulated by IL-6 via the JAK/STAT pathway and subsequently inhibit STAT-mediated signal transduction[166;167].

Only few data exist on the catabolic intracellular signaling pathways of IL-6 in skeletal muscles itself. It has been shown that both lysosomal cathepsin B and cathepsin B+L levels and activities were increased in the gastrocnemius of transgenic mice overexpressing IL-6, as were the mRNA levels of both poly- and mono-ubiquitins. In contrast, the mRNA levels of muscle-specific calpain 3 were decreased while no alterations were observed in the mRNA levels of subunits of the 26S proteasome (S4 and S7) and S20 proteasome (C2 and C8)[135;136]. It has recently been suggested that IL-6 might also interfere with the growth hormone (GH)-IGF-I axis as decreases in the phosphorylation of p70-S6 kinase (S6K1) protein were observed after IL-6 infusion in the tibialis anterior muscle[142]. In normal circumstances, IGF-I is known to increase the phosphorylation of S6K1, notably as part of the phosphoinositol 3-kinase signaling pathway, and the phosphorylated S6K1 is known to be associated with skeletal muscle hypertrophy. In contrast to the decreased functioning of the IGF-I-signaling pathway, significant increases in the mRNA for IGF-I have been observed, likely to maintain muscle development. Moreover, these elevated IGF-I mRNA levels were independent of the GH-signaling

pathway. In addition, IL-6 infusion in humans has been shown to increase the amount of IGF-I binding protein 1 while no changes were found in total IGF-I or IGF-I binding protein 3, therefore suggesting that less IGF-I was available to activate the IGF-I-signaling pathway[168]. Moreover, mRNAs for the E3-ubiquitin-protein ligases atrogin-1 and MURF-1 did not change significantly in response to direct infusion of IL-6 in the tibialis anterior, indicating that IL-6 does not appear to mediate muscle atrophy via pretranslational modulation of these proteins[142]. Recently, it has also been shown that high levels of intracellular IL-6 might interfere with the insulin-signaling pathway in mouse C2C12 myoblasts, as they provoked a reduction in the expression levels of glucose transporter 4 and insulin-stimulated glucose uptake[169].

1.3 Systemic inflammation and other diseases

As discussed above, elevated systemic or local cytokine levels might not only be clinically relevant in inducing pulmonary damage and skeletal muscle dysfunction in stable COPD and in patients suffering from acute exacerbations of this disease. Circulating levels of TNF-α, both soluble TNF-Rs, IL-6 and IL-8 are also elevated in various other conditions such as heart failure[170;171], sepsis[172], burns[173], pneumonia and the acute respiratory stress syndrome[174], and are further upregulated when the disease becomes more severe, a similar phenomenon as occurring during exacerbations of COPD. Moreover, in all the above-mentioned diseases, clinically significant skeletal muscle weakness is known to be present[175-180]. However, whether circulating cytokines per se might be responsible for the observed skeletal muscle weakness still remains the issue of a debate, as direct effects of several cytokines on skeletal muscle function are rather controversial, as already discussed above.

Similarly to COPD, dyspnea and muscle fatigue are clinically relevant outcomes in myocardial failure[177]. Furthermore, systolic ventricular dysfunction is known to induce selective diaphragm atrophy in rats 3 months after left coronary artery ligation[178]. Hence it appears plausible that the aforementioned effects of several cytokines on skeletal muscles might be caused by a primary detrimental effect on the myocardium.

Indeed, IL-6 has been shown to act as an independent predictor of worsening of left ventricular congestive failure[181] and both IL-6 and TNF-α act as major mediators of myocardial depression in patients with meningococcal septic shock[182;183]. Furthermore, IL-6 and IL-8 have been shown to be associated with left ventricular wall motion abnormalities after coronary artery bypass grafting[184]. High levels of IL-6 and CRP were also significantly related to an increased risk for coronary heart disease[185]. Interesting is the recent finding in patients admitted to the hospital for myocardial infarction, that IL-6, IL-1β, TNF-α and both soluble TNF-Rs are related to outcome after acute myocardial infarction. However, in a multivariable analysis with adjustment for baseline and clinical characteristics, only soluble TNF-R1 seems to be a major short- and long-term predictor of mortality and heart failure in these patients[186].

1.3.1 Effects of cytokines on the myocardium

Several animal studies have shown that cytokines such as IL-1α, IL-1β, IL-2, IL-6 and TNF-α might indeed cause myocardial depression.

Concentric myocyte hypertrophy and decreases in left ventricular volume were observed in 5 months old IL-6^+/IL-$6R^+$-transgenic mice, with human IL-6 plasma levels ranging between 0.1-5 ng/mL[187]. Intravenous administration of either TNF-α or

IL-1β in intact animals recapitulated the haemodynamic changes of endotoxemia and endotoxemic shock, whereas administration of IL-1β receptor antagonist or anti-TNF-α-antibodies ameliorated the cardiovascular abnormalities or mortality[183]. In general, numerous studies examining the delayed response after intravenous or intracoronary administration of TNF-α or IL-1β to rats or dogs showed negative inotropic effects of both cytokines as measured by left ventricular ejection fraction, preload recruitable stroke work, end-systolic elastance, maximum elastance or left ventricular and myocyte shortening. In contrast, the few studies that have examined the immediate contractile effects of TNF-α generally reported a distinct early stimulatory effect on inotropy and lusitropy regarding the above mentioned haemodynamic variables[183]. Taken together, some proinflammatory cytokines likely induce a biphasic effect on instrinsic cardiac function comprised of an early positive inotropic and lusitropic effect of relatively short duration, followed by a delayed and prolonged phase of profound systolic and diastolic dysfunction (Table 1.1).

The rapid onset of the early stimulatory response therefore suggests a direct myocardial effect via mechanisms not requiring gene expression, whereas the delayed onset and prolonged duration of the late cardiodepressant response likely suggest an indirect effect requiring *de novo* gene expression and the activation of secondary mediators.

Cytokine	Dose	Route	Species	Inotropic effects	Parameter(s) examined	Mechanism suggested
Early effects (0 to 3 hours)						
rhTNF-α	100 μg/kg	Intravenously over 1 hour	Dog	Positive	dP/dt_{max} (normalized)	
rhTNF-α	60 μg/kg	Intravenously over 1 hour	Dog	No change	dP/dt_{max} (normalized)	
rhTNF-α	40 μg/kg	Intravenously over 1 hour	Dog	Positive	E_{es}, dP/dt_{max} (normalized)	
rhTNF-α	50-200 μg/kg	Intravenously over 1 hour	Dog	Positive	PRSW	Reflex independent
Delayed effects (hours to days)						
rhTNF-α	60 μg/kg	Intravenously over 1 hour	Dog	Negative	LVEF	
rhTNF-α	2.5 μg/kg/min	15 days osmotic fusion	Rat	Negative	LV and myocyte shortening	Sphingolipid mediators
rhTNF-α	30-120 μg/kg	Intravenously over 1 hour	Dog	Negative	LVEF	
rhTNF-α	100 μg/kg	Intravenously over 1 hour	Dog	Negative	dP/dt_{max}, PRSW	
rhTNF-α	60 μg/kg	Intravenously over 1 hour	Dog	Negative	dP/dt_{max}, E_{max}	
rhTNF-α	40 μg/kg	Intravenously over 1 hour	Dog	Negative	E_{es}, PRSW, dE/dt_{max}	
rhTNF-α	40 μg/kg	Intravenously over 1 hour	Dog	Negative	Ees, dP/dt_{max}	No effect of NOS inhibition
rhIL-1β	1 μg/kg	Intracoronary	Dog	Negative	LVEF	iNOS-derived NO, $ONOO^-$
rhIL-1β	1 μg/kg	Intracoronary	Dog	Negative	LVEF	Adhesion molecules
rhIL-1β	1 μg/kg	Intracoronary	Dog	Negative	LVEF	Superoxide, NO, $ONOO^-$

Table 1.1. Contractile effects of TNF-α and IL-1β on left ventricular function *in vivo*.

(Adapted from Prabhu. Circulation Research. 2004; 95(12): 1140-53)

In agreement with the *in vivo* investigations, a biphasic contractile response has also been observed in single myocytes, papillary muscle strips, and isolated heart preparations, with early effects generally generated within 30 minutes and delayed effects thereafter and up to 48 to 72 hours. Delayed cytokine-mediated depression of either basal or stimulated myocardial function has been uniformly reported, whereas results were conflicting regarding the immediate effects, which also indicated an early cytokine-induced cardiodepression after exposure to TNF-α, IL-1β, IL-1α, IL-2, or IL-6, even at low cytokine concentrations[183].

For IL-6 in particular, minutes of exposure to 1 ng/mL has been shown to depress the intracellular Ca^{2+} transients and the amplitude of cell contraction in both cultured chick embryo or guinea-pig ventricular myocytes by the Ca^{2+}-dependent nitric oxide (NO)-cyclic guanosine monophosphate-mediated pathway[188;189], whereas 24-hours exposure may induce Ca^{2+}-independent NO synthase (NOS)[189]. Moreover, in adult rat ventricular myocytes, 10 ng/mL of IL-6 enhanced the *de novo* synthesis of the earlier described Ca^{2+}-independent inducible NOS protein, increased NO production, and decreased cardiac contractility after 2 hours by primary activation of the JAK2/STAT3 signaling pathway[190]. The upregulation of NO was found to decrease the phosphorylation of phospholamban, which was in turn responsible for the inhibition of Ca^{2+} reuptake in the sarcoplasmatic reticulum[191]. Forty-eight hours later, total sarcoendoplasmic reticulum Ca^{2+} adenosine triphosphatase 2 (SERCA2) protein was also shown to be decreased with 60%, suggesting a reduced Ca^{2+} uptake in the sarcoplasmatic reticulum[192]. Acute dose-dependent negative inotropic effects of IL-6 on hamster papillary muscle strips were also found to be mediated by a constitutive myocardial NOS[193]. Recently, a reduced expression of α-myosin heavy chain (MHC), β-MHC and cardiac α-actin has been shown to occur after 24 hours of treatment of cultured rat cardiac myocytes with 2 ng/mL of mouse IL-6[194].

CHAPTER 2: AIMS OF THE STUDY

The general objective of this work was to investigate the effects of circulating cytokines on both respiratory and peripheral skeletal muscle function.

Three specific objectives have been focused on:

1. To identify whether IL-6 could induce respiratory and peripheral skeletal muscle dysfunction in experimental animals and by which mechanisms this might occur.
2. To examine the effects of IL-8 on respiratory and peripheral skeletal muscle function in experimental animals, in a similar manner as for the first objective.
3. To explore whether increased cytokine levels might also be involved in inducing physiological effects in patients suffering from myocardial failure.

CHAPTER 3: MATERIALS AND METHODS

3.1 Animal experiments

The ethics committee of the medical faculty of the Katholieke Universiteit Leuven, Leuven, Belgium, approved the experiments described below.

3.1.1 Study design

3.1.1.1 rhIL-6 administration to rats

Six series of experiments were conducted with recombinant human interleukin-6 (rhIL-6; gift of Dr Okano, Ajinomoto Co., Inc, Japan) on 139 male Wistar rats, 8 to 10 weeks old and weighing between 350 and 450 g.

3.1.1.1.1 *In vivo* experiments

In vivo studies were performed during or at the end of 7 days of continuous infusions with different doses of rhIL-6. The obtained results were compared to those of controls treated with phosphate buffered saline (PBS).

In a first series, 24 rats received during 7 days continuous infusions of either a low (50 μg/kg/day, n=8) or moderate rhIL-6 dose (100 μg/kg/day, n=8) or PBS (n=8). In a second series, 15 rats received a high rhIL-6 dose (250 μg/kg/day, n=9) or PBS (n=6). In both series, body weight was measured daily while body and tissue mass, diaphragm *in vitro* contractile properties and morphometry of the diaphragm and gastrocnemius were performed after the 7 day treatment period.

In a third series, invasive haemodynamic measurements either combined with determination of body and tissue mass, lung histology and water content, and blood sampling (control, n=4; 100 μg rhIL-6/kg/day, n=8; 250 μg rhIL-6/kg/day, n=5) or with

examination of heart histology (control, n=4; 100 μg rhIL-6/kg/day, n=6; 250 μg rhIL-6/kg/day, n=4) were performed in 31 rats after 7 days of treatment.

In a fourth series, organ and muscle blood flow were assessed with colored microspheres in 17 rats after 7 days (control, n=4; 100 μg rhIL-6/kg/day, n=6; 250 μg rhIL-6/kg/day, n=7).

In a fifth series, food intake was measured daily in 24 rats during the 7 day treatment period (control; 100 μg rhIL-6/kg/day; 250 μg rhIL-6/kg/day, n=8/group) whereas 18 rats were used to assess activity levels on the last day of treatment (control; 100 μg rhIL-6/kg/day; 250 μg rhIL-6/kg/day, n=6/group). Plasma rhIL-6, endogenous rat IL-6, albumin and IGF-I levels were measured at the end of treatment in both the moderate and high dose group of the third and fifth experimental series, and were compared to controls.

3.1.1.1.2 *In vitro* experiments

In a sixth series of experiments, diaphragm contractile properties of untreated animals were assessed *in vitro* after 30 minutes of incubation either with 12 ng/mL rhIL-6 or with Krebs (n=5/group).

3.1.1.2 rhIL-8 administration to rats

Two series of experiments were conducted with recombinant human interleukin-8 (rhIL-8; gift of Novartis, Austria) on 36 male Wistar rats, 8 to 10 weeks old on weighing between 350 and 450 g.

No *in vitro* experiments were performed. *In vivo* studies were conducted after 7 days of continuous infusions with different doses of rhIL-8. The obtained results were compared to those of controls treated with PBS.

In a first series, 24 rats were divided into 3 groups (n=8/group) to receive during 7 days continuous infusions of rhIL-8 (25 or 50 μg/kg/day) or PBS. In a second series, two higher doses of rhIL-8 (100 or 250 μg/kg/day) were administered to 12 rats and were compared to controls (n=4/group). In both experiments, body weight was measured daily. After 7 days, body and tissue mass, diaphragm *in vitro* contractile properties, and histochemical analyses of the diaphragm and gastrocnemius were performed together with lung histology, determination of lung wet-to-dry ratio and determination of rhIL-8 and albumin plasma levels.

3.1.2 Experimental methodology

3.1.2.1 Pump implantation

Rats were anesthetized by intraperitoneal injection of sodium pentobarbital (Nembutal, Sanofi, Brussels, Belgium, 60 mg/kg). Subsequently, Alzet mini-osmotic pumps (model 2001, Iffa Credo, Bruxelles, Belgium) with a continuous delivery of 1.0 μL/h during 7 days were implanted subcutaneously on the back of the animal. Pumps of experimental animals were filled with sterile PBS (Cambrex Bio Science Verviers, Verviers, Belgium), rhIL-6 or rhIL-8, and rat serum (1% v/v). Control rats were given the same volume of PBS, human albumin (ICN Biomedicals Inc., Aurora, 0.1% w/v) and rat serum. The number of pumps implanted per rat varied from 1 to 3, depending on the concentration of the cytokine used for administration. After this procedure, all rats were housed in individual cages.

3.1.2.2 *In vitro* contractile properties of the diaphragm

Animals were anesthetized by intraperitoneal injection of sodium pentobarbital (60 mg/kg), tracheotomized (Insyte catheter, 14 GA, BD) and artificially ventilated at

a constant rate of 60 cycles min^{-1} (Harvard pump respirator, Harvard Apparatus, Co., South Natick, MA). This mechanical ventilation was necessary as laparotomy, performed to remove the diaphragm, made spontaneous breathing impossible. After laparotomy with transverse extension of incision, the diaphragm was immediately placed in an aerated (95% O_2 – 5% CO_2) and cooled Krebs solution (NaCl 137, KCl 4, $CaCl_2$ 2, $MgCl_2$ 1, KH_2PO_4 1, $NaHCO_3$ 12 and glucose 6.5 mM). A small amount of D-tubocurarine chloride (0.025 mM) was added to this solution to inhibit neuromuscular activation. Two small rectangular strips of both left and right costal diaphragm regions were then dissected, parallel to the long axis of the fibers. Both ends of each bundle were tied with silk sutures to serve as anchoring points. The paired bundles were subsequently mounted vertically in a tissue bath containing the aerated Krebs solution at 37°C. The temperature was maintained constant by circulating water running through an external jacket with a thermostatically controlled water pump. The bundles were then placed in between two large platinum stimulating electrodes, anchored at the bottom to a rigid support and fastened at the top to an isometric force transducer (Maywood Ltd., Hampshire, U.K.) mounted to a micrometer. The preparations were stimulated by a Harvard 50-5016 stimulator (Edenbridge, Kent), connected in series to a power amplifier (Power one model HS-24-4.8). Stimulations were performed with 0.2 ms supramaximal square wave pulses and a train duration of 250 ms. Therefore, the muscle bundles were first placed at their optimal length (L_0), defined as the length at which maximal isometric twitch tension was obtained. The signals were amplified and recorded on a computer via analog to digital conversion (DT 2801-A) using Labdat software (Labdat/Anadat, RHT-Infodat, Montréal, Canada). Measurements were analyzed with Anadat.

After a 15 min equilibration period at L_0, the following measurements were successively performed for each bundle:

- twitch characteristics (1 Hz stimulation) were determined from two successive measurements; the highest value of peak twitch force (P_t) and its corresponding time to peak tension (TPT) and half-relaxation time (1/2 RT) were used for further analysis.
- fused tetanic force (P_o, 160 Hz stimulation) was determined from two successive stimulations with a two minutes interval; the highest value was taken for further analysis.
- the force-frequency relationship was measured with two minutes of interval in between the stimulations, using the following order: 25, 160, 50, 160, 80, 160, 120, and 160 Hz. Deterioration of the preparations because of successive stimulations was evaluated by measuring the decline in force developed at 160 Hz after each stimulus.
- fatiguability of the bundles was assessed using a fatigue run consisting of repeated 25 Hz stimulations in trains of 330 ms duration with one each 3 s during 5 minutes.

After completion of the experiment, the bundles' length, thickness and width were measured at L_0 using fine calipers. The bundles were then blotted dry and weighed. Unstrechted length was also determined. CSA was obtained by dividing weight by muscle specific density (1.056) and length obtained at L_0. All forces were expressed in g per unit CSA (g/cm^2). Twitch-to-tetanus ratio (P_t/P_o) was also calculated for each muscle bundle[195].

The whole diaphragm (including the bundles), right scalenus medius, gastrocnemius, soleus, EDL, and plantaris, heart, lungs, and liver were dissected and weighed after trimming and blotting dry.

3.1.2.3 Histochemical and histological examination

3.1.2.3.1 Diaphragm and gastrocnemius

Part of the costal diaphragm samples and gastrocnemius were curled up, cut transversely and fixed into tissue glue (Tissue-Tek, Elkard, IN, USA) with their fibers oriented perpendicularly to a cork holder. Subsequently, each muscle specimen was immediately frozen in isopentane cooled with liquid nitrogen. Serial 10-μm cross-sections were then cut using a cryostat at -20°C and stained for myofibrillar adenosine triphosphatase (ATPase) after acid preincubation to identify the different fiber types i.e. type I (slow-twitch oxidative), IIa (fast-twitch oxidative and glycolytic) or IIx/b (fast-twitch glycolytic)[196].

Acid preincubation pH (buffer acetate solution, pH 4.3 or 4.5) makes it possible to distinguish easily between the above-mentioned fiber types because it strongly inactivates the myosin ATPase enzyme of fast oxidative glycolytic fibers and to a lesser extent that of fast glycolytic fibers.

Staining primarily occurs in an alkaline solution containing ATP and Ca^{2+} at 37°C for 45 minutes. The enzyme ATPase splits off the terminal phosphate from ATP and, because of the presence of calcium in the solution, this phosphate immediately combines to form calcium phosphate. At an alkaline pH, calcium phosphate is insoluble and is therefore deposited at the site of the enzyme activity. The tissue section is then removed from the solution and placed in a solution of cobalt chloride 2% for 3 minutes. The cobalt is exchanged for the calcium, forming cobalt phosphate

at the site where calcium phosphate was previously seen. Finally, the tissue is placed in ammonium sulphide for 2 minutes, resulting in the formation of black, insoluble cobaltous sulphide and consequently demonstrating the site of enzyme activity[196].

Morphometric examination was carried out microscopically (Leitz Laborlux S., Wetzlar, Germany) at 20x magnification, using a digital video camera (Sanyo B/W CCD Camera, Model VC-2512; Osaka, Japan) connected to a computerized image analysis system (Quantimet 500, Leica, Cambridge Ltd., UK). At least 150 fibers were analyzed in both diaphragm and gastrocnemius muscle specimens. Areas in which fiber orientation was not transverse to the long axis were not analyzed. Boundaries of individual muscle fibers were delineated, and fiber CSA was then determined from the number of pixels within the outlined fiber. Fiber diameters were determined by measuring the maximum diameter perpendicular to the long axis. In addition, measured diaphragm fiber CSAs and diameters were corrected for the shortening occurring from L_0 to excised length by dividing CSA by a correction factor. This correction factor was the ratio of L_0 to unstretched length. The residual interstitial space (RIS) was evaluated by measuring the interstitial space between muscle fibers and was expressed as a percentage of total fiber area. Finally, fiber type proportion was expressed as a percentage of total amount of fibers[195].

3.1.2.3.2 Heart

After inserting a winged needle (BD Valu-Set, 21 GA) into the left ventricle, a small hole was made into the right atrium and 2 mL 0.1 N $CdCl_2$ was injected *in situ* into the left ventricle to arrest the heart in dilatation, as it is known that $CdCl_2$ blocks the L-type Ca^{2+}-channels. After perfusion with 0.9% NaCl, fixation occurred with 4%

formaldehyde. Hearts were then excised and stored in 70% methanol at 4°C. After dehydration in solutions with an increasing percentage of methanol, and incubation in toluene (5 minutes for each solution), hearts were divided in 4 transverse slices and embedded in paraffin. Subsequently, serial 7-μm slices were cut (Micron HM340E) and stained with hematoxylin-eosin (H&E) after deparaffination (toluene and solutions with decreasing percentage of methanol, 5 minutes each) and rehydration in distilled water. H&E staining was performed by incubating the slices for 5 minutes in hematoxyline de Marris, followed by incubation in acid alcohol for several seconds and by a short-period incubation in a Li-carbonate solution. Finally, slices were incubated in eosine for 20 seconds. Between all incubation steps, slices were rinsed with distilled water.

Right ventricular cavity was measured using a microscope digital video camera, connected to a computerized image analysis system, as described above. Values were expressed as a percentage of the total heart cross-sectional area limited by the outer margin of the ventricular wall.

3.1.2.3.3 Lungs

Lung lobes were excised after treatment and left lobes were immediately fixed in 4% formaldehyde for 72 hrs. Five-μm histological paraffin slices were stained with H&E as described above and examined by a pathologist, who was blinded to the experimental protocol.

In addition, right lung lobes were used to determine water content by measuring wet-to-dry ratio after desiccation for 3 days at 80°C.

3.1.2.4 Measurement of cytokine, albumin and IGF-I plasma levels

During removal of the diaphragm, the vena cava inferior was cut and blood was sampled from the abdomen. Blood was collected in tubes coated with potassium ethylenediaminetetraacetic, lithium heparin or clot activator silica (BD Vacutainer systems, Plymouth, UK) for determination of plasma cytokines, albumin and IGF-I respectively. Plasma was obtained by centrifugation (1,900 g; 10 minutes at 4°C for cytokines and albumin – 1,900 g; 10 minutes at room temperature for IGF-I) and stored at -80°C.

Plasma levels of rhIL-6, rhIL-8 and rat IL-6 were measured by a sandwich enzyme linked-immuno-sorbent assay (ELISA: human IL-6 Flexia kit – sensitivity: 3 pg/mL, human IL-8 cytoset CHC1304 – sensitivity: 2 pg/mL and rat IL-6 ELISA kit – sensitivity: < 8 pg/mL; all Biosource Europe, Nivelles, Belgium). Albumin plasma levels were determined using a colorimetric method with bromcresol green binding (Roche, Basel, Switzerland)[197] while IGF-I plasma levels were measured in acid-ethanol-extracted plasma by a radio-immunoassay using a guinea-pig polyclonal antiserum (Ciba-Geigy, Basel, Switzerland)[198].

3.1.2.5 Invasive haemodynamic measurements

Rats were anesthetized by intraperitoneal injection of urethane (600 mg/kg) α-chloralose (160 mg/kg) to minimally alter myocardial performance. Thereafter, animals were tracheotomized, and ventilated with a pressure-controlled respirator (end-inspiratory pressure=12 mm Hg, end-expiratory pressure=2 mm Hg, Hugo Sachs Elektronik, D-7806 March-Hugstetten, Germany) set at a constant rate of 60 cycles min^{-1}. The right carotid artery was exposed and a micro-tip pressure-conductance combination catheter (SPR-847 catheter connected to an ARIA-1 setup,

Millar Instruments, Houston, TX), consisting of 4 electrodes with a high-fidelity pressure transducer mounted between electrodes 2 and 3, was advanced into the left ventricular cavity to measure basal haemodynamic and cardiac contractility parameters under both load-dependent and load-independent conditions by generating pressure-volume loops.

The outer excitation electrodes, which are located at the apex and just below the aortic valve, were used to generate an electric field. The conductance of the ventricular blood pool constantly changes during expansion and contraction of the ventricle. The inner sensing electrodes could in turn deduce the conductance as a function of time G(t) which is proportional to the intraventricular volume by $V(t)= 1/\alpha \times \rho \times L^2 \times (G(t)-G(p))$ where α is the volume calibration factor, ρ is the specific resistivity of blood, L is the distance across the sensing electrodes and G(p) is the parallel conductance (i.e. conductance formed by the tissues surrounding the left ventricular cavity), causing overestimation of intraventricular conductance G(t). The parallel conductance volume was therefore determined by a 50 µL bolus injection of 15% NaCl solution into the exposed external jugular vein, leading to an increased ventricular conductance, without affecting left ventricular pressure. The intercept of the regression line between the end-diastolic (EDV) and end-systolic volume (ESV) with the identity line (EDV=ESV; intraventricular blood volume equals zero) then corresponds to the parallel volume. Most important haemodynamic variables measured under baseline conditions included:

- heart rate (HR)
- end-systolic and end-diastolic volume (ESV and EDV)
- end-systolic and end-diastolic pressure (ESP and EDP)
- stroke volume (SV=EDV-ESV)

- ejection fraction (EF=SV/EDV)
- cardiac output (CO=SV.HR)
- stroke work (SW=ESP.SV)
- arterial elastance (Ea=ESP/SV)
- positive and negative first derivate of pressure to time (+/- dP/dt)
- tau (time constant of isovolumetric relaxation)

For years, both + dP/dt and EF were used to determine ventricular contractility, but these variables are rather dependent on pre- and afterload respectively. Ea has been widely used to determine this afterload, while EDV represents preload conditions. Tau and – dP/dt can both be seen as time determinants of pressure changes during the process of active relaxation.

To measure contractility parameters, left ventricular preload was decreased by temporary occlusion of the inferior vena cava exposed via a small laparotomy, causing pressure-volume loops to shift to the left. Variables measured during occlusion included:

- preload recruitable stroke work (PRSW)
- end-systolic elastance (Ees)
- the slope of the end-diastolic pressure-volume relation (EDPVR)

PRSW has been considered as the most reliable contractility parameter as it is independent of both pre- and afterload conditions; this in contrast with Ees which is both pre- and afterload dependent. The slope of the EDPVR has in turn been used to assess passive ventricle stiffness or ventricle compliance.

Volume calibrations of the *in vivo* measured conductance were performed *ex vivo* at the end of each experiment in cuvettes of known blood volume[199].

3.1.2.6 Blood flow measurements

Rats were anesthetized intraperitoneally with urethane (600 mg/kg) α-chloralose (160 mg/kg), tracheotomized, and ventilated with a pressure-controlled respirator, set at a constant rate of 60 cycles min^{-1} as mentioned before. Subsequently, two PE50 catheters (Intramedic, Clay Adams, NY) were inserted into the left ventricle via the right carotid artery, guided by the pressure curve, and into the left femoral artery to determine blood flow of both the right and left ventricle, diaphragm, right gastrocnemius, right and left kidney, spleen, jejunum and colon. After 30 minutes of stabilisation, 15-μm yellow colored microspheres (400 μL Dye-Trak, Triton Technology, San Diego, CA) were injected over 15 seconds into the left ventricle. The line was flushed with 0.5 mL of saline solution over 30 seconds while a reference sample was withdrawn with a syringe driver (Harvard apparatus nr 22, South Natick, MA, USA) at a precalibrated rate of 600 μL/min for 90 seconds, starting 10 seconds before the start of microsphere injection.

Subsequently, the right and left ventricle, diaphragm, right gastrocnemius, right and left kidney, spleen, jejunum and colon were excised, weighed, digested overnight by a 4 M potassium hydroxide solution and filtered through 8-μm filters (Millipore, Ireland). The dyes were in turn extracted from the microspheres with 200 μL dimethylformamide, and their concentrations were determined by automated spectrophotometry at 448 nm.

Organ blood flow was calculated according to the following formula: organ blood flow = (reference sample withdrawal rate x number of microspheres in organ) / number of microspheres in reference sample. Blood flow was divided by tissue weight and expressed as mL/minute/g wet weight.

To exclude experiments with inhomogeneous mixing of microspheres, only those measurements where blood flow in the right and left kidney differed by less than 10%, were retained[200].

3.1.2.7 Food intake

Free fed animals were individually housed in metabolic cages at an ambient temperature of 23°C with a 14 hrs light and 10 hrs dark cycle. During the 7 day treatment period, ad libitum food intake and body mass were recorded daily. Water was available ad libitum.

3.1.2.8 Activity level

Behavioural responses were tested for 16 hrs on day 7 of treatment (8 hrs under light conditions and 8 hrs in the dark) using an infrared camera system (AGEMA Thermovision 570), placed above the cages, coupled to a video digitiser board (PIP-1024B). The images were formatted into 256x256 pixels, a black pixel receiving the grey-value 0 and a white pixel the grey-value 225. The animals were represented by white dots, from which the pixels were subtracted from the black background. Activity index could then be calculated by comparing the position of the animal in 2 successive images. The pixels in which 'background' is changed to 'animal' are classified as pixels of moving animals[201]. Values were expressed as cm displacement per hour (cm/hr).

3.1.2.9 Statistical analysis

Analyses of haemodynamic and blood flow variables were performed using Statistica 6 (StatSoft, Inc., USA). All other statistical analyses were performed by the

Statistical Analysis System Statistical package (Version 6.12, SAS Institute Inc., Cary, NC). Data from both left and right diaphragm strips obtained from each rat were averaged. Differences between means of rats treated with rhIL-6 or rhIL-8 and control rats were assessed using a one-way analysis of variance (ANOVA) with appropriate Gabriel, Scheffé, Duncan or Fisher post-hoc comparison, or using a Wilcoxon or unpaired t-test. Pearson's correlation analysis was performed to assess relationships as data were normally distributed. A p value ≤ 0.05 two-sided was considered statistically significant. Data are expressed as mean $\pm$ standard deviation.

3.2 Patient experiments

This observational study was approved by the Institutional Review Board of the University Hospitals of the Katholieke Universiteit Leuven, Leuven, Belgium. The Institutional Review Board waived the need for individual informed consent as interventions took place under non-disturbing or non-detrimental circumstances.

3.2.1 Patient characteristics

Twenty-two patients with a minimum age of 12 years undergoing heart valve surgery using extracorporeal circulation were recruited as the use of cardiopulmonary bypass is known to release extremely high levels of many inflammatory mediators such as IL-1β, IL-2, IL-6, IL-8, IL-10 and TNF-α[202]. No exclusion criteria were handled.

A wide range of procedures was performed including two re-operations: 8 classical aortic valve replacements, 2 Ross procedures, 4 aortic valve replacements

combined with coronary artery bypass grafting, 1 aortic valve replacement combined with coronary artery bypass grafting and carotid endarterectomy, 1 combined aortic and mitral valve procedure, 1 combined mitral and tricuspid valve procedure, 1 mitral valve procedure with excision of left atrial myxoma, 2 mitral valve reconstructions, and 2 mitral valve reconstructions combined with coronary artery bypass grafting. All operations were performed at moderate hypothermia of 28°C, with continuous retrograde cold blood cardioplegia used as cardioprotective strategy.

3.2.2 Experimental methodology

3.2.2.1 Clinical and haemodynamic variables

Clinical variables such as age, weight, type of procedure, aortic cross-clamp time, extracorporeal circulation time, duration of procedure, time to extubation, and intensive care stay were determined initially.

Haemodynamic variables including cardiac output (CO: L/min), arterial blood pressure (systolic, diastolic, mean – ABP: mm Hg), mean central venous pressure (CVP: mm Hg), mean left atrial pressure (LAP: mm Hg), heart rate (HR: bpm), pulmonary artery pressure (systolic, diastolic, mean – PAP: mm Hg), partial oxygen pressure (PaO_2: mm Hg), and central and peripheral temperature (°C) were registered at 4 different time points: preoperatively (i.e. after induction of anesthesia and full installation of the patient), at the end of the operation (i.e. immediately before transfer to the intensive care unit), and 12 and 24 hrs later on the intensive care unit.

The use of inotropic, vasopressor, and vasodilator drugs (dopamine and dobutamine, norepinephrine and phosphodiesterase inhibitors, respectively) was noted at the end of the operation, and 12 and 24 hrs later.

3.2.2.2 Measurement of cytokine and troponin-I plasma levels

Blood was sampled in tubes coated with potassium ethylenediaminetetraacetic or lithium heparin (BD Vacutainer systems, Plymouth, UK) for determination of plasma cytokine and troponin-I levels, respectively, at the same time points as determination of haemodynamic variables, meaning preoperatively, at the end of operation, and 12 and 24 hrs later at the intensive care. Plasma was obtained by centrifugation (1,900 g; 10 minutes at 4°C) and stored at -80°C.

Plasma levels of IL-6, IL-1β, IL-8, IL-10, IL-11, IL-17, TNF-α, soluble (s)TNF-R1 and sTNF-R2 were determined by multiplex sandwich ELISA (SearchLight Cytokine Array, Perbio, USA) at all above mentioned time points except for 24 hrs after surgery. Sensitivity levels were different for all cytokines (IL-6: 0.4 pg/mL, IL-1β: 0.2 pg/mL, IL-8: 0.4 pg/mL, IL-10: 0.4 pg/mL, IL-11: 1.0 pg/mL, IL-17: 0.8 pg/mL, TNF-α: 2.3 pg/mL, sTNF-R1: 1.6 pg/mL and sTNF-R2: 0.4 pg/mL).

Troponin-I was determined 12 and 24 hrs after surgery only, using a heterogenous one step enzyme immunoassay (Cardia Troponin-I Flex reagent cartridge, Dade Behring, UK). Sensitivity level was set at 0.04 µg/L.

3.2.2.3 Statistical analysis

All analyses were performed using Statistica 6 (StatSoft, Inc., USA). Correlations between plasma cytokine levels and haemodynamic variables were expressed using Spearman correlation coefficients as the haemodynamic and cytokine data were not normally distributed. Correlations were considered highly significant with a p value ≤ 0.01, except for IL-6, a p value ≤ 0.05 was used to express its significance level. The evolution in time was tested with Friedman ANOVA, with significance level p ≤ 0.05.

Post-hoc testing was performed with the sign test corrected for multiple testing by Bonferroni correction. All data are presented as median [range].

CHAPTER 4: EFFECTS OF IL-6 ON SKELETAL AND CARDIAC MUSCLE FUNCTION

In this section, we wanted to examine to effects of IL-6 on skeletal muscle function using an animal model.

Rats were divided in 4 groups receiving PBS (controls) or rhIL-6 at different concentrations (50 – 100 – 250 µg/kg/day) during 7 days. At the end of treatment, body, muscle and organ masses were determined, contractile properties of the diaphragm were measured, and diaphragm and gastrocnemius morphometry was performed. Plasma levels of the subcutaneously administered rhIL-6 were also determined. Subsequently, haemodynamics, food intake, activity level, and direct effects of rhIL-6 on the diaphragm were examined in order to unravel the possible mechanisms involved in skeletal muscle dysfunction.

4.1 *In vivo* experiments

4.1.1 Body and tissue weight

Body weight was similar between controls and experimental groups at the time of pump implantation. Only for the high rhIL-6 dose (250 µg/kg/day), body weight decreased significantly by 8% at the time of dissection when compared to controls ($p<0.005$).

The low rhIL-6 dose (50 µg/kg/day) had no effect on any tissue weights. In rats treated with the moderate rhIL-6 dose (100 µg/kg/day), solely diaphragm weight tended to decrease by 15% ($p=0.0561$) whereas heart weight increased significantly by 9% ($p<0.05$). However, in rats treated with the high rhIL-6 dose the mass of all skeletal muscles studied decreased significantly by about 15% ($p<0.05$). (Table 4.1)

	control	low	moderate	high
body weight (g)				
at beginning of exp I	369±20	383±20	376±12	
at end of exp I	367±21	370±31	361±13	
at beginning of exp II	400±14			401±7
at end of exp II	417±18			382±8***
respiratory muscle weight (g)				
diaphragm exp I	0.552±0.080	0.498±0.075	0.468±0.034^{+}	
exp II	0.600±0.056			0.510±0.047*
scalenus medius exp I	0.482±0.035	0.478±0.080	0.458±0.046	
exp II	0.630±0.098			0.540±0.063*
peripheral muscle weight (g)				
gastrocnemius exp I	1.829±0.242	1.673±0.338	1.673±0.114	
exp II	2.170±0.133			1.770±0.107***
soleus exp I	0.143±0.015	0.154±0.014	0.143±0.010	
exp II	0.211±0.018			0.183±0.024*
plantaris exp I	0.355±0.041	0.355±0.032	0.329±0.030	
exp II	0.414±0.030			0.350±0.029***
EDL exp I	0.155±0.012	0.158±0.014	0.145±0.011	
exp II	0.193±0.019			0.168±0.011**
organ weight (g)				
heart exp I	0.857±0.052	0.901±0.039	0.934±0.045*	
exp II	1.170±0.056			1.100±0.108
liver exp III	14.69±0.05		13.48±1.35	15.65±1.47

Table 4.1. Body and tissue weights of rats treated with 50-100-250 µg/kg/day of rhIL-6, compared to controls. EDL indicates extensor digitorum longus, exp I = first experiment, exp II = second experiment, exp III = third experiment. Gabriel post-hoc: $^{+}$p=0.0561 vs control, *p<0.05 vs control, **p<0.01 vs control, ***p<0.005 vs control.

4.1.2 Diaphragm *in vitro* contractile properties

Maximal twitch (P_t) and tetanic tension (P_o) were similar between all groups (pooled values of 465±84 and 2,407±418 g/cm^2 respectively), although P_t/P_o decreased significantly in the high dose group (0.20±0.01 vs 0.21±0.01 in control rats, p<0.05). TPT was also identical in all groups (pooled value of 20±2 ms) while

1/2 RT slightly tended to decrease in the high dose group (22±3 vs 23±3 ms in controls, p=0.0584).

Diaphragm force as deduced from the force-frequency curve was comparable in all groups (Figure 4.1, upper panel). Furthermore, during the low frequency fatigue run, no differences in force decline (pooled values of 56±5%, Figure 4.1, lower panel) were observed between the differently treated rats.

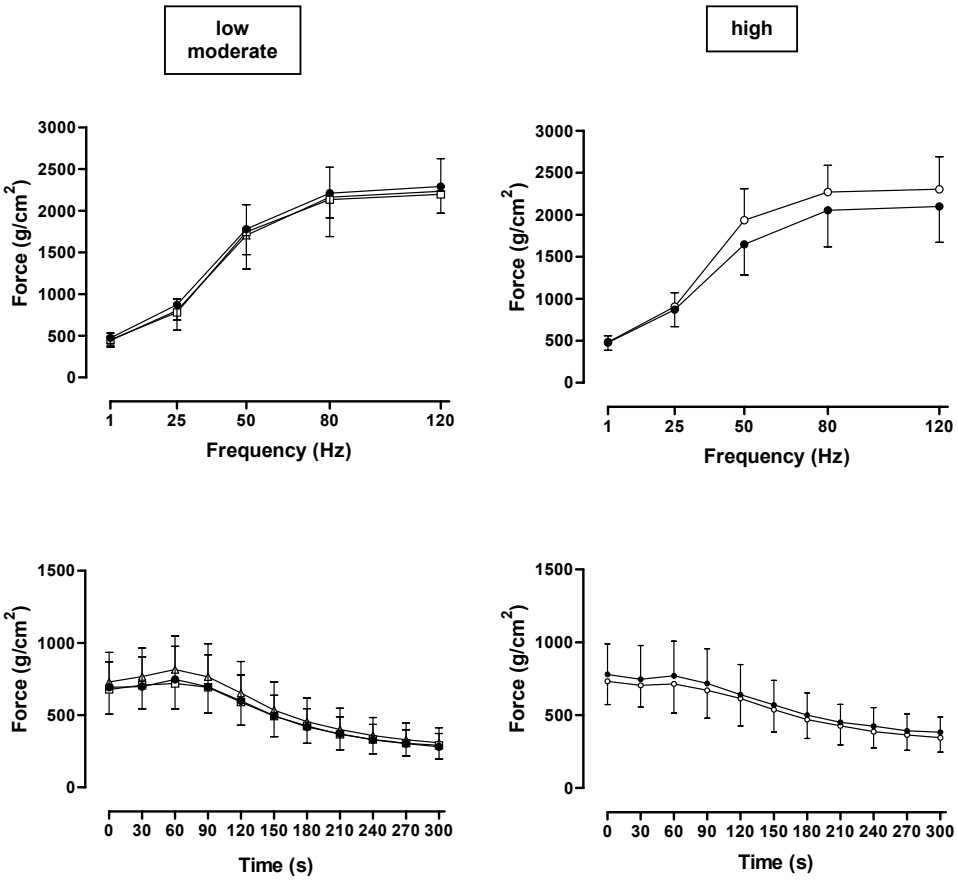


Figure 4.1. Diaphragm force-frequency (upper panels) – fatigue (lower panels) data in low (50 µg/kg/day, open squares), moderate (100 µg/kg/day, open triangles) and high dose (250 µg/kg/day, open circles) group rats, compared to controls (solid circles). Forces are expressed in absolute values, frequency in Hz, and time in s.

4.1.3 Morphometry of diaphragm and gastrocnemius

Fiber proportion and RIS remained unchanged both in the diaphragm and gastrocnemius at all doses. Also no changes in fiber dimensions of both muscles were observed in the low and moderate dose group.

Compared to controls, the diameter of all fiber types in the diaphragm of rats treated with a high dose of rhIL-6 was significantly lower by about 14% (type I: 30±3 vs 35±4; type IIa: 35±1 vs 40±4; type IIx/b: 49±4 vs 58±7 μm; all $p<0.05$). Moreover, the CSA of type IIa fibers decreased significantly by 19% (799±93 vs 987±158 μm^2, $p<0.01$) while that of type IIx/b and type I fibers tended to decrease by 24% and 17% respectively when compared to controls (1,587±302 vs 2,078±518 μm^2, p=0.0518 and 625±120 vs 756±159 μm^2, p=0.099 respectively) (Figure 4.2).

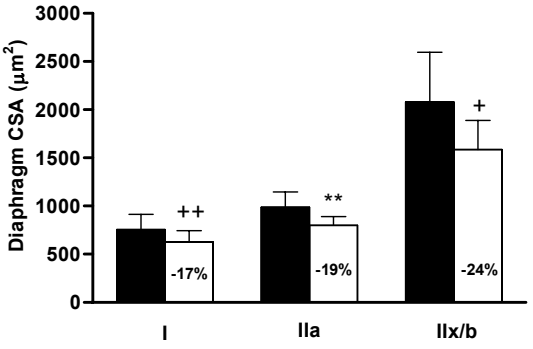


Figure 4.2. CSA of the different fiber types in the diaphragm, expressed in μm^2, in rats treated with 250 μg/kg/day of rhIL-6. Solid bars represent data of control rats, open bars represent data of rats treated with 250 μg/kg/day.
**p<0.01, $^{+}$p=0.0518, $^{++}$p=0.099

Compared to controls, the diameter of the internal type I and IIx/b fibers in the gastrocnemius tended to decrease with 9% in the high dose group (type I: 49±5 vs 54±2, p=0.0731; type IIx/b: 50±6 vs 55±3 μm, p=0.0855) while that of internal type IIa fibers remained unchanged. For the external part, the diameter of type IIx/b fibers tended to decrease with 5% (60±2 versus 64.0±4 μm, p=0.0747). The CSA of fiber types I and IIa also tended to decrease with respectively 15% and 14% when compared to controls (type I: 2,184±384 vs 2,575±283, p=0.0677; type IIa:

2,036±371 vs 2,384±170 μm^2, p=0.0875) while the CSA of both internal and external IIx/b fiber type did not change (Figure 4.3).

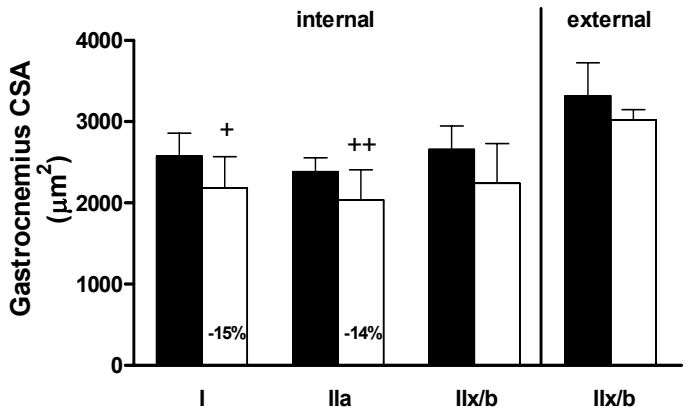


Figure 4.3. CSA of the different fiber types in the gastrocnemius, expressed in μm^2, in rats treated with 250 µg/kg/day of rhIL-6 (open bars) and in control rats (solid bars). $^{+}$p=0.0677, $^{++}$p=0.0875

4.1.4 Plasma levels

RhIL-6 plasma levels averaged 765±529 pg/mL in the moderate dose group and 12±10 ng/mL in the high dose group.

Conversely, endogenous IL-6 concentrations were negligible and did not differ between controls and both moderate and high dose groups (average value of 23±53 pg/mL), as did IGF-I plasma levels (pooled value of 647±84 ng/mL).

Albumin concentrations were equally and significantly decreased in animals treated with moderate (19±3 g/L) and high dose of rhIL-6 (19±2 g/L) when compared to controls (31±2 g/L, p<0.001).

4.1.5 Invasive haemodynamic analysis

rhIL-6 elicited a significant and dose-dependent increase in steady state end-diastolic volume (p<0.005) and stroke volume (p<0.005), causing a remarkable shift to the right of the pressure-volume loops (Figure 4.4, upper panels). End-diastolic pressure was somewhat higher in treated groups, but failed to reach statistical

significance. Heart rate, ejection fraction, +/- dP/dt and tau, were not affected by treatment. End-systolic pressure ($p<0.05$) and arterial elastance ($p<0.001$) decreased significantly, with both the moderate and high rhIL-6 dose. (Table 4.2)

	control	moderate	high
steady state			
heart rate (bpm)	435±18	421±54	427±46
end-systolic volume (μL)	42.9±11.7	70.0±13.9*	74.3±24.3**
end-diastolic volume (μL)	77.6±12.1	123.2±11.8***	137.3±22.9***
end-systolic pressure (mm Hg)	113.0±26.6	86.5±17.0^{+}	90.1±16.4^{+}
end-diastolic pressure (mm Hg)	1.6±1.5	1.9±0.7	2.9±1.4
stroke volume (μL)	50.1±4.5	79.7±15.3*	87.5±28.7***
ejection fraction (%)	58.5±6.7	58.7±9.9	58.4±13.9
cardiac output (mL/min)	21.9±2.5	33.4±6.8*	37.1±11.4***
stroke work (mm Hg.mL)	4.2±0.7	5.6±1.6	6.5±1.6**
arterial elastance (mm Hg/μL)	2.4±0.7	1.2±0.3***	1.2±0.5***
dPdt max (mm Hg/s)	7,800±2,400	6,100±1,800	7,100±2,400
dPdt min (mm Hg/s)	-9,100±2,700	-6,500±2,300	-7,100±2,300
tau (ms)	6.8±0.8	6.9±1.0	7.1±1.2
occlusions			
end-systolic elastance (mm Hg/μL)	1.8±0.6	0.9±0.7*	0.4±0.1***
preload recruitable stroke work (mm Hg)	79.3±14.2	66.9±7.7$^{\|}$	48.4±11.3***
EDPVR slope (mm Hg/μL)	0.04±0.02	0.14±0.30	0.03±0.01

Table 4.2. Invasive haemodynamic steady state and contractility parameters in controls and rats treated with a moderate (100 μg/kg/day) or high (250 μg/kg/day) dose of rhIL-6. EDPVR indicates end-diastolic pressure volume relation. Scheffé post-hoc: $^{+}p<0.094$ vs control, $^{*}p<0.05$ vs control, $^{**}p<0.01$ vs control, ***$p<0.005$ vs control, $^{\|}p=0.016$ vs high dose.

Preload recruitable stroke work and end-systolic elastance decreased significantly in a dose-dependent manner ($p<0.001$, Figure 4.4, lower panels).

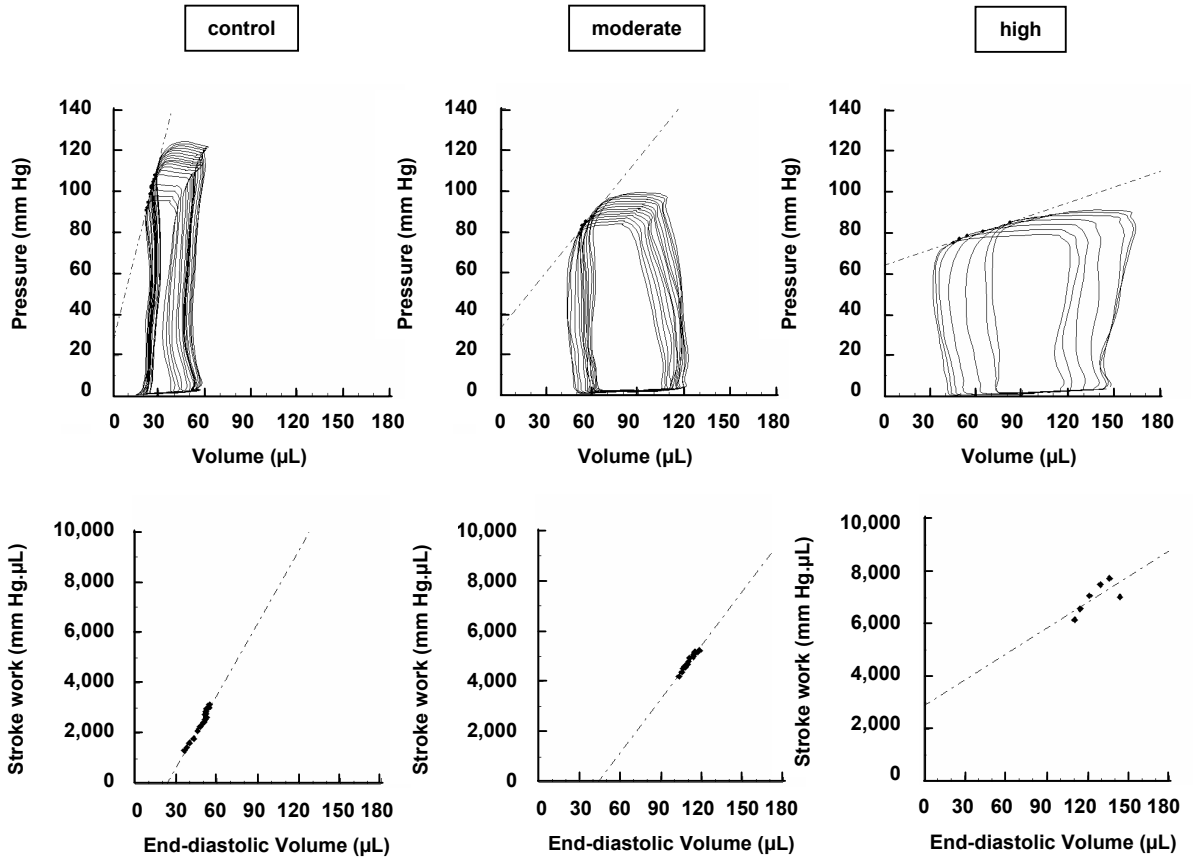


Figure 4.4. Pressure-volume (upper panels) and stroke work-volume (lower panels) relationships of the left ventricle in control (left), moderate (100 µg/kg/day, middle) and high dose rhIL-6 (250 µg/kg/day, right) in three representative animals. Pressure is expressed in mm Hg, volume in µL, and stroke work in mmHg.µL. The dashed line in the upper panels corresponds to end-systolic pressure-volume relation of the left ventricle. The slope of this line, termed Ees, denotes end-systolic elastance. In the lower panels the slope corresponds to preload recruitable stroke work, PRSW. Note dose-dependent decrease in Ees, increase in end-diastolic volume, and decrease in PRSW after IL-6 administration.

From the above mentioned parameters it is clear that despite the reduced contractility, cardiac output ($p<0.005$) increased due to larger stroke volumes combined with a reduced afterload (Table 4.2).

4.1.6 Correlations: muscle weight - cardiovascular functional parameters

Positive correlations were found between diaphragm weight - Ees and PRSW ($0.50<r<0.63$, $0.012<p<0.056$). Inverse correlations were present between diaphragm weight – ESV, EDV and SW ($-0.62<r<-0.51$, $0.013<p<0.052$). Similar relationships were present between the weight of the gastrocnemius, plantaris, soleus, lungs and heart, and body weight - haemodynamic variables.

4.1.7 Blood flow analysis

All measured organ blood flows, except for kidneys, tended to decrease after rhIL-6 treatment. This was also observed for the gastrocnemius (control: 0.12±0.05, moderate dose: 0.10±0.05, high dose: 0.08±0.02 mL/min/g). However, this tendency reached statistical significance only for the diaphragm (Figure 4.5) and jejunum (control: 1.89±0.51, moderate dose: 1.33±0.47, high dose: 1.10±0.24 mL/min/g; p=0.021).

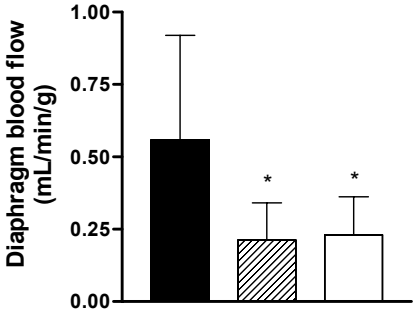


Figure 4.5. Diaphragm blood flow, expressed in mL/min/g, in control rats (solid bar) or rats treated with moderate (100 µg/kg/day, hatched bar) or high rhIL-6 doses (250 µg/kg/day, open bar).
*p<0.05 vs control

4.1.8 Heart histology

Microscopic examination of the right ventricular diastolic cavity dimension revealed significant dose-dependent increases in cross-sectional area when

compared with control rats (15.4±3.4 in controls vs 28.6±5.2 in moderate dose group and 31.9±8.1 μm^2 in high dose group, p<0.01) (Figure 4.6).

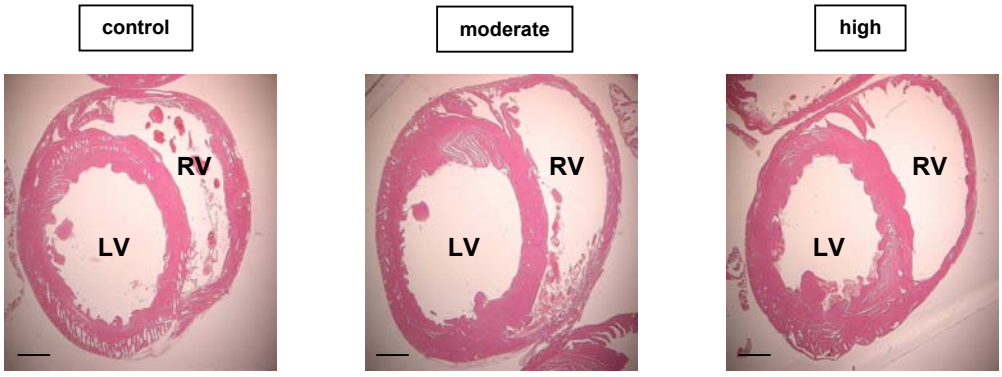


Figure 4.6. Heart H&E staining of a representative control (left), moderate (100 µg/kg/day, middle) and high (250 µg/kg/day, right) dose rhIL-6 animal. Panels correspond to 8x magnification, bar=875 µm. Note dose-dependent dilatation of right ventricular (RV) cavity area in both treated groups when expressed as a percentage of total cross-sectional area. Left ventricular (LV) dilatation did not occur.

4.1.9 Lung histology and water content

Left lung microscopic sections of treated animals showed congestion and interstitial edema whereas alveolar edema was only seen in some sections (Figure 4.7). Neither alveolar septa thickening nor focal edema were present in control rats. There were no signs of inflammatory infiltrates in any of the three groups.

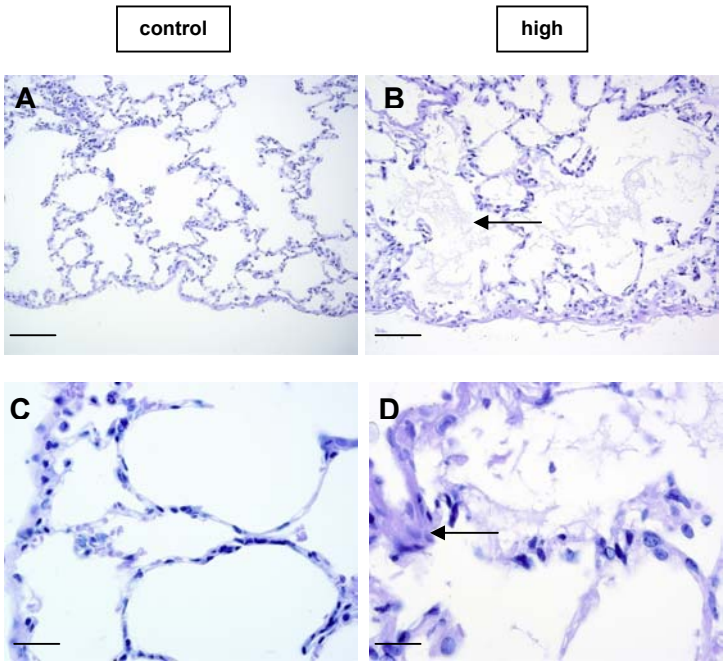


Figure 4.7. Left lung H&E staining of a representative control (left panels) and high dose rhIL-6 animal (250 μg/kg/day, right panels). Upper panels correspond to 200x magnification, bar=50 μm; lower panels to 650x magnification, bar=15 μm. Note alveolar edema, identified as pale eosinophilic fluid within groups of alveoli (arrow in B), and congestion or interstitial edema, marked by thickened septa engorged by red blood cells (arrow in D), in the micrographs of the high dose group. None of these characteristics were present in control rats.

Wet-to-dry ratio of the right lung was significantly higher in moderate (4.6±0.10) and high dose group animals (4.5±0.05) than in controls (4.2±0.13, $p<0.001$).

4.1.10 Food intake

Food intake decreased in all groups directly after pump implantation (control -26%, moderate dose -53%, high dose -45%; $p<0.001$). However, at day 1, food intake started to increase in all groups, still yielding a significantly lower food intake in both treated groups ($p<0.005$). Conversely, from day 5 on, food intake increased more in treated rats, so that at the end of treatment food intake was again similar between all groups (control: 26.10±7.21, moderate dose: 25.92±2.65, high dose: 22.88±2.68 g). (Figure 4.8)

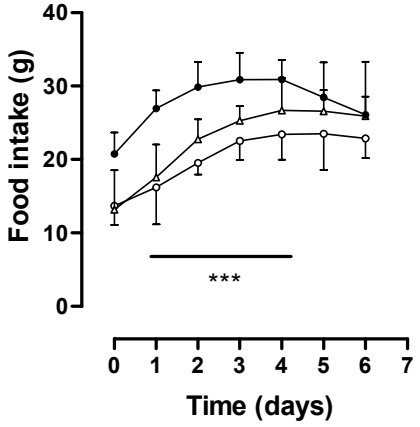


Figure 4.8. Daily food intake, expressed in g, in control rats (solid circles) and rats treated with moderate (100 µg/kg/day, open triangles) and high (250 µg/kg/day, open circles) doses of rhIL-6.
*** p<0.005 vs control

4.1.11 Activity level

Displacement distance was similar between treated and control rats, both during the day (control: 1,286±451, moderate dose: 1,063±414, high dose: 1,165±314 cm/hr) and during the night (control: 710±521, moderate dose: 537±363, high dose: 541±256 cm/hr).

4.2 *In vitro* experiments

Addition of 12 ng/mL of rhIL-6 to the tissue bath did not affect diaphragm *in vitro* P_t (366±75 vs 381±50 g/cm^2) or P_o (1,965±457 vs 1,975±165 g/cm^2), P_t/P_o (0.19±0.03 vs 0.19±0.01), TPT (23±1 vs 21±2 ms) and 1/2 RT (22±2 vs 27±5 ms) when compared to control strips. Also during the force-frequency curve and the low frequency fatigue run, generated forces were similar in both groups.

CHAPTER 5: EFFECTS OF IL-8 ON SKELETAL MUSCLE FUNCTION

In this section, we wanted to examine to effects of IL-8 on skeletal muscle function using an animal model.

Rats were divided in 5 groups receiving PBS (controls) or rhIL-8 at different concentrations (25 – 50 – 100 – 250 µg/kg/day) during 7 days. At the end of treatment, body, muscle and organ masses were determined, contractile properties of the diaphragm were measured, and diaphragm and gastrocnemius morphometry was performed. Plasma levels of the subcutaneously administered rhIL-8 were also determined.

5.1 Body and tissue weight

Body weight was similar between controls and experimental groups both at the time of pump implantation and at the time of dissection, as were all muscle and organ masses (Table 5.1), except for the scalenus medius that was significantly increased by 36% in rats treated with 100 µg/kg/day.

	control	25µg/kg/day	50µg/kg/day	100µg/kg/day	250µg/kg/day
body weight (g)					
at the beginning of exp I	364±29	366±25	368±31		
at the end of exp I	400±25	404±19	406±26		
at the beginning of exp II	409±13			405±19	404±17
at the end of exp II	433±14			435±11	425±16
respiratory muscle weight (g)					
diaphragm exp I	0.570±0.046	0.592±0.060	0.589±0.053		
exp II	0.576±0.033			0.607±0.053	0.589±0.033
scalenus medius exp I	0.561±0.033	0.558±0.092	0.560±0.078		
exp II	0.499±0.034			0.681±0.075*	0.587±0.128
peripheral muscle weight (g)					
gastrocnemius exp I	1.972±0.238	1.977±0.194	1.992±0.175		
exp II	2.156±0.087			2.121±0.070	2.134±0.236
soleus exp I	0.204±0.039	0.212±0.029	0.201±0.027		
exp II	0.221±0.018			0.245±0.022	0.229±0.019
plantaris exp I	0.391±0.075	0.394±0.039	0.393±0.052		
exp II	0.402±0.024			0.414±0.030	0.406±0.047
EDL exp I	0.186±0.021	0.194±0.015	0.193±0.023		
exp II	0.201±0.017			0.208±0.016	0.202±0.016
organ weight (g)					
heart	1.177±0.057	1.118±0.067	1.183±0.080	1.225±0.028	1.166±0.115
liver	15.28±1.75	15.09±0.96	15.81±2.13	15.36±1.38	13.89±1.07

Table 5.1. Body and tissue masses in rats treated with 25-50-100 or 250 µg/kg/day of rhIL-8, compared to controls. EDL indicates extensor digitorum longus, exp I = first experiment, exp II = second experiment. Duncan post-hoc: *p<0.05 vs control.

5.2 Diaphragm *in vitro* contractile properties

P_t and P_o were similar among all groups (pooled values of 382±92 and 1,993±330 g/cm^2, respectively), as were P_t/P_o (0.19±0.02), TPT (20±3 ms) and 1/2 RT (19±2 ms).

Moreover, no differences in diaphragm force during the force-frequency curve and in force decline during the low frequency fatigue run were observed (Figure 5.1).

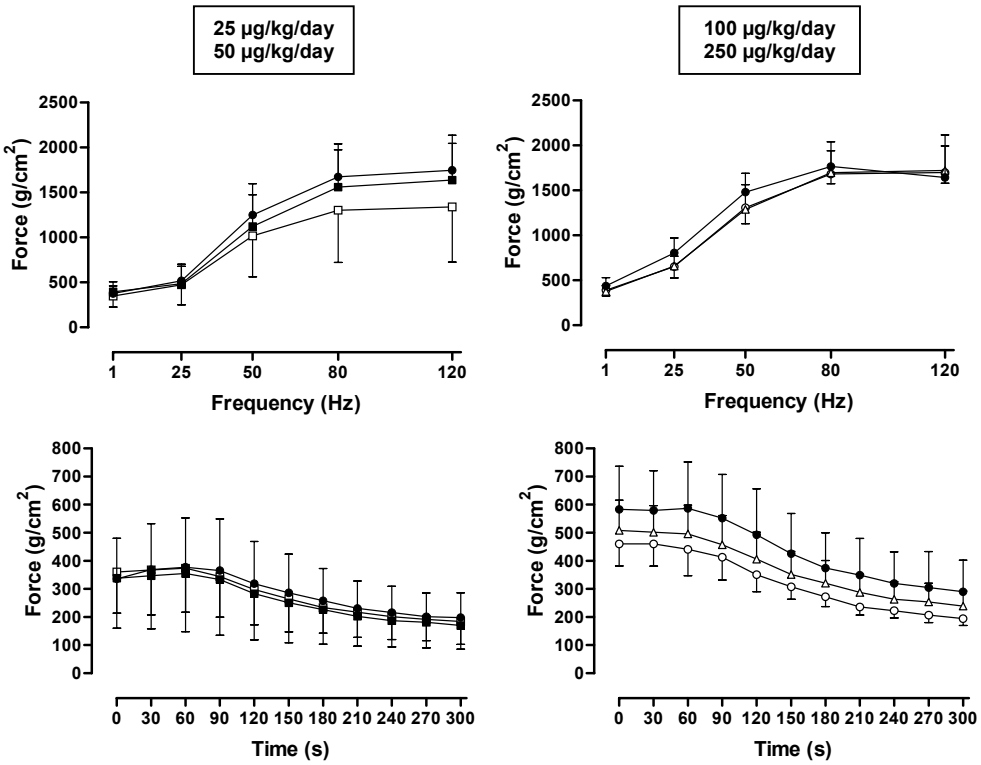


Figure 5.1. Diaphragm force-frequency (upper panels) – fatigue (lower panels) data in rats treated with 25 µg/kg/day (solid squares), 50 µg/kg/day (open squares), 100 µg/kg/day (open triangles) and 250 µg/kg/day of rhIL-8 (open circles) compared with controls (solid circles). Forces are expressed in g/cm^2, frequency in Hz, and time in s.

5.3 Morphometry of diaphragm and gastrocnemius

No changes in diaphragm (Figure 5.2) and gastrocnemius (Figure 5.3) fiber dimensions and RIS were observed whatever the dose.

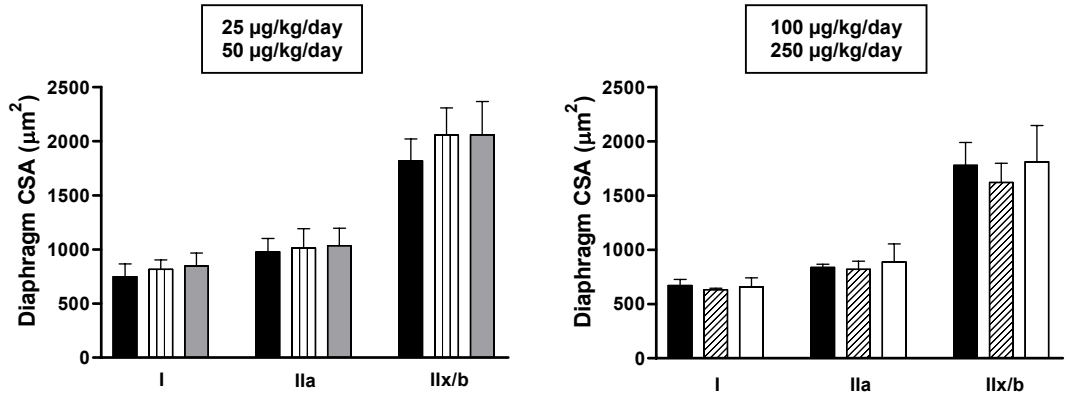


Figure 5.2. CSA of diaphragm fiber type I, IIa and IIx/b in animals treated with 25 µg/kg/day (vertical hatched bars), 50 µg/kg/day (gray bars), 100 µg/kg/day (hatched bars) and 250 µg/kg/day of rhIL-8 (open bars) compared with controls (solid bars). CSA is expressed in μm^2.

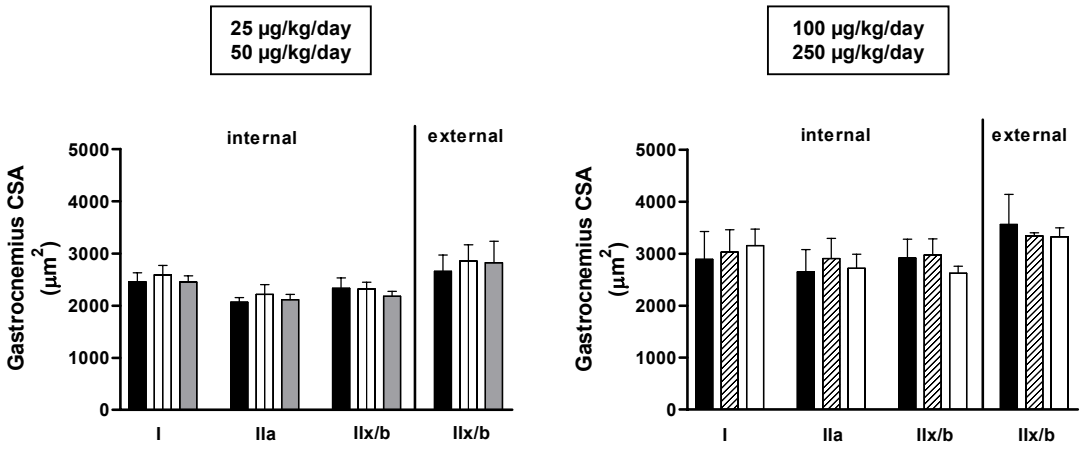


Figure 5.3. CSA of gastrocnemius internal fiber type I, IIa, IIx/b and external fiber type IIx/b in animals treated with 25 µg/kg/day (vertical hatched bars), 50 µg/kg/day (gray bars), 100 µg/kg/day (hatched bars) and 250 µg/kg/day of rhIL-8 (open bars) compared with controls (solid bars). CSA is expressed in μm^2.

Moreover, fiber proportions of both muscles remained unaffected by rhIL-8 treatment (Table 5.2).

	diaphragm			gastrocnemius		
	I	IIa	IIx/b	I	IIa	IIx/b
control	36±4	32±6	32±3	45±11	25±4	30±10
25 µg/kg/day	34±2	36±6	30±7	45±5	31±3	24±5
50 µg/kg/day	35±4	31±5	34±5	50±8	24±9	26±3
control	39±3	28±3	33±2	48±14	19±4	33±12
100 µg/kg/day	36±5	28±4	36±3	51±3	23±6	26±7
250 µg/kg/day	37±3	28±2	35±3	56±4	20±5	24±5

Table 5.2. Diaphragm and gastrocnemius fiber proportions, expressed as a percentage of total number of fibers (%).

5.4 Plasma levels

RhIL-8 plasma levels averaged 369±123, 460±111, 2472±1404 and 9445±6363 pg/mL after treatment with 25-50-100-250 µg/kg/day of rhIL-8, respectively.

Albumin plasma concentrations did not differ between controls and rats treated with different doses of rhIL-8 (average value of 35±1 g/L).

5.5 Lung histology and water content

No signs of inflammation, congestion, and interstitial or alveolar edema were seen on H&E sections.

Moreover, wet-to-dry ratio was similar in all groups (pooled value of 4.6±0.2).

CHAPTER 6: CLINICAL RELEVANCE OF PERI-OPERATIVE CYTOKINE LEVELS IN HEART VALVE SURGERY

In this section, we wanted to explore the range of cytokine levels, with particular interest in IL-6, in a clinical setting of 22 patients undergoing hart valve surgery with the use of extracorporeal circulation. Furthermore, we wanted to examine whether elevated cytokine levels might be predictive for patient's clinical outcome.

Blood was sampled at 4 different moments (preoperatively, at the end of surgery, and 12 and 24 hours later). Haemodynamis, and need for inotropic, vasopressor or vasodilator support were also determined at these time points.

6.1 Clinical variables

No mortality was seen in this series. Median [range] for age and weight was 68 years [16-81] and 72 kg [40-100], respectively. Male/female ratio was 9/13.

Duration of operation was 250 min [185-410], accompanied by an extracorporeal circulation of 118 min [44-180] and an aortic cross-clamp time of 78 min [19-136]. Patients were extubated after 20 hrs [11-720]. Median intensive care stay was 49 hrs [20-1,870].

Inotropics (dopamine - DOPA and dobutamine - DOB combined), vasopressor (norepinephrine - NA) and vasodilator (phosphodiesterase inhibitors – PDE inhibitors) drugs were administered as described in Table 6.1.

	0 hr	+ 12 hrs	+ 24 hrs
DOPA + DOB	17 patients	19 patients	2 patients
	< 4 µg/kg/day	< 4 µg/kg/day	> 4 µg/kg/day
NA	8 patients	11 patients	5 patients
	0.2 µg/kg/min	0.25 µg/kg/min	0.2 µg/kg/min
PDE-inhibitors	4 patients	/	/
	< 25 mg		

Table 6.1. Inotropics, vasopressor and vasodilator support administered at the end of surgery, and 12 and 24 hrs later. DOPA = dopamine, DOB = dobutamine, NA = norepinephrine, PDE-inhibitors = phosphodiesterase inhibitors. 0 hr = at the end of surgery, + 12 hrs = 12 hrs after the end of surgery, and + 24 hrs = 24 hrs after the end of operation.

6.2 Haemodynamic variables

The central venous pressure (CVP) and left atrial pressure (LAP) remained stable during the whole observation period, as were the mean pulmonary artery pressure (PAP) and systemic arterial blood pressure (ABP). Pulmonary vascular resistance (PVR) was also relatively stable. Heart rate (HR) increased postoperatively, remained elevated 12 hrs later, and returned to baseline levels after 24 hrs. Cardiac output (CO) increased postoperatively and remained elevated up to 24 hrs after surgery. Conversely, systemic vascular resistance (SVR) decreased postoperatively and remained low. (Table 6.2)

	preoperative	0 hr	+ 12 hrs	+ 24 hrs
HR (bpm)	68 [50-105]	80 [68-117]*	85 [72-106]*	77 [60-102]$^{|}$
CO (L/min)	3.8 [2.2-5.8]	5.4 [2.8-8.2]*	6.1 [2.6-7.8]*	5.3 [2.6-7.0]*
CVP (mm Hg)	10 [1-16]	11 [6-17]	10 [5-15]	12 [7-16]
PAP (mm Hg)	22 [13-66]	22 [15-47]	24 [17-36]	24 [17-38]
PVR (dyne.s/cm^5)	149 [54-489]	141 [21-446]	143 [12-315]	188 [12-412]
LAP (mm Hg)	14 [6-44]	14 [3-22]	13 [8-19]	14 [6-20]
ABP (mm Hg)	71 [52-98]	64 [51-94]	73 [42-113]	77 [61-102]
SVR (dyne.s/cm^5)	1312 [728-2800]	896 [496-1360]*	848 [464-1904]*	984 [680-2248]$^{*‖}$

Table 6.2. Haemodynamic variables obtained at the end of surgery, and 12 and 24 hrs later.
0 hr = at the end of surgery, + 12 hrs = 12 hrs after the end of surgery, + 24 hrs = 24 hrs after the end of surgery.
Sign post-hoc: $^{*}p<0.05$ vs preoperative; $^{‖}p<0.05$ vs 0 hr; $^{|}p<0.05$ vs + 12 hrs.

6.3 Cytokine and troponin-I plasma levels

Cytokine plasma levels were significantly higher at the end of operation compared with preoperative levels. After 12 hrs, IL-1β and IL-8 returned to preoperative levels, while IL-6, IL-10 and both sTNF-R1 and 2 (sTNF-Rs) remained elevated, and IL-11, IL-17 and TNF-α fell below preoperative values. Moreover, 12 hrs after surgery, cytokine levels were lower than immediate postoperative levels, except for sTNF-R2. (Table 6.3, Figure 6.1)

Troponin-I plasma levels were 5.04 [1.91-18.06] and 5.18 [1.37-31.14] µg/L 12 and 24 hrs after surgery respectively.

	preoperative	0 hr	+ 12 hrs
IL-6	3 [0-16]	133 [19-3080]***	59 [10-242]*** $
IL-1β	6 [0-25]	68 [27-199]***	2 [0-28] $
IL-8	1 [0-43]	294 [53-2340]***	1 [0-23] $
IL-10	1 [0-88]	85 [15-532]***	12 [5-184]*** $
IL-11	8 [0-52]	350 [199-1792]***	0 [0-25]*** $
IL-17	107 [0-681]	727 [373-1968]***	31 [0-296]*** $
TNF-α	73 [0-232]	952 [378-3163]***	26 [0-73]*** $
sTNF-R1	520 [218-2331]	2768 [1128-6310]***	1313 [523-3840]*** $
sTNF-R2	2066 [760-10739]	5382 [2230-17640]***	4737 [1581-13461]***

Table 6.3. Plasma cytokine levels measured preoperatively, at the end of surgery and 12 hrs later. 0 = below detection limit, 0 hr = at the end of surgery, + 12 hrs = 12 hrs after the end of surgery.
For all cytokines, ANOVA $p \leq 0.01$. Sign test with Bonferroni correction: $^{***}p<0.005$ vs preoperative, $^{\$}p<0.005$ vs 0 hr.

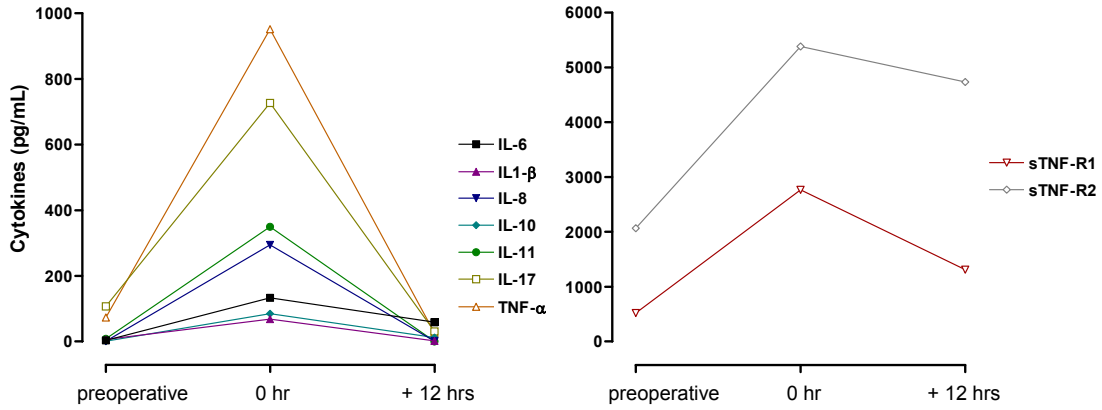


Figure 6.1. IL-6, IL-1β, IL-8, IL-10, IL-11, IL-17, and TNF-α plasma levels (left panel), and both sTNF-R plasma levels (right panel) determined preoperatively, at the end of surgery and 12 hrs later. Plasma cytokine levels are expressed in pg/mL. For statistics, see Table 6.3.
0 hr = at the end of surgery, + 12 hrs = 12 hrs after the end of surgery.

6.4 Correlates of preoperative cytokine plasma levels

Preoperative IL-10 levels were positively correlated with PVR for all time points after surgery (r=0.611, p=0.004, and r=0.667, p=0.001, and r=0.667, p=0.001 at the end of operation, and 12 and 24 hrs later, respectively). Furthermore, it correlated

positively with the need for inotropic support immediately after surgery (r=0.613, p=0.002). (Table 6.4)

Preoperative levels of sTNF-R1 were positively correlated with the need for vasopressor support 12 hrs after surgery (r=0.610, p=0.003) while preoperative sTNF-R2 levels were positively correlated with PVR 24 hrs postoperatively (r=0.559, p=0.010). (Table 6.4)

Preoperative IL-6 levels were positively correlated with the need for inotropic support 12 hrs after the end of surgery (r=0.515, p=0.014). Furthermore, IL-6 correlated positively with PVR 12 hrs (r=0.522, p=0.018) and 24 hrs (r=0.532, p=0.016) after surgery. (Table 6.5)

Preoperative plasma cytokine levels were always positively correlated ($p \leq 0.01$). The preoperative levels of IL-6 were correlated with the preoperative levels of IL-10 and sTNF-R1. The preoperative levels of IL-1β were correlated with these of IL-11 and TNF-α. IL8 was furthermore correlated with IL-11, IL-17 and TNF-α, and IL-11 with IL-17 and TNF-α. IL-17 was in turn correlated with TNF-α. Finally, the preoperative levels of sTNF-R1 were correlated with those of sTNF-R2.

6.5 Correlates of cytokine plasma levels at the end of surgery

IL-6 levels at the end of operation were positively correlated with norepinephrine dose administered 12 hrs (r=0.549, p=0.008, Table 6.4) and 24 hrs (r=0.505, p=0.016) after surgery (Tables 6.4-6.5).

	PVR_0	$inotr_0$	PVR_{12}	CVP_{12}	$vasopr_{12}$	PVR_{24}	CO_{24}
preoperative							
IL-10	0.611	0.613	0.667			0.667	
sTNF-R1					0.610		
sTNF-R2						0.559	
at the end of surgery							
IL-6					0.549		
12 hrs after the end of surgery							
IL-10							-0.702
IL-11				0.542	0.540		
IL-1β				0.538			

Table 6.4. Spearman correlation coefficients between plasma cytokine levels and haemodynamic variables. Plasma cytokines were determined preoperatively, at the end of surgery and 12 hrs later while haemodynamic variables were also determined 24 hrs later. Always $p \leq 0.01$.
PVR_0 = PVR at the end of surgery, $inotr_0$ = inotropic support at the end of surgery, PVR_{12} = PVR 12 hrs after the end of surgery, CVP_{12} = CVP 12 hrs after the end of surgery, $vasopr_{12}$ = vasopressor support 12 hrs after the end of surgery, PVR_{24} = PVR 24 hrs after the end of surgery, CO_{24} = CO 24 hrs after the end of surgery.

	$inotr_{12}$	PVR_{12}	$vasopr_{12}$	SVR_{12}	CO_{12}	HR_{24}	PVR_{24}	$vasopr_{24}$
preoperative								
IL-6	0.515	0.522					0.532	
at the end of surgery								
IL-6			0.549					0.505
12 hrs after the end of surgery								
IL-6				-0.538	0.447	0.570	0.474	

Table 6.5. Spearman correlation coefficients between plasma IL-6 levels and haemodynamic variables. IL-6 was determined preoperatively, at the end of surgery and 12 hrs later while haemodynamic variables were also determined 24 hrs later. Always $p<0.05$.
$inotr_{12}$ = inotropic support 12 hrs after the end of surgery, PVR_{12} = PVR 12 hrs after the end of surgery, $vasopr_{12}$ = vasopressor support 12 hrs after the end of surgery, SVR_{12} = SVR 12 hrs after the end of surgery, CO_{12} = CO 12 hrs after the end of surgery, HR_{24} = HR 24 hrs after the end of surgery, PVR_{24} = PVR 24 hrs after the end of surgery, $vasopr_{24}$ = vasopressor support 24 hrs after the end of surgery.

Plasma cytokine levels were always positively correlated. The IL-6 levels at the end of the operation were highly correlated with sTNF-R1 and sTNF-R2 levels. The

immediately postoperative levels of IL-1β were correlated with IL-8, IL-11, IL-17, TNF-α, and sTNF-R1 at that time. Further correlations existed between IL-8 and TNF-α, sTNF-R1, and sTNF-R2. IL-10 and sTNF-R1 were furthermore correlated with sTNF-R2, IL-11 with IL-7, TNF-α, and sTNF-R1; and IL-17 in turn with TNF-α.

6.6 Correlates of cytokine and troponin-I plasma levels 12 hrs after the end of surgery

Twelve hrs after the operation, IL-1β was positively correlated with CVP (r=0.538, p=0.010), while IL-11 correlated positively with CVP and norepinephrine use at that time point (r=0.542, p=0.009 and r=0.540, p=0.009, respectively). (Table 6.4)

IL-10 12 hrs after the operation was inversely correlated with CO 24 hrs after surgery (r=-0.702, p=0.001). (Table 6.4)

IL-6 levels 12 hrs after the end of surgery were positively correlated with CO at that time (r=0.447, p=0.048) and with HR (r=0.57, p=0.016) and PVR (r=0.474, p=0.035) 12 hrs later. It was furthermore inversely correlated with SVR (r=-0.538, p=0.014) 12 hrs after surgery. (Table 6.5)

Plasma cytokine levels were always positively correlated. IL-1β was only correlated with IL-11. IL8 was correlated with IL-17, TNF-α, sTNF-R1, and sTNF-R2 at the same time point. IL-17 was correlated with TNF-α and sTNF-R2, TNF-α with sTNF-R2, and sTNF-R1 with sTNF-R2 at that time.

As could be expected, there was a positive relationship between the aortic cross-clamp time and troponine-I levels 12 hrs after surgery (r=0.570, p=0.006).

CHAPTER 7: GENERAL DISCUSSION

7.1 Effects of IL-6 on skeletal muscle function

The data obtained in the present study showed that 7 days administration of moderate (100 µg/kg/day) and high (250 µg/kg/day) doses of rhIL-6 to male Wistar rats resulted in a dose-dependent respiratory and peripheral skeletal muscle atrophy without alterations in diaphragm *in vitro* contractile properties. Both doses also caused a dose-dependent myocardial contractile deterioration, as was evident from alterations in invasive cardiovascular functional parameters, increased lung wet-to-dry ratios and lung microscopic examination. It appears likely that the observed diaphragm and peripheral skeletal muscle atrophy predominantly resulted from blood flow redistribution, and not from a direct effect of rhIL-6 on skeletal muscle function, or from alterations in food intake and activity level. (Tabel 7.1)

SYSTEMIC EFFECTS OF IL-6	**100 µg/kg/day**	**250 µg/kg/day**
• **diaphragm weight**	↓ (NS)	↓
• **gastrocnemius weight**		↓
• **diaphragm fiber cross-sectional area**		I, IIx/b: ↓ (NS) IIa: ↓
• **gastrocnemius fiber cross-sectional area**		I: ↓ (NS) IIa: ↓ (NS)
• **IL-6 plasma levels**	765 pg/mL	12 ng/mL
• **high-output failure**	↑	↑↑
• **diaphragm blood flow**	↓	↓

Table 7.1. Overview of the most important changes observed after 7 days of treatment with rhIL-6. NS = non-significant. For all groups, comparison vs controls.

To mimic the condition of chronically elevated systemic cytokine concentrations as found in COPD patients[14;20;22;24;25;203], mini-osmotic pumps were implanted subcutaneously in rats to deliver continuous infusions of rhIL-6. Despite the low

amino acid homology between human IL-6 and its murine or rat counterpart (± 42% homology at the protein level)[204], rhIL-6 was administered to rats as it has been shown to act with the same biological activity on murine or rat cells as murine or rat IL-6 itself[205]. Moreover, numerous studies have shown that rhIL-6 was active in rats.

All these changes were observed with clinically relevant rhIL-6 plasma levels. Indeed, in rats treated with moderate doses of rhIL-6, plasma levels averaged 765 pg/mL, while those in rats treated with high rhIL-6 doses averaged 12 ng/mL. Both values are in the range of individual IL-6 plasma levels observed in patients suffering from sepsis, acute respiratory distress syndrome, and pneumonia[30;172]. Furthermore, all these illnesses are known to be accompanied by clinically significant skeletal muscle weakness[30;172]. However, due to the fact that rats are less susceptible to IL-6 than humans, as demonstrated in human toxicity experiments[206], the clinical relevance of IL-6 in inducing skeletal muscle weakness could not be excluded for patients with COPD.

Although the *in vitro* contractile properties of the diaphragm remained unchanged, a significant diaphragm type II atrophy was observed in rats treated with the high rhIL-6 dose. This apparent discrepancy might be related to the fact that contractility was expressed in g/cm^2, meaning that all generated forces were corrected for potential reductions in fiber cross-sectional area. In particular, this indicates that there was in essence less muscle but the quality of the remaining muscle contractile apparatus was preserved, therefore excluding myopathy. Furthermore, no changes in diaphragm fiber proportions were observed which is compatible with the unchanged contractile properties. For the gastrocnemius, solely a tendency for type I and IIa fibers to decrease was observed in rats treated with the high rhIL-6 dose, without any changes in fiber type proportions. All the above-mentioned results were

in accordance with decreases in the weight of both the diaphragm and gastrocnemius of rats treated with the high rhIL-6 dose, and furthermore with decreases in body weight in high dose group animals. These findings are fully in line with the observed decrease in the weight of the gastrocnemius muscle of IL-6 transgenic mice[135-137], and also with decreases in plasma albumin levels as observed in the present study, as albumin can be seen as a measure for total protein content.

In this study, heart weight increased significantly in rats treated with the moderate rhIL-6 dose, while it was unchanged in rats treated with the high rhIL-6 dose, suggesting myocardial hypertrophy and dilatation in moderate and high dose group animals, respectively. The deleterious effects of IL-6 on myocardial function have already been well documented *in vitro* and in transgenic mice. Indeed, reversible concentration-dependent negative inotropic effects, and depression of the amplitude of cell contraction and of Ca^{2+} transients have been reported after minutes of incubation with IL-6, both in isolated hamster papillary muscles[193] and in cultured chick embryo or guinea-pig ventricular myocytes[188;189], respectively. IL-6 has also been shown to downregulate SERCA2 protein content to about 60% in neonatal rat ventricular myocytes after 2 days of incubation[207], while reduced RNA expression of both cardiac MHC isoforms and a loss in cardiac actin has already been reported in cultured rat cardiac myocytes after treatment for 24 hours[194]. Moreover, IL-6 double-transgenic mice overexpressing both IL-6 and soluble IL-6R are known to suffer from concentric myocyte hypertrophy and decreases in left ventricular volume[187]. Although *in vivo* experiments concerning the effects of IL-6 administration on myocardial function are missing, *in vivo* experiments with cardiotrophin-1, a cytokine belonging to the same family as IL-6[208], showed that increases in ventricular-to-body weight ratio associated with reduced mean arterial pressure and systemic vascular

resistance occurred after daily injections for 14 days[209;210]. This cytokine has also been shown to induce hypertrophic responses in neonatal rat ventricular myocytes after 2 days of treatment[208].

As the increase in heart weight in the present study might implicate a detrimental effect of IL-6 on myocardial performance, invasive haemodynamic measurements were performed. The pattern of *in vivo* haemodynamic alterations after 7 days of rhIL-6 treatment in the present study is remarkable. Indeed, a dose-dependent heart dilatation was observed as was evident from increases in end-diastolic volume, leading to functioning at lower end-systolic pressures. Significantly higher stroke volumes were compatible with an unaltered ejection fraction. Moreover, due to unchanged heart rates, cardiac output increased dose-dependently. In contrast, both load-independent contractility parameters, preload recruitable stroke work and end-systolic elastance decreased in a dose-dependent fashion. The increase in cardiac output, accompanied by a decreased ventricular contractility, is somewhat controversial. However, due to the fact that peripheral resistance decreased, stroke volume and cardiac output could increase despite the reduced cardiac contractility.

All these haemodynamic changes are not in contradiction with myocyte hypertrophy and decreases in left ventricular volume found in IL-6-double-transgenic mice, where human IL-6 plasma levels averaged 0.1-5 ng/mL[187], which is less than the concentration observed in our high dose group rats (12.1 ng/mL). This low IL-6 concentration might rather produce ventricular hypertrophy while higher concentrations as seen in the present study might further affect the myocardium and produce dilatation. However, transgenic models are not fully comparable with the model used in our study due to overexpression during both pre- and postnatal development, which certainly influences chronic morphological findings such as

ventricular hypertrophy and remodeling. Furthermore, cardiotrophin-1 administration, at lower doses than the doses of rhIL-6 used in the present study, also induced myocyte hypertrophy[209], decreases in mean arterial pressure and systemic vascular resistance without changes in left ventricular + dP/dt[210]. This is fully in line with the results obtained in the present study.

Congestion and interstitial or alveolar edema as observed in histological lung slices furthermore confirmed the presence of myocardial dysfunction after rhIL-6 treatment. Edema was further confirmed by an increased lung wet-to-dry ratio, however without any signs of inflammatory cell infiltrates as has been deduced from the histological lung slices. The edema formation is likely due to the increased end-diastolic pressure after rhIL-6 treatment. However, increases in end-diastolic pressure were not statistically different between control rats and both experimentally treated groups, most likely due to the large standard deviation observed in the present study.

The above-mentioned type of myocardial dysfunction is known in the literature as high-output myocardial failure, and is a frequently occurring phenomenon in patients suffering from septic shock. Indeed, the commonest effect of septic shock on the cardiovascular system is a haemodynamic profile characterized by an elevated cardiac index and decreased systemic vascular resistance[211]. These two factors were reflected in the present study by an increase in cardiac output and by a decrease in peripheral resistance. Furthermore, high IL-6 plasma values have been shown to act as a predictor of mortality in these patients[212]. Also in patients suffering from left ventricular dysfunction[170] or after reperfusion of the ischemic heart in patients undergoing cardiopulmonary bypass[213], systemic IL-6 levels are known to be elevated. This may consequently lead to further deterioration of cardiac function as

IL-6 is known to be an independent predictor for worsening of heart failure in patients with end-stage heart failure[181]. From this point of view, anti-IL-6 strategies might be useful in patients with sepsis or in patients undergoing cardiac surgery to improve clinical outcome. This has already been shown by the beneficial effects of TNF-α and IL-6 removal through haemofiltration in children undergoing cardiopulmonary bypass[214].

There is abundant evidence in the literature that myocardial failure induces ventilatory and peripheral skeletal muscle atrophy. However, in studies concurrently addressing respiratory and peripheral muscle strength in heart failure patients, the impairment in respiratory muscles' contractility was proportionally greater[215-217] or even existed in the absence of peripheral skeletal muscle dysfunction[216]. Ventricular dysfunction induced by experimental coronary ligation in rats confirmed the above mentioned findings, i.e. moderate ventricular dysfunction affected the diaphragm only whereas severe heart failure also affected other respiratory and peripheral muscles[178].

It appears plausible from the present study that the observed skeletal muscle atrophy resulted from the cardiac failure induced by rhIL-6 as the pattern of muscle atrophy observed in the present study is similar to the pattern observed in clinical studies of myocardial failure[218;219]. Furthermore, systolic ventricular dysfunction in rats in which the alterations in haemodynamic variables resulted in a similar pattern of heart failure as in the present study, led to an identical pattern of skeletal muscle atrophy, without changes in diaphragm *in vitro* contractile properties[178]. Finally, in the present study, haemodynamic functional parameters correlated highly with diaphragm weight, and to a lesser extent with the weight of the gastrocnemius.

Although paradoxically at first sight, the increase in cardiac output was associated with reductions in diaphragm blood flow in both treated groups. In addition, decreases in systolic arterial pressure as observed in the present study are known to decrease diaphragmatic blood flow[220]. This latter decrease is likely responsible for the observed diaphragm atrophy. A similar trend was present for blood flow to peripheral muscles although less pronounced. This is in keeping with the fact that only a tendency to atrophy was observed in the gastrocnemius. Nevertheless, since blood flow reductions were also observed in all measured organs except kidneys and both left and right ventricles, increases in other tissues are expected. The exact mechanism for blood flow decreases particularly in the diaphragm is not known. A high autoregulatory mechanism such as found in the renal, cerebral and coronary circulations is likely lacking in the diaphragm. Hence the decreases in diaphragm blood flow are largely related to decreases in diaphragm perfusion pressure. This is in accordance with the earlier mentioned systemic vasodilation as organ perfusion pressure is characterized as the difference between arterial and venous organ pressure. It might furthermore be possible that some kind of regional arterio-venous shunting process is involved, inhibiting blood flow through the capillaries of the diaphragm. This hypothesis might be strengthened by the fact that decreases in blood flow to skeletal muscles, cutaneous regions and jejunum were found after experimental induction of an abdominal aortocaval shunt in rats, whereas blood flow to the cerebral, coronary and renal beds was protected[221]. However, it should be kept in mind that arterio-venous shunts itself are known to increase cardiac output[222] and might therefore be the primary cause of the pattern of high-output failure observed in the present study.

Attention must be paid to the fact that diaphragm blood flow decreased equally in both treated groups, while only a dose-dependent atrophic pattern was observed after rhIL-6 treatment. First, it has to be mentioned that it is not known whether a linear relation exists between diaphragm blood flow and diaphragm fiber atrophy. Second, blood flow was only determined after 7 days of treatment and this time point might not be fully representative. Indeed, it is likely that blood flow reductions occurred at an earlier time point in animals treated with high rhIL-6 doses when compared to animals treated with moderate rhIL-6 doses, explaining the significant atrophy and the tendency to atrophy in high and moderate dose group animals, respectively.

Other factors might also be implicated in the observed skeletal muscle atrophy but probably contributed to a lesser extent. Indeed, short-term nutritional deprivation as occurring immediately after pump implantation for 4 consecutive days, would be expected to result in a selective type IIx/b atrophy in the diaphragm[223], which is in contrast with the more generalized atrophic pattern observed in the present study. Furthermore, deconditioning was unlikely to be responsible as well, as activity levels were similar between all groups. A direct effect of rhIL-6 on diaphragm performance could also be ruled out as no changes in diaphragmatic contractility were observed after *in vitro* rhIL-6 administration when compared to controls. This is in agreement with previous *in vitro* experiments on soleus or EDL muscles reporting no protein breakdown after IL-6 incubation for several hours[138;145]. Conversely, skeletal muscle insulin resistance could not be ruled out in our study and might have somewhat contributed to the observed skeletal muscle atrophy, as it is known that IL-6 administration to mice resulted in hepatic insulin resistance by inhibiting the insulin-dependent insulin receptor signal transduction at serum concentrations of 112 pg/mL.

However, at this concentration it did not affect the signal transduction pathway in skeletal muscles[169]. Finally, endogenous rat IL-6, which might be activated by the subcutaneous administered rhIL-6, and circulating IGF-I could also be ruled out from contributing to the observed skeletal muscle atrophy as plasma values did not differ between controls and experimentally treated groups.

7.2 Effects of IL-8 on skeletal muscle function

The present study was the first to examine the effects of IL-8 on skeletal muscle function and showed that 7 days administration of low or high doses of rhIL-8 to male Wistar rats did not affect body, organ or muscle weight, except for the scalenus medius. Moreover, *in vitro* diaphragmatic contractile properties, and diaphragm and gastrocnemius fiber dimensions and proportions remained unchanged.

As for the study with IL-6, mini-osmotic pumps delivering IL-8 continously were used to mimic the chronic situation of elevated cytokine levels seen in COPD patients[14;20;22;24;25;203]. RhIL-8 was chosen to administer to rats knowing that the rodent IL-8 receptor has a 71% homology with the human IL-8 type B receptor[224]. Moreover, previous *in vivo* studies reported proliferation of rats ovarian follicle cells[225] and mobilization of mice myeloid progenitor and stem cells into the circulation[226] after rhIL-8 administration, thus demonstrating its activity in rodents. As humans do not possess keratinocyte-derived chemokine (KC) or macrophage inflammatory protein (MIP)-2, we chose to use rhIL-8 in order to assess the extent to which human IL-8 could affect skeletal muscle, keeping in mind the data previously obtained in COPD patients[29;152].

The rhIL-8 plasma levels yielded in the present study were however clinically relevant since rats treated with 25 and 50 µg/kg/day reached plasma levels of about

400 pg/mL, which are similar to those observed in some COPD patients[20]. Nevertheless, as it has been shown in *in vitro* neutrophil chemotaxis experiments that rats are less susceptible to rhIL-8 than to KC or MIP-2[227], two higher doses were tested. However, no deleterious effects on skeletal muscle function were observed in the present study even with the high dose yielding high plasma levels of rhIL-8. This likely suggests that the correlations between IL-8 plasma levels and peripheral muscle function seen in COPD and in meningococcal disease, with circulating IL-8 levels in the same range as those observed in the present study, did not reflect a causal relation, but were a mere coincidental finding[29;151]. In this context, it is moreover worthwhile to mention that anti-IL-8 treatment of stable COPD patients reduced their severity of dyspnea, while it did not alter lung function parameters or 6-min walking distance[152]. Together with our findings, this likely indicates that a reduced amount of active IL-8 had no effect on improving respiratory and peripheral skeletal muscle function.

Surprisingly, an increased weight of the scalenus medius was found in the present study after 7 days of rhIL-8 administration. This unexpected finding might underline the effectiveness of rhIL-8 administration to rats, which is in line with the previous mentioned studies on rats ovarian follicle cells[225] and mice myeloid progenitor and stem cells[226].

7.3 Clinical relevance of peri-operative cytokine levels in heart valve surgery

In the present setting, IL-6, TNF-α and IL-10 seemed to be the most relevant circulating cytokines to predict the early postoperative haemodynamic status after heart valve surgery using extracorporeal circulation. Indeed, although precaution is needed to blame cytokines as the causal factors, the present study showed that both

preoperative IL-10 and IL-6 levels might be predictive for a postoperative decrease in myocardial inotropy as well as for pulmonary vasoconstriction, while both sTNF-Rs seemed to be responsible for postoperative systemic vasodilation and pulmonary vasoconstriction. Instead, IL-6 levels at the end of surgery might induce a postoperative systemic vasodilation. Postoperative levels of IL-1β and IL-11 might in turn be responsible for venous vasoconstriction and systemic vasodilation, while IL-10 and IL-6 might decrease or increase myocardial performance, respectively. At this time point, IL-6 might also be involved in postoperative pulmonary vasoconstriction and systemic vasodilation.

Many studies have already described the effect of cardiac surgery on cytokine levels, but only few were able to relate these cytokine levels to clinical outcome after cardiac surgery[228;229]. However, most of these studies were performed in patients undergoing coronary artery bypass grafting[230-236]. This type of surgery however carries a low risk of inducing a systemic inflammatory response syndrome, and is currently performed in many centers without the use of extracorporeal circulation, which further reduces the inflammatory reaction[230]. Therefore, we appealed to patients undergoing heart valve surgery, as this type of surgery is mostly performed with the use of extracorporeal circulation in our center.

Systemic cytokine levels were measured at 4 different time points - preoperatively, at the end of surgery, and 12 and 24 hrs later - chosen arbitrarily as literature data showed that most peak cytokine levels after myocardial surgery with extracorporeal circulation occurred at day 1 postoperatively. To the best of our knowledge, at the beginning of this study, determination of systemic cytokine levels several hours after myocardial surgery with cardio-pulmonary bypass was not available in the literature.

In the present study, particular interest went to the relation between IL-6 and haemodynamic parameters in patients undergoing extracorporeal circulation as the rat study (chapter 4) demonstrated a direct cardiodepressive action of IL-6[237]. In addition, pro-inflammatory cytokines like IL-1β[183], IL-11[238] and TNF-α[183;193] were also measured as these cytokines have been shown to exert negative inotropic effects on myocardial function or to cause atrial remodelling. Because plasma levels of TNF-α are quite instable, both sTNF-Rs were measured to properly reflect the levels of circulating TNF-α. IL-8 and IL-17 were chosen too as IL-8 is one of the most prominent inflammatory mediators, likely preceded by IL-17[239]. Finally, anti-inflammatory mediators during cardiopulmonary bypass are predominantly reflected by systemic IL-10[202].

The present study was a first but necessary step to define the actual routine cytokine levels and their clinical correlates in order to possibly plan an interventional study. However, the observational nature of the study precluded the generation of definite causal relationships, so only correlations were studied. The large number of variables recorded and the considerable number of cytokine levels measured at different time points in a limited population dictates some caution in interpreting the data. Therefore, only highly significant correlations were retained ($p \leq 0.01$), except for IL-6 ($p < 0.05$). Nevertheless, interesting correlations with potential pathophysiological meaning could be found.

It is interesting to mention that the postoperative haemodynamic parameters were correlated with the levels of IL-10, and both sTNF-receptors preoperatively. The global image that arises is that this preoperative cocktail of cytokines was correlated with a postoperative status of increased pulmonary vascular resistance, an increased need for inotropic and vasopressor support, and systemic vasodilation as the need

for inotropic support increased while arterial blood pressure did not change. The above-mentioned correlations are thus compatible with the fact that these cytokines could be mere markers for the degree of heart failure. Interesting in this context is the recent finding in 184 patients that although IL-6, IL-10, TNF-α and both sTNF-Rs were univariately related to outcome after acute myocardial infarction, in a multivariable analysis only sTNF-R1 was a major short- and long-term predictor of mortality and heart failure in these patients[186].

The correlations between the postoperative haemodynamic parameters with the systemic levels of IL-10 and both sTNF-Rs immediately after surgery were less strict ($0.01<p<0.05$), while the correlation between IL-6 and the need for vasopressor support became highly significant. This is fully in line with the haemodynamic status reported in rats after 7 days of exogenous rhIL-6 administration (chapter 4)[237]. The levels of IL-6 found in patients immediately after surgery reached values in the same order as those obtained in the rat experiments[237]. Therefore, the correlations between IL-6 and haemodynamic variables found in patients likely imply a potential causal effect, and not a mere coincidental finding.

Plasma levels of IL-1β, IL-8, IL-11, IL-17 and TNF-α measured preoperatively and immediately after surgery seemed to have no correlate with any postoperative haemodynamic parameter, and are thus less attractive for potential therapeutic interventions. However, it should be kept in mind that three confounding variables might hinder the recognition of clinical correlates: 1) systemic cytokine levels might not reflect the relevant, local concentrations, 2) the method of stimulation and mediation of effect may be different, and 3) the clinical responses may not be related to the agent measured per se but by the action of that agent to stimulate the production of mediators at other parts in the amplification pathway.

Twelve hours after surgery only IL-6, IL-10 and sTNF-R1 and R2 levels remained significantly elevated over preoperative levels, and from these only IL-10 had haemodynamic correlates, i.e. reduced cardiac output 12 hrs later. It is interesting that the anti-inflammatory cytokine IL-10 correlated with decreased cardiac output in the present study. It is striking that glucocorticoid administration during cardiac surgery decreases IL-6 levels but increases IL-10 levels, which might thus have mixed advantageous and disadvantageous effects, possibly partly explaining the inconsistent clinical effects of glucocorticoid administration[240;241]. Furthermore in severe inflammatory states, such as found with high fever, septicaemia and meningococcal disease, an increased mortality has been shown to be associated with increased IL-10 levels[242].

In this soup of cytokines, it seemed that IL-6, TNF-α and IL-10 are most relevant from haemodynamic point of view in the current practice of cardiac surgery using extracorporeal circulation. It is interesting that IL-6 and TNF-α are generally recognized as pro-inflammatory cytokines, whereas IL-10 is mainly anti-inflammatory. In the present study, IL-10 immediately after surgery seemed to have no significant clinical correlates. This might be caused by a biphasic dose-effect relationship on the haemodynamic effects of IL-10, or because the vasoconstrictive correlate of IL-10 was lost in the soup of (interactions of) cytokine effects.

The haemodynamic profile that correlated with the IL-6 levels in patients as observed in the present study ($p<0.05$) corresponded highly to that found in the rat study (chapter 4) where similar plasma concentrations were reached[237]. Indeed, preoperative levels of IL-6 correlated positively with the postoperative need for inotropic support. Immediately after surgery, circulating IL-6 correlated positively with the need for vasopressor support 12 and 24 hrs later, indicating the presence of

systemic vasodilation. Twelve hours after the end of surgery, IL-6 concentrations were found to be positively correlated with cardiac output and heart rate, suggesting an identical pattern of high-output failure as seen after rhIL-6 administration to rats. Furthermore, at that time point, IL-6 levels were negatively correlated with the systemic vascular resistance, and might therefore be indicative for systemic vasodilation (Table 7.2).

	12 hrs after surgery				24 hrs after surgery	
IL-6	**dopamine + dobutamine**	**nor-epinephrine (NA)**	**systemic vascular resistance**	**cardiac output**	**heart rate**	**NA**
preoperative	+					
end of surgery		+				+
12 hrs later			-	+	+	

Table 7.2. Significant correlations between IL-6 plasma levels and inotropic/vasopressor support, or haemodynamic variables, showing an identical pattern of heart failure as that observed in rats after 7 days of treatment with rhIL-6.

Although caution has to be taken concerning definitive statements, the findings in rats make a causal relation between the IL-6 levels and the described haemodynamic profile at least possible and even likely. In the rat study, IL-6 has been shown to cause skeletal muscle and diaphragm contractile dysfunction[237], which might further complicate the postoperative course after myocardial surgery. Moreover, it seemed that patients with the GG genotype of the -174G/C interleukin-6 polymorphism have higher postoperative IL-6 levels and might be more vulnerable to postoperative atrial fibrillation[228]. Therefore, this clinical observational study, together with the rat study, warrants further research on the haemodynamic effects of the high IL-6 levels early after surgery in patients and might justify an interventional study to block this effect.

7.4 Summary and general conclusion

In chapter 4, we investigated the effects of circulating IL-6 on respiratory and peripheral skeletal muscle function in rats. We found that clinically relevant levels of IL-6 induced a dose-dependent respiratory and peripheral skeletal muscle atrophy, without alterations in diaphragm contractile properties. These alterations were likely caused by a primary effect of IL-6 on the myocardium, as changes in blood flow were observed in both muscle types.

In chapter 5, we examined the effects of circulating IL-8 on respiratory and peripheral skeletal muscle function in rats. In this setting, no deleterious effects of IL-8 were observed with clinically relevant IL-8 plasma levels.

Finally, in chapter 6, we explored whether increased circulating cytokines could induce a deleterious outcome in patients suffering from heart valve disease. We found that of the 9 examined cytokines, IL-6, IL-10 and TNF-α were the most important cytokines in patients undergoing myocardial surgery with the use of extracorporeal circulation. Moreover, the profile deduced from the correlations between IL-6 and haemodynamic variables in these patients was similar to the type of myocardial failure observed in rats after exogenous IL-6 administration.

In conclusion, this observational study, together with the findings in rats, warrants further research on the deleterious effect of IL-6 on the myocardium and subsequently on respiratory and peripheral skeletal muscles in patients undergoing myocardial surgery with extracorporeal circulation, and might moreover justify an interventional study to block its effect. However, further studies are needed to unravel the precise mechanism by which IL-6 causes high-output myocardial failure, keeping in mind that IL-6 is also known to be necessary for correct wound healing.

REFERENCES

1. Sin, D. D., F. A. McAlister, S. F. Man, and N. R. Anthonisen. 2003. Contemporary management of chronic obstructive pulmonary disease: scientific review. *JAMA* 290:2301-2312.

2. 2005. Workshop Report, Global Strategy for Diagnosis, Management, and Prevention of COPD: NHLBI/WHO Workshop. *Global Initiative for Chronic Obstructive Lung Disease*.

3. Celli, B. R. and W. MacNee. 2004. Standards for the diagnosis and treatment of patients with COPD: a summary of the ATS/ERS position paper. *Eur Respir J* 23:932-946.

4. Siafakas, N. M., P. Vermeire, N. B. Pride, P. Paoletti, J. Gibson, P. Howard, J. C. Yernault, M. Decramer, T. Higenbottam, and D. S. Postma. 1995. Optimal assessment and management of chronic obstructive pulmonary disease (COPD). The European Respiratory Society Task Force. *Eur Respir J* 8:1398-1420.

5. Hogg, J. C. 2004. Pathophysiology of airflow limitation in chronic obstructive pulmonary disease. *Lancet* 364:709-721.

6. Hamid, Q., M. Cosio, and S. Lim. 2004. Inflammation and remodeling in chronic obstructive pulmonary disease. *J Allergy Clin Immunol* 114:1479-1481.

7. Pettersen, C. A. and K. B. Adler. 2002. Airways inflammation and COPD: epithelial-neutrophil interactions. *Chest* 121:142S-150S.

8. Barnes, P. J. 2000. Chronic obstructive pulmonary disease. *N Engl J Med* 343:269-280.

9. Sethi, S. 2005. Pathogenesis and treatment of acute exacerbations of chronic obstructive pulmonary disease. *Semin Respir Crit Care Med* 26:192-203.

10. Selby, C., E. Drost, S. Lannan, P. K. Wraith, and W. MacNee. 1991. Neutrophil retention in the lungs of patients with chronic obstructive pulmonary disease. *Am Rev Respir Dis* 143:1359-1364.

11. Noguera, A., X. Busquets, J. Sauleda, J. M. Villaverde, W. MacNee, and A. G. Agusti. 1998. Expression of adhesion molecules and G proteins in circulating neutrophils in chronic obstructive pulmonary disease. *Am J Respir Crit Care Med* 158:1664-1668.

12. Noguera, A., S. Batle, C. Miralles, J. Iglesias, X. Busquets, W. MacNee, and A. G. Agusti. 2001. Enhanced neutrophil response in chronic obstructive pulmonary disease. *Thorax* 56:432-437.

13. Burnett, D., A. Chamba, S. L. Hill, and R. A. Stockley. 1987. Neutrophils from subjects with chronic obstructive lung disease show enhanced chemotaxis and extracellular proteolysis. *Lancet* 2:1043-1046.

14. Dentener, M. A., E. C. Creutzberg, A. M. Schols, A. Mantovani, C. van't Veer, W. A. Buurman, and E. F. Wouters. 2001. Systemic anti-inflammatory mediators in COPD: increase in soluble interleukin 1 receptor II during treatment of exacerbations. *Thorax* 56:721-726.

15. Riise, G. C., S. Larsson, C. G. Lofdahl, and B. A. Andersson. 1994. Circulating cell adhesion molecules in bronchial lavage and serum in COPD patients with chronic bronchitis. *Eur Respir J* 7:1673-1677.

16. Hageman, G. J., I. Larik, H. J. Pennings, G. R. Haenen, E. F. Wouters, and A. Bast. 2003. Systemic poly(ADP-ribose) polymerase-1 activation, chronic inflammation, and oxidative stress in COPD patients. *Free Radic Biol Med* 35:140-148.

17. Wouters, E. F. 2005. Local and systemic inflammation in chronic obstructive pulmonary disease. *Proc Am Thorac Soc* 2:26-33.

18. Kluchova, Z., D. Petrasova, P. Joppa, Z. Dorkova, and R. Tkacova. 2006. The association between oxidative stress and obstructive lung impairment in patients with COPD. *Physiol Res* (In press)

19. Calikoglu, M., A. Unlu, L. Tamer, B. Ercan, R. Bugdayci, and U. Atik. 2002. The levels of serum vitamin C, malonyldialdehyde and erythrocyte reduced glutathione in chronic obstructive pulmonary disease and in healthy smokers. *Clin Chem Lab Med* 40:1028-1031.

20. Schols, A. M., W. A. Buurman, Staal van den Brekel AJ, M. A. Dentener, and E. F. Wouters. 1996. Evidence for a relation between metabolic derangements and increased levels of inflammatory mediators in a subgroup of patients with chronic obstructive pulmonary disease. *Thorax* 51:819-824.

21. Dahl, M., A. Tybjaerg-Hansen, J. Vestbo, P. Lange, and B. G. Nordestgaard. 2001. Elevated plasma fibrinogen associated with reduced pulmonary function and increased risk of chronic obstructive pulmonary disease. *Am J Respir Crit Care Med* 164:1008-1011.

22. Di Francia, M., D. Barbier, J. L. Mege, and J. Orehek. 1994. Tumor necrosis factor-alpha levels and weight loss in chronic obstructive pulmonary disease. *Am J Respir Crit Care Med* 150:1453-1455.

23. Eid, A. A., A. A. Ionescu, L. S. Nixon, V. Lewis-Jenkins, S. B. Matthews, T. L. Griffiths, and D. J. Shale. 2001. Inflammatory response and body composition in chronic obstructive pulmonary disease. *Am J Respir Crit Care Med* 164:1414-1418.

24. Takabatake, N., H. Nakamura, S. Abe, T. Hino, H. Saito, H. Yuki, S. Kato, and H. Tomoike. 1999. Circulating leptin in patients with chronic obstructive pulmonary disease. *Am J Respir Crit Care Med* 159:1215-1219.

25. Yasuda, N., K. Gotoh, S. Minatoguchi, K. Asano, K. Nishigaki, M. Nomura, A. Ohno, M. Watanabe, H. Sano, H. Kumada, T. Sawa, and H. Fujiwara. 1998. An increase of soluble Fas, an inhibitor of apoptosis, associated with progression of COPD. *Respir Med* 92:993-999.

26. Calikoglu, M., G. Sahin, A. Unlu, C. Ozturk, L. Tamer, B. Ercan, A. Kanik, and U. Atik. 2004. Leptin and TNF-alpha levels in patients with chronic obstructive pulmonary disease and their relationship to nutritional parameters. *Respiration* 71:45-50.

27. Creutzberg, E. C., E. F. Wouters, I. M. Vanderhoven-Augustin, M. A. Dentener, and A. M. Schols. 2000. Disturbances in leptin metabolism are related to energy imbalance during acute exacerbations of chronic obstructive pulmonary disease. *Am J Respir Crit Care Med* 162:1239-1245.

28. Yang, Y. M., T. Y. Sun, and X. M. Liu. 2006. The role of serum leptin and tumor necrosis factor-alpha in malnutrition of male chronic obstructive pulmonary disease patients. *Chin Med J (Engl)* 119:628-633.

29. Spruit, M. A., R. Gosselink, T. Troosters, A. Kasran, G. Gayan-Ramirez, P. Bogaerts, R. Bouillon, and M. Decramer. 2003. Muscle force during an acute exacerbation in hospitalised patients with COPD and its relationship with CXCL8 and IGF-I. *Thorax* 58:752-756.

30. Wedzicha, J. A., T. A. Seemungal, P. K. MacCallum, E. A. Paul, G. C. Donaldson, A. Bhowmik, D. J. Jeffries, and T. W. Meade. 2000. Acute exacerbations of chronic obstructive pulmonary disease are accompanied by elevations of plasma fibrinogen and serum IL-6 levels. *Thromb Haemost* 84:210-215.

31. Schols, A. M., J. Slangen, L. Volovics, and E. F. Wouters. 1998. Weight loss is a reversible factor in the prognosis of chronic obstructive pulmonary disease. *Am J Respir Crit Care Med* 157:1791-1797.

32. Schols, A. M., P. B. Soeters, A. M. Dingemans, R. Mostert, P. J. Frantzen, and E. F. Wouters. 1993. Prevalence and characteristics of nutritional depletion in patients with stable COPD eligible for pulmonary rehabilitation. *Am Rev Respir Dis* 147:1151-1156.

33. Creutzberg, E. C., A. M. Schols, F. C. Bothmer-Quaedvlieg, and E. F. Wouters. 1998. Prevalence of an elevated resting energy expenditure in patients with chronic obstructive pulmonary disease in relation to body composition and lung function. *Eur J Clin Nutr* 52:396-401.

34. Baarends, E. M., A. M. Schols, K. R. Westerterp, and E. F. Wouters. 1997. Total daily energy expenditure relative to resting energy expenditure in clinically stable patients with COPD. *Thorax* 52:780-785.

35. Decramer, M., F. De Benedetto, A. Del Ponte, and S. Marinari. 2005. Systemic effects of COPD. *Respir Med* 99 Suppl B:S3-10.

36. 1999. Skeletal muscle dysfunction in chronic obstructive pulmonary disease. American Thoracic Society/European Respiratory Society. *Am J Respir Crit Care Med* 159:S1-S40.

37. Decramer, M. 1997. Hyperinflation and respiratory muscle interaction. *Eur Respir J* 10:934-941.

38. De Troyer, A., J. B. Leeper, D. K. McKenzie, and S. C. Gandevia. 1997. Neural drive to the diaphragm in patients with severe COPD. *Am J Respir Crit Care Med* 155:1335-1340.

39. Scott, K. W. and J. Hoy. 1976. The cross sectional area of diaphragmatic muscle fibres in emphysema, measured by an automated image analysis system. *J Pathol.* 120:121-128.

40. Steele, R. H. and B. E. Heard. 1973. Size of the diaphragm in chronic bronchitis. *Thorax* 28:55-60.

41. Arora, N. S. and D. F. Rochester. 1987. COPD and human diaphragm muscle dimensions. *Chest* 91:719-724.

42. Similowski, T., S. Yan, A. P. Gauthier, P. T. Macklem, and F. Bellemare. 1991. Contractile properties of the human diaphragm during chronic hyperinflation. *N Engl J Med* 325:917-923.

43. Morrison, N. J., J. Richardson, L. Dunn, and R. L. Pardy. 1989. Respiratory muscle performance in normal elderly subjects and patients with COPD. *Chest* 95:90-94.

44. Orozco-Levi, M., J. Gea, J. L. Lloreta, M. Felez, J. Minguella, S. Serrano, and J. M. Broquetas. 1999. Subcellular adaptation of the human diaphragm in chronic obstructive pulmonary disease. *Eur Respir J* 13:371-378.

45. Ottenheijm, C. A., L. M. Heunks, G. C. Sieck, W. Z. Zhan, S. M. Jansen, H. Degens, T. de Boo, and P. N. Dekhuijzen. 2005. Diaphragm Dysfunction in Chronic Obstructive Pulmonary Disease. *Am J Respir Crit Care Med*.

46. Levine, S., L. Kaiser, J. Leferovich, and B. Tikunov. 1997. Cellular adaptations in the diaphragm in chronic obstructive pulmonary disease. *N Engl J Med* 337:1799-1806.

47. Hughes, R. L., H. Katz, V. Sahgal, J. A. Campbell, R. Hartz, and T. W. Shields. 1983. Fiber size and energy metabolites in five separate muscles from patients with chronic obstructive lung diseases. *Respiration* 44:321-328.

48. Levine, S., T. Nguyen, L. R. Kaiser, N. A. Rubinstein, G. Maislin, C. Gregory, L. C. Rome, G. A. Dudley, G. C. Sieck, and J. B. Shrager. 2003. Human diaphragm remodeling associated with chronic obstructive pulmonary disease: clinical implications. *Am J Respir Crit Care Med* 168:706-713.

49. Doucet, M., R. Debigare, D. R. Joanisse, C. Cote, P. LeBlanc, J. Gregoire, J. Deslauriers, R. Vaillancourt, and F. Maltais. 2004. Adaptation of the diaphragm and the vastus lateralis in mild-to-moderate COPD. *Eur Respir J* 24:971-979.

50. Levine, S., C. Gregory, T. Nguyen, J. Shrager, L. Kaiser, N. Rubinstein, and G. Dudley. 2002. Bioenergetic adaptation of individual human diaphragmatic myofibers to severe COPD. *J Appl Physiol* 92:1205-1213.

51. Wijnhoven, J. H., A. J. Janssen, T. H. van Kuppevelt, R. J. Rodenburg, and P. N. Dekhuijzen. 2005. Metabolic capacity of the diaphragm in patients with COPD. *Respir Med* 100:1064-1071.

52. Ribera, F., B. N'Guessan, J. Zoll, D. Fortin, B. Serrurier, B. Mettauer, X. Bigard, R. Ventura-Clapier, and E. Lampert. 2003. Mitochondrial electron transport chain function is enhanced in inspiratory muscles of patients with chronic obstructive pulmonary disease. *Am J Respir Crit Care Med* 167:873-879.

53. Sanchez, J., C. Bastien, G. Medrano, M. Riquet, and J. P. Derenne. 1984. Metabolic enzymatic activities in the diaphragm of normal men and patients with moderate chronic obstructive pulmonary disease. *Bull Eur Physiopathol Respir* 20:535-540.

54. Orozco-Levi M, Gea J, Aguar C, Felez M, Jimenez-Fuentes MA, and Broquetas J. Changes in the capillary content in the diaphragm of COPD patients: a sort of muscle remodelling? Am J Respir Crit Care Med 153. 1996.

55. Gosselin, N., S. Matecki, M. Poulain, M. Ramonatxo, F. Ceugniet, C. Prefaut, and A. Varray. 2003. Electrophysiologic changes during exercise testing in patients with chronic obstructive pulmonary disease. *Muscle Nerve* 27:170-179.

56. Jeffery, M. M., T. J. Kufel, and L. Pineda. 2000. Quadriceps fatigue after cycle exercise in patients with chronic obstructive pulmonary disease. *Am J Respir Crit Care Med* 161:447-453.

57. Bernard, S., P. LeBlanc, F. Whittom, G. Carrier, J. Jobin, R. Belleau, and F. Maltais. 1998. Peripheral muscle weakness in patients with chronic obstructive pulmonary disease. *Am J Respir Crit Care Med* 158:629-634.

58. Gosselink, R., T. Troosters, and M. Decramer. 1996. Peripheral muscle weakness contributes to exercise limitation in COPD. *Am J Respir Crit Care Med* 153:976-980.

59. Gosselink, R., T. Troosters, and M. Decramer. 2000. Distribution of muscle weakness in patients with stable chronic obstructive pulmonary disease. *J Cardiopulm Rehabil* 20:353-360.

60. Martinez-Llorens, J. M., M. Orozco-Levi, M. J. Masdeu, C. Coronell, A. Ramirez-Sarmiento, C. Sanjuas, J. M. Broquetas, and J. Gea. 2004. Global muscle dysfunction and exacerbation of COPD: a cohort study. *Med Clin (Barc)* 122:521-527.

61. Pitta, F., T. Troosters, V. S. Probst, M. A. Spruit, M. Decramer, and R. Gosselink. 2006. Physical activity and hospitalization for exacerbation of COPD. *Chest* 129:536-544.

62. Couillard, A., C. Koechlin, J. P. Cristol, A. Varray, and C. Prefaut. 2002. Evidence of local exercise-induced systemic oxidative stress in chronic obstructive pulmonary disease patients. *Eur Respir J* 20:1123-1129.

63. Zattara-Hartmann, M. C., M. Badier, C. Guillot, C. Tomei, and Y. Jammes. 1995. Maximal force and endurance to fatigue of respiratory and skeletal muscles in chronic hypoxemic patients: the effects of oxygen breathing. *Muscle Nerve* 18:495-502.

64. Couillard, A., F. Maltais, D. Saey, R. Debigare, A. Michaud, C. Koechlin, P. LeBlanc, and C. Prefaut. 2003. Exercise-induced quadriceps oxidative stress and peripheral muscle dysfunction in patients with chronic obstructive pulmonary disease. *Am J Respir Crit Care Med* 167:1664-1669.

65. Mador, M. J., T. J. Kufel, L. A. Pineda, A. Steinwald, A. Aggarwal, A. M. Upadhyay, and M. A. Khan. 2001. Effect of pulmonary rehabilitation on quadriceps fatiguability during exercise. *Am J Respir Crit Care Med* 163:930-935.

66. Whittom, F., J. Jobin, P. M. Simard, P. LeBlanc, C. Simard, S. Bernard, R. Belleau, and F. Maltais. 1998. Histochemical and morphological characteristics of the vastus lateralis muscle in patients with chronic obstructive pulmonary disease. *Med Sci Sports Exerc* 30:1467-1474.

67. Maltais, F., P. LeBlanc, F. Whittom, C. Simard, K. Marquis, M. Belanger, M. J. Breton, and J. Jobin. 2000. Oxidative enzyme activities of the vastus lateralis muscle and the functional status in patients with COPD. *Thorax* 55:848-853.

68. Gosker, H. R., H. van Mameren, P. J. van Dijk, M. P. Engelen, G. J. van der Vusse, E. F. Wouters, and A. M. Schols. 2002. Skeletal muscle fibre-type shifting and metabolic profile in patients with chronic obstructive pulmonary disease. *Eur Respir J* 19:617-625.

69. Jakobsson, P., L. Jorfeldt, and J. Henriksson. 1995. Metabolic enzyme activity in the quadriceps femoris muscle in patients with severe chronic obstructive pulmonary disease. *Am J Respir Crit Care Med* 151:374-377.

70. Maltais, F., A. A. Simard, C. Simard, J. Jobin, P. Desgagnes, and P. LeBlanc. 1996. Oxidative capacity of the skeletal muscle and lactic acid kinetics during exercise in normal subjects and in patients with COPD. *Am J Respir Crit Care Med* 153:288-293.

71. Jakobsson, P., L. Jorfeldt, and A. Brundin. 1990. Skeletal muscle metabolites and fibre types in patients with advanced chronic obstructive pulmonary disease (COPD), with and without chronic respiratory failure. *Eur Respir J* 3:192-196.

72. Jobin, J., F. Maltais, J. F. Doyon, P. LeBlanc, P. M. Simard, A. A. Simard, and C. Simard. 1998. Chronic obstructive pulmonary disease: capillarity and fiber-type characteristics of skeletal muscle. *J Cardiopulm Rehabil* 18:432-437.

73. Gosker, H. R., B. Kubat, G. Schaart, G. J. van der Vusse, E. F. Wouters, and A. M. Schols. 2003. Myopathological features in skeletal muscle of patients with chronic obstructive pulmonary disease. *Eur Respir J* 22:280-285.

74. Agusti, A. G., J. Sauleda, C. Miralles, C. Gomez, B. Togores, E. Sala, S. Batle, and X. Busquets. 2002. Skeletal muscle apoptosis and weight loss in chronic obstructive pulmonary disease. *Am J Respir Crit Care Med* 166:485-489.

75. Marquis, K., R. Debigare, Y. Lacasse, P. LeBlanc, J. Jobin, G. Carrier, and F. Maltais. 2002. Midthigh muscle cross-sectional area is a better predictor of mortality than body mass index in patients with chronic obstructive pulmonary disease. *Am J Respir Crit Care Med* 166:809-813.

76. Decramer, M., R. Gosselink, T. Troosters, M. Verschueren, and G. Evers. 1997. Muscle weakness is related to utilization of health care resources in COPD patients. *Eur Respir J* 10:417-423.

77. Yohannes, A. M., J. Roomi, K. Waters, and M. J. Connolly. 1998. Quality of life in elderly patients with COPD: measurement and predictive factors. *Respir Med* 92:1231-1236.

78. Larsson, L. and T. Ansved. 1985. Effects of long-term physical training and detraining on enzyme histochemical and functional skeletal muscle characteristic in man. *Muscle Nerve* 8:714-722.

79. Coyle, E. F., W. H. Martin, III, S. A. Bloomfield, O. H. Lowry, and J. O. Holloszy. 1985. Effects of detraining on responses to submaximal exercise. *J Appl Physiol* 59:853-859.

80. Decramer, M., V. de Bock, and R. Dom. 1996. Functional and histologic picture of steroid-induced myopathy in chronic obstructive pulmonary disease. *Am J Respir Crit Care Med* 153:1958-1964.

81. Barreiro, E., J. Gea, J. M. Corominas, and S. N. Hussain. 2003. Nitric oxide synthases and protein oxidation in the quadriceps femoris of patients with chronic obstructive pulmonary disease. *Am J Respir Cell Mol Biol* 29:771-778.

82. Barreiro, E., B. de la Puente, J. Minguella, J. M. Corominas, S. Serrano, S. N. Hussain, and J. Gea. 2005. Oxidative stress and respiratory muscle dysfunction in severe chronic obstructive pulmonary disease. *Am J Respir Crit Care Med* 171:1116-1124.

83. Scano, G., A. Spinelli, R. Duranti, M. Gorini, F. Gigliotti, P. Goti, and J. Milic-Emili. 1995. Carbon dioxide responsiveness in COPD patients with and without chronic hypercapnia. *Eur Respir J* 8:78-85.

84. Gertz, I., G. Hedenstierna, G. Hellers, and J. Wahren. 1977. Muscle metabolism in patients with chronic obstructive lung disease and acute respiratory failure. *Clin Sci Mol Med* 52:396-403.

85. Ottenheijm, C. A., L. M. Heunks, T. Hafmans, P. F. van der Ven, C. Benoist, H. Zhou, S. Labeit, H. L. Granzier, and P. N. Dekhuijzen. 2006. Titin and diaphragm dysfunction in chronic obstructive pulmonary disease. *Am J Respir Crit Care Med* 173:527-534.

86. Ottenheijm, C. A., L. M. Heunks, Y. P. Li, B. Jin, R. Minnaard, H. W. van Hees, and P. N. Dekhuijzen. 2006. Activation of Ubiquitin-Proteasome Pathway in the Diaphragm in Chronic Obstructive Pulmonary Disease. *Am J Respir Crit Care Med* (In press)

87. Schols, A. M. and E. F. Wouters. 2000. Nutritional abnormalities and supplementation in chronic obstructive pulmonary disease. *Clin Chest Med* 21:753-762.

88. Casaburi, R. 1998. Rationale for anabolic therapy to facilitate rehabilitation in chronic obstructive pulmonary disease. *Baillieres Clin Endocrinol Metab* 12:407-418.

89. Semple, P. D., G. H. Beastall, W. S. Watson, and R. Hume. 1980. Serum testosterone depression associated with hypoxia in respiratory failure. *Clin Sci (Lond)* 58:105-106.

90. Supinski, G. S. and L. A. Callahan. 2005. Diaphragmatic free radical generation increases in an animal model of heart failure. *J Appl Physiol* 99:1078-1084.

91. Rabinovich, R. A., M. Figueras, E. Ardite, N. Carbo, T. Troosters, X. Filella, J. A. Barbera, J. C. Fernandez-Checa, J. M. Argiles, and J. Roca. 2003. Increased tumour necrosis factor-alpha plasma levels during moderate-intensity exercise in COPD patients. *Eur Respir J* 21:789-794.

92. van Helvoort, H. A., Y. F. Heijdra, L. M. Heunks, P. L. Meijer, W. Ruitenbeek, H. M. Thijs, and P. N. Dekhuijzen. 2006. Supplemental oxygen prevents exercise-induced oxidative stress in muscle-wasted patients with chronic obstructive pulmonary disease. *Am J Respir Crit Care Med* 173:1122-1129.

93. Sin, D. D. and S. F. Man. 2003. Why are patients with chronic obstructive pulmonary disease at increased risk of cardiovascular diseases? The potential role of systemic inflammation in chronic obstructive pulmonary disease. *Circulation* 107:1514-1519.

94. Rennard, S. I. 2005. Clinical approach to patients with chronic obstructive pulmonary disease and cardiovascular disease. *Proc Am Thorac Soc* 2:94-100.

95. Burns, D. M. 2003. Tobacco-related diseases. *Semin Oncol Nurs* 19:244-249.

96. Willerson, J. T. and P. M. Ridker. 2004. Inflammation as a cardiovascular risk factor. *Circulation* 109:II2-10.

97. Engstrom, G., P. Lind, B. Hedblad, P. Wollmer, L. Stavenow, L. Janzon, and F. Lindgarde. 2002. Lung function and cardiovascular risk: relationship with inflammation-sensitive plasma proteins. *Circulation* 106:2555-2560.

98. Jousilahti, P., E. Vartiainen, J. Tuomilehto, and P. Puska. 1996. Symptoms of chronic bronchitis and the risk of coronary disease. *Lancet* 348:567-572.

99. Sin, D. D. and S. F. Man. 2005. Chronic obstructive pulmonary disease as a risk factor for cardiovascular morbidity and mortality. *Proc Am Thorac Soc* 2:8-11.

100. Mathur, R., I. J. Cox, A. Oatridge, D. T. Shephard, R. J. Shaw, and S. D. Taylor-Robinson. 1999. Cerebral bioenergetics in stable chronic obstructive pulmonary disease. *Am J Respir Crit Care Med* 160:1994-1999.

101. Rose, C., L. Wallace, R. Dickson, J. Ayres, R. Lehman, Y. Searle, and P. S. Burge. 2002. The most effective psychologically-based treatments to reduce anxiety and panic in patients with chronic obstructive pulmonary disease (COPD): a systematic review. *Patient Educ Couns* 47:311-318.

102. Hynninen, K. M., M. H. Breitve, A. B. Wiborg, S. Pallesen, and I. H. Nordhus. 2005. Psychological characteristics of patients with chronic obstructive pulmonary disease: a review. *J Psychosom Res* 59:429-443.

103. Brenes, G. A. 2003. Anxiety and chronic obstructive pulmonary disease: prevalence, impact, and treatment. *Psychosom Med* 65:963-970.

104. Miller, D. B. and J. P. O'Callaghan. 2005. Depression, cytokines, and glial function. *Metabolism* 54:33-38.

105. Wright, C. E., P. C. Strike, L. Brydon, and A. Steptoe. 2005. Acute inflammation and negative mood: mediation by cytokine activation. *Brain Behav Immun* 19:345-350.

106. Liesker, J. J., D. S. Postma, R. J. Beukema, N. H. ten Hacken, M. T. van der, R. A. Riemersma, E. H. van Zomeren, and H. A. Kerstjens. 2004. Cognitive performance in patients with COPD. *Respir Med* 98:351-356.

107. Stuss, D. T., I. Peterkin, D. A. Guzman, C. Guzman, and A. K. Troyer. 1997. Chronic obstructive pulmonary disease: effects of hypoxia on neurological and neuropsychological measures. *J Clin Exp Neuropsychol* 19:515-524.

108. Soriano, J. B., G. T. Visick, H. Muellerova, N. Payvandi, and A. L. Hansell. 2005. Patterns of comorbidities in newly diagnosed COPD and asthma in primary care. *Chest* 128:2099-2107.

109. Incalzi, R. A., P. Caradonna, P. Ranieri, S. Basso, L. Fuso, F. Pagano, G. Ciappi, and R. Pistelli. 2000. Correlates of osteoporosis in chronic obstructive pulmonary disease. *Respir Med* 94:1079-1084.

110. Nishimura, Y., H. Nakata, M. Tsutsumi, H. Maeda, and M. Yokoyama. 1997. Relationship between changes of bone mineral content and twelve-minute walking distance in men with chronic obstructive pulmonary disease: a longitudinal study. *Intern Med* 36:450-453.

111. Goldstein, M. F., J. J. Fallon, Jr., and R. Harning. 1999. Chronic glucocorticoid therapy-induced osteoporosis in patients with obstructive lung disease. *Chest* 116:1733-1749.

112. Gross, N. J. 2001. Extrapulmonary effects of chronic obstructive pulmonary disease. *Curr Opin Pulm Med* 7:84-92.

113. Leech, J. A., C. Dulberg, S. Kellie, L. Pattee, and J. Gay. 1990. Relationship of lung function to severity of osteoporosis in women. *Am Rev Respir Dis* 141:68-71.

114. John, M., A. Lange, S. Hoernig, C. Witt, and S. D. Anker. 2005. Prevalence of anemia in chronic obstructive pulmonary disease: Comparison to other chronic diseases. *Int J Cardiol* 111:365-370.

115. Similowski, T., A. Agusti, W. MacNee, and B. Schonhofer. 2006. The potential impact of anaemia of chronic disease in COPD. *Eur Respir J* 27:390-396.

116. John, M., S. Hoernig, W. Doehner, D. D. Okonko, C. Witt, and S. D. Anker. 2005. Anemia and inflammation in COPD. *Chest* 127:825-829.

117. Debigare, R., K. Marquis, C. H. Cote, R. R. Tremblay, A. Michaud, P. LeBlanc, and F. Maltais. 2003. Catabolic/anabolic balance and muscle wasting in patients with COPD. *Chest* 124:83-89.

118. Yende, S., G. W. Waterer, E. A. Tolley, A. B. Newman, D. C. Bauer, D. R. Taaffe, R. Jensen, R. Crapo, S. Rubin, M. Nevitt, E. M. Simonsick, S. Satterfield, T. Harris, and S. B. Kritchevsky. 2006. Inflammatory markers are associated with ventilatory limitation and muscle dysfunction in obstructive lung disease in well functioning elderly subjects. *Thorax* 61:10-16.

119. Montes, d. O., S. H. Torres, J. De Sanctis, A. Mata, N. Hernandez, and C. Talamo. 2005. Skeletal muscle inflammation and nitric oxide in patients with COPD. *Eur Respir J* 26:390-397.

120. Li, X., M. R. Moody, D. Engel, S. Walker, F. J. Clubb, Jr., N. Sivasubramanian, D. L. Mann, and M. B. Reid. 2000. Cardiac-specific overexpression of tumor necrosis factor-alpha causes oxidative stress and contractile dysfunction in mouse diaphragm. *Circulation* 102:1690-1696.

121. Cheema, I. R., C. Hermann, S. Postell, and P. Barnes. 2000. Effect of chronic excess of tumour necrosis factor-alpha on contractile proteins in rat skeletal muscle. *Cytobios* 103:169-176.

122. Cheema, I. R., C. Hermann, S. Postell, and B. Holifield. 1999. Effect of tumour necrosis factor-alpha on total myofibrillar and sarcoplasmic protein synthesis and polysomal aggregation in rat skeletal muscles. *Cytobios* 97:133-139.

123. Llovera, M., F. J. Lopez-Soriano, and J. M. Argiles. 1993. Effects of tumor necrosis factor-alpha on muscle-protein turnover in female Wistar rats. *J Natl Cancer Inst* 85:1334-1339.

124. Flores, E. A., B. R. Bistrian, J. J. Pomposelli, C. A. Dinarello, G. L. Blackburn, and N. W. Istfan. 1989. Infusion of tumor necrosis factor/cachectin promotes muscle catabolism in the rat. A synergistic effect with interleukin 1. *J Clin Invest* 83:1614-1622.

125. Garcia-Martinez, C., N. Agell, M. Llovera, F. J. Lopez-Soriano, and J. M. Argiles. 1993. Tumour necrosis factor-alpha increases the ubiquitinization of rat skeletal muscle proteins. *FEBS Lett* 323:211-214.

126. Wilcox, P. G., Y. Wakai, K. R. Walley, D. J. Cooper, and J. Road. 1994. Tumor necrosis factor alpha decreases in vivo diaphragm contractility in dogs. *Am J Respir Crit Care Med* 150:1368-1373.

127. Hopkins, P. M. 1996. Human recombinant TNF alpha affects rat diaphragm muscle in vitro. *Intensive Care Med* 22:359-362.

128. Wilcox, P., C. Milliken, and B. Bressler. 1996. High-dose tumor necrosis factor alpha produces an impairment of hamster diaphragm contractility - Attenuation with a prostaglandin inhibitor. *Am J Respir Crit Care Med* 153:1611-1615.

129. Diaz, P. T., M. W. Julian, M. D. Wewers, and T. L. Clanton. 1993. Tumor necrosis factor and endotoxin do not directly affect in vitro diaphragm function. *Am Rev Respir Dis* 148:281-287.

130. Kettelhut, I. C. and A. L. Goldberg. 1988. Tumor necrosis factor can induce fever in rats without activating protein breakdown in muscle or lipolysis in adipose tissue. *J Clin Invest* 81:1384-1389.

131. Li, Y. P., R. J. Schwartz, I. D. Waddell, B. R. Holloway, and M. B. Reid. 1998. Skeletal muscle myocytes undergo protein loss and reactive oxygen-mediated NF-kappaB activation in response to tumor necrosis factor alpha. *FASEB J* 12:871-880.

132. Langen, R. C., A. M. Schols, M. C. Kelders, E. F. Wouters, and Y. M. Janssen-Heininger. 2001. Inflammatory cytokines inhibit myogenic differentiation through activation of nuclear factor-kappaB. *FASEB J* 15:1169-1180.

133. Alvarez, B., L. S. Quinn, S. Busquets, F. J. Lopez-Soriano, and J. M. Argiles. 2001. Direct effects of tumor necrosis factor alpha (TNF-alpha) on murine skeletal muscle cell lines. Bimodal effects on protein metabolism. *Eur Cytokine Netw* 12:399-410.

134. el Naggar, E. A., F. Kanda, S. Okuda, N. Maeda, K. Nishimoto, H. Ishihara, and K. Chihara. 2004. Direct effects of tumor necrosis factor alpha (TNF-alpha) on L6 myotubes. *Kobe J Med Sci* 50:39-46.

135. Fujita, J., T. Tsujinaka, C. Ebisui, M. Yano, H. Shiozaki, A. Katsume, Y. Ohsugi, and M. Monden. 1996. Role of interleukin-6 in skeletal muscle protein breakdown and cathepsin activity in vivo. *Eur Surg Res* 28:361-366.

136. Tsujinaka, T., C. Ebisui, J. Fujita, M. Kishibuchi, T. Morimoto, A. Ogawa, A. Katsume, Y. Ohsugi, E. Kominami, and M. Monden. 1995. Muscle undergoes atrophy in association with increase of lysosomal cathepsin activity in interleukin-6 transgenic mouse. *Biochem Biophys Res Commun* 207:168-174.

137. Tsujinaka, T., J. Fujita, C. Ebisui, M. Yano, E. Kominami, K. Suzuki, K. Tanaka, A. Katsume, Y. Ohsugi, H. Shiozaki, and M. Monden. 1996. Interleukin 6 receptor antibody inhibits muscle atrophy and modulates proteolytic systems in interleukin 6 transgenic mice. *J Clin Invest* 97:244-249.

138. Goodman, M. N. 1994. Interleukin-6 induces skeletal muscle protein breakdown in rats. *Proc Soc Exp Biol Med* 205:182-185.

139. Williams, A., J. J. Wang, L. Wang, X. Sun, J. E. Fischer, and P. O. Hasselgren. 1998. Sepsis in mice stimulates muscle proteolysis in the absence of IL-6. *Am J Physiol* 275:R1983-R1991.

140. Castell, J. V., T. Geiger, V. Gross, T. Andus, E. Walter, T. Hirano, T. Kishimoto, and P. C. Heinrich. 1988. Plasma clearance, organ distribution and target cells of interleukin-6/hepatocyte-stimulating factor in the rat. *Eur J Biochem* 177:357-361.

141. Tsujinaka, T., M. Kishibuchi, M. Yano, T. Morimoto, C. Ebisui, J. Fujita, A. Ogawa, H. Shiozaki, E. Kominami, and M. Monden. 1997. Involvement of interleukin-6 in activation of lysosomal cathepsin and atrophy of muscle fibers induced by intramuscular injection of turpentine oil in mice. *J Biochem (Tokyo)* 122:595-600.

142. Haddad, F., F. P. Zaldivar, D. M. Cooper, and G. R. Adams. 2004. IL-6 Induced Skeletal Muscle Atrophy. *J Appl Physiol* 98:911-917.

143. Strassmann, G., M. Fong, J. S. Kenney, and C. O. Jacob. 1992. Evidence for the involvement of interleukin 6 in experimental cancer cachexia. *J Clin Invest* 89:1681-1684.

144. Pedersen, B. K., A. Steensberg, and P. Schjerling. 2001. Muscle-derived interleukin-6: possible biological effects. *J Physiol* 536:329-337.

145. Garcia-Martinez, C., F. J. Lopez-Soriano, and J. M. Argiles. 1994. Interleukin-6 does not activate protein breakdown in rat skeletal muscle. *Cancer Lett* 76:1-4.

146. Ebisui, C., T. Tsujinaka, T. Morimoto, K. Kan, S. Iijima, M. Yano, E. Kominami, K. Tanaka, and M. Monden. 1995. Interleukin-6 induces proteolysis by activating intracellular proteases (cathepsins B and L, proteasome) in C2C12 myotubes. *Clin Sci (Lond)* 89:431-439.

147. Jove, M., A. Planavila, J. C. Laguna, and M. Vazquez-Carrera. 2005. Palmitate-induced interleukin 6 production is mediated by protein kinase C and nuclear-factor kappaB activation and leads to glucose transporter 4 down-regulation in skeletal muscle cells. *Endocrinology* 146:3087-3095.

148. Alvarez, B., L. S. Quinn, S. Busquets, M. T. Quiles, F. J. Lopez-Soriano, and J. M. Argiles. 2002. Tumor necrosis factor-alpha exerts interleukin-6-dependent and - independent effects on cultured skeletal muscle cells. *Biochim Biophys Acta* 1542:66-72.

149. Cantini, M., M. L. Massimino, E. Rapizzi, K. Rossini, C. Catani, L. L. Dalla, and U. Carraro. 1995. Human satellite cell proliferation in vitro is regulated by autocrine secretion of IL-6 stimulated by a soluble factor(s) released by activated monocytes. *Biochem Biophys Res Commun* 216:49-53.

150. Bartoccioni, E., D. Michaelis, and R. Hohlfeld. 1994. Constitutive and cytokine-induced production of interleukin-6 by human myoblasts. *Immunol Lett* 42:135-138.

151. Carrol, E. D., A. P. Thomson, K. J. Mobbs, W. D. Fraser, J. A. Sills, and C. A. Hart. 2002. Myositis in children with meningococcal disease: a role for tumour necrosis factor-alpha and interleukin-8? *J Infect* 44:17-21.

152. Mahler, D. A., S. Huang, M. Tabrizi, and G. M. Bell. 2004. Efficacy and safety of a monoclonal antibody recognizing interleukin-8 in COPD: a pilot study. *Chest* 126:926-934.

153. Harver, A., D. A. Mahler, and J. A. Daubenspeck. 1989. Targeted inspiratory muscle training improves respiratory muscle function and reduces dyspnea in patients with chronic obstructive pulmonary disease. *Ann Intern Med* 111:117-124.

154. Costelli, P., P. Reffo, F. Penna, R. Autelli, G. Bonelli, and F. M. Baccino. 2005. Ca(2+)-dependent proteolysis in muscle wasting. *Int J Biochem Cell Biol* 37:2134-2146.

155. Franch, H. A. and S. R. Price. 2005. Molecular signaling pathways regulating muscle proteolysis during atrophy. *Curr Opin Clin Nutr Metab Care* 8:271-275.

156. Sharma, R. and S. Anker. 2002. Cytokines, apoptosis and cachexia: the potential for TNF antagonism. *Int J Cardiol* 85:161.

157. Debigare, R., C. H. Cote, and F. Maltais. 2001. Peripheral muscle wasting in chronic obstructive pulmonary disease. Clinical relevance and mechanisms. *Am J Respir Crit Care Med* 164:1712-1717.

158. Langen, R. C., J. L. Van Der Velden, A. M. Schols, M. C. Kelders, E. F. Wouters, and Y. M. Janssen-Heininger. 2004. Tumor necrosis factor-alpha inhibits myogenic differentiation through MyoD protein destabilization. *FASEB J* 18:227-237.

159. Reid, M. B. and Y. P. Li. 2001. Tumor necrosis factor-alpha and muscle wasting: a cellular perspective. *Respir Res* 2:269-272.

160. Benbassat, C. A., D. D. Lazarus, S. B. Cichy, T. M. Evans, L. L. Moldawer, S. F. Lowry, and T. G. Unterman. 1999. Interleukin-1 alpha (IL-1 alpha) and tumor necrosis factor alpha (TNF alpha) regulate insulin-like growth factor binding protein-1 (IGFBP-1) levels and mRNA abundance in vivo and in vitro. *Horm Metab Res* 31:209-215.

161. Li, Y. P., Y. Chen, J. John, J. Moylan, B. Jin, D. L. Mann, and M. B. Reid. 2005. TNF-alpha acts via p38 MAPK to stimulate expression of the ubiquitin ligase atrogin1/MAFbx in skeletal muscle. *FASEB J* 19:362-370.

162. de Alvaro, C., T. Teruel, R. Hernandez, and M. Lorenzo. 2004. Tumor necrosis factor alpha produces insulin resistance in skeletal muscle by activation of inhibitor kappaB kinase in a p38 MAPK-dependent manner. *J Biol Chem* 279:17070-17078.

163. Coletti, D., E. Yang, G. Marazzi, and D. Sassoon. 2002. TNFalpha inhibits skeletal myogenesis through a PW1-dependent pathway by recruitment of caspase pathways. *EMBO J* 21:631-642.

164. Zhang, Y., G. Pilon, A. Marette, and V. E. Baracos. 2000. Cytokines and endotoxin induce cytokine receptors in skeletal muscle. *Am J Physiol Endocrinol Metab* 279:E196-E205.

165. Thibault, V., C. D. Richards, F. Botelho, and J. Gauldie. 1997. Antibodies to rat soluble IL-6 receptor stimulate B9 hybridoma cell proliferation. *FEBS Lett* 408:182-186.

166. Jones, S. A., S. Horiuchi, N. Topley, N. Yamamoto, and G. M. Fuller. 2001. The soluble interleukin 6 receptor: mechanisms of production and implications in disease. *FASEB J* 15:43-58.

167. Heinrich, P. C., I. Behrmann, S. Haan, H. M. Hermanns, G. Muller-Newen, and F. Schaper. 2003. Principles of interleukin (IL)-6-type cytokine signalling and its regulation. *Biochem J* 374:1-20.

168. Pihl, S., C. Carlsson-Skwirut, U. Berg, K. Ekstrom, and P. Bang. 2006. Acute interleukin-6 infusion increases IGFBP-1 but has no short-term effect on IGFBP-3 proteolysis in healthy men. *Horm Res* 65:177-184.

169. Klover, P. J., T. A. Zimmers, L. G. Koniaris, and R. A. Mooney. 2003. Chronic exposure to interleukin-6 causes hepatic insulin resistance in mice. *Diabetes* 52:2784-2789.

170. Torre-Amione, G., S. Kapadia, C. Benedict, H. Oral, J. B. Young, and D. L. Mann. 1996. Proinflammatory cytokine levels in patients with depressed left ventricular ejection fraction: A report from the studies of left ventricular dysfunction (SOLVD). *J Am Coll Cardiol* 27:1201-1206.

171. Torre-Amione, G., S. Kapadia, J. Lee, J. B. Durand, R. D. Bies, J. B. Young, and D. L. Mann. 1996. Tumor necrosis factor-alpha and tumor necrosis factor receptors in the failing human heart. *Circulation* 93:704-711.

172. Kragsbjerg, P., H. Holmberg, and T. Vikerfors. 1996. Dynamics of blood cytokine concentrations in patients with bacteremic infections. *Scand J Infect Dis* 28:391-398.

173. Yamada, Y., S. Endo, and K. Inada. 1996. Plasma cytokine levels in patients with severe burn injury - With reference to the relationship between infection and prognosis. *Burns* 22:587-593.

174. Schutte, H., J. Lohmeyer, S. Rosseau, S. Ziegler, C. Siebert, H. Kielisch, H. Pralle, F. Grimminger, H. Morr, and W. Seeger. 1996. Bronchoalveolar and systemic cytokine profiles in patients with ARDS, severe pneumonia and cardiogenic pulmonary oedema. *Eur Resp J* 9:1858-1867.

175. Bolton, C. F. 1996. Sepsis and the systemic inflammatory response syndrome: Neuromuscular manifestations. *Crit Care Med* 24:1408-1416.

176. Herridge, M. S., A. M. Cheung, C. M. Tansey, A. Matte-Martyn, N. Diaz-Granados, F. Al Saidi, A. B. Cooper, C. B. Guest, C. D. Mazer, S. Mehta, T. E. Stewart, A. Barr, D. Cook, and A. S. Slutsky. 2003. One-year outcomes in survivors of the acute respiratory distress syndrome. *N Engl J Med* 348:683-693.

177. Stassijns, G., R. Lysens, and M. Decramer. 1996. Peripheral and respiratory muscles in chronic heart failure. *Eur Respir J* 9:2161-2167.

178. Stassijns, G., G. Gayan-Ramirez, P. De Leyn, G. Verhoeven, P. Herijgers, V. de Bock, R. Dom, R. Lysens, and M. Decramer. 1998. Systolic ventricular dysfunction causes selective diaphragm atrophy in rats. *Am J Respir Crit Care Med* 158:1963-1967.

179. Vassilakopoulos, T., E. Zakynthinos, C. Roussos, and S. Zakynthinos. 1999. Respiratory muscles in heart failure. *Monaldi Arch Chest Dis* 54:150-153.

180. Yasuhara, S., E. Kanakubo, M. E. Perez, M. Kaneki, T. Fujita, T. Okamoto, and J. A. Martyn. 1999. The 1999 Moyer award. Burn injury induces skeletal muscle apoptosis and the activation of caspase pathways in rats. *J Burn Care Rehabil* 20:462-470.

181. Gwechenberger, M., M. Hulsmann, R. Berger, S. Graf, C. Springer, B. Stanek, and R. Pacher. 2004. Interleukin-6 and B-type natriuretic peptide are independent predictors for worsening of heart failure in patients with progressive congestive heart failure. *J Heart Lung Transplant* 23:839-844.

182. Pathan, N., C. A. Hemingway, A. A. Alizadeh, A. C. Stephens, J. C. Boldrick, E. E. Oragui, C. McCabe, S. B. Welch, A. Whitney, P. O'Gara, S. Nadel, D. A. Relman, S. E. Harding, and M. Levin. 2004. Role of interleukin 6 in myocardial dysfunction of meningococcal septic shock. *Lancet* 363:203-209.

183. Prabhu, S. D. 2004. Cytokine-induced modulation of cardiac function. *Circ Res* 95:1140-1153.

184. Hennein, H. A., H. Ebba, J. L. Rodriguez, S. H. Merrick, F. M. Keith, M. H. Bronstein, J. M. Leung, D. T. Mangano, L. J. Greenfield, and J. S. Rankin. 1994. Relationship of the proinflammatory cytokines to myocardial ischemia and dysfunction after uncomplicated coronary revascularization. *J Thorac Cardiovasc Surg* 108:626-635.

185. Pai, J. K., T. Pischon, J. Ma, J. E. Manson, S. E. Hankinson, K. Joshipura, G. C. Curhan, N. Rifai, C. C. Cannuscio, M. J. Stampfer, and E. B. Rimm. 2004. Inflammatory markers and the risk of coronary heart disease in men and women. *N Engl J Med* 351:2599-2610.

186. Valgimigli, M., C. Ceconi, P. Malagutti, E. Merli, O. Soukhomovskaia, G. Francolini, G. Cicchitelli, A. Olivares, G. Parrinello, G. Percoco, G. Guardigli, D. Mele, R. Pirani, and R. Ferrari. 2005. Tumor Necrosis Factor-{alpha} Receptor 1 Is a Major Predictor of Mortality and New-Onset Heart Failure in Patients With Acute Myocardial Infarction. The Cytokine-Activation and Long-term Prognosis in Myocardial Infarction (C-ALPHA) Study. *Circulation* 111:863-870.

187. Hirota, H., K. Yoshida, T. Kishimoto, and T. Taga. 1995. Continuous activation of gp130, a signal-transducing receptor component for interleukin 6-related cytokines, causes myocardial hypertrophy in mice. *Proc Natl Acad Sci U S A* 92:4862-4866.

188. Sugishita, K., K. Kinugawa, T. Shimizu, K. Harada, H. Matsui, T. Takahashi, T. Serizawa, and O. Kohmoto. 1999. Cellular basis for the acute inhibitory effects of IL-6 and TNF- alpha on excitation-contraction coupling. *J Mol Cell Cardiol* 31:1457-1467.

189. Kinugawa, K., T. Takahashi, O. Kohmoto, A. Yao, T. Aoyagi, S. Momomura, Y. Hirata, and T. Serizawa. 1994. Nitric oxide-mediated effects of interleukin-6 on [Ca2+]i and cell contraction in cultured chick ventricular myocytes. *Circ Res* 75:285-295.

190. Yu, X., R. H. Kennedy, and S. J. Liu. 2003. JAK2/STAT3, not ERK1/2, mediates interleukin-6-induced activation of inducible nitric-oxide synthase and decrease in contractility of adult ventricular myocytes. *J Biol Chem* 278:16304-16309.

191. Yu, X. W., Q. Chen, R. H. Kennedy, and S. J. Liu. 2005. Inhibition of sarcoplasmic reticular function by chronic interleukin-6 exposure via iNOS in adult ventricular myocytes. *J Physiol* 566:327-340.

192. Villegas, S., F. J. Villarreal, and W. H. Dillmann. 2000. Leukemia Inhibitory Factor and Interleukin-6 downregulate sarcoplasmic reticulum Ca2+ ATPase (SERCA2) in cardiac myocytes. *Basic Res Cardiol* 95:47-54.

193. Finkel, M. S., C. V. Oddis, T. D. Jacob, S. C. Watkins, B. G. Hattler, and R. L. Simmons. 1992. Negative inotropic effects of cytokines on the heart mediated by nitric oxide. *Science* 257:387-389.

194. Patten, M., E. Kramer, J. Bunemann, C. Wenck, M. Thoenes, T. Wieland, and C. Long. 2001. Endotoxin and cytokines alter contractile protein expression in cardiac myocytes in vivo. *Pflugers Arch* 442:920-927.

195. Dekhuijzen, P. N., G. Gayan-Ramirez, V. de Bock, R. Dom, and M. Decramer. 1993. Triamcinolone and prednisolone affect contractile properties and histopathology of rat diaphragm differently. *J Clin Invest* 92:1534-1542.

196. Dubowitz, V. 1985. Muscle Biopsy: A Practical Approach Balliere Tindall, London, UK.

197. Doumas, B. T., W. A. Watson, and H. G. Biggs. 1971. Albumin standards and the measurement of serum albumin with bromcresol green. *Clin Chim Acta* 31:87-96.

198. Furlanetto, R. W. and J. M. Marino. 1987. Radioimmunoassay of somatomedin C/insulin-like growth factor I. *Methods Enzymol* 146:216-226.

199. Kass, D. A. and W. L. Maughan. 1988. From 'Emax' to pressure-volume relations: a broader view. *Circulation* 77:1203-1212.

200. Herijgers, P., V. Leunens, T. B. Tjandra-Maga, K. Mubagwa, and W. Flameng. 1996. Changes in organ perfusion after brain death in the rat and its relation to circulating catecholamines. *Transplantation* 62:330-335.

201. Bloemen, H., J. M. Aerts, D. Berckmans, and V. Goedseels. 1997. Image analysis to measure activity index of animals. *Equine Vet J Suppl* 23:16-19.

202. Paparella, D., T. M. Yau, and E. Young. 2002. Cardiopulmonary bypass induced inflammation: pathophysiology and treatment. An update. *Eur J Cardiothorac Surg* 21:232-244.

203. Takabatake, N., H. Nakamura, S. Abe, S. Inoue, T. Hino, H. Saito, H. Yuki, S. Kato, and H. Tomoike. 2000. The relationship between chronic hypoxemia and activation of the tumor necrosis factor-alpha system in patients with chronic obstructive pulmonary disease. *Am J Respir Crit Care Med* 161:1179-1184.

204. Van Snick, J., S. Cayphas, J. P. Szikora, J. C. Renauld, E. Van Roost, T. Boon, and R. J. Simpson. 1988. cDNA cloning of murine interleukin-HP1: homology with human interleukin 6. *Eur J Immunol* 18:193-197.

205. Ehlers, M., J. Grotzinger, F. D. deHon, J. Mullberg, J. P. Brakenhoff, J. Liu, A. Wollmer, and S. Rose-John. 1994. Identification of two novel regions of human IL-6 responsible for receptor binding and signal transduction. *J Immunol* 153:1744-1753.

206. Olencki, T., J. Finke, R. Tubbs, P. Elson, D. McLain, P. Herzog, G. T. Budd, H. Gunn, and R. M. Bukowski. 2000. Phase 1 trial of subcutaneous IL-6 in patients with refractory cancer: clinical and biologic effects. *J Immunother* 23:549-556.

207. Villegas, S., F. J. Villarreal, and W. H. Dillmann. 2000. Leukemia Inhibitory Factor and Interleukin-6 downregulate sarcoplasmic reticulum Ca2+ ATPase (SERCA2) in cardiac myocytes. *Basic Res Cardiol* 95:47-54.

208. Pennica, D., K. L. King, K. J. Shaw, E. Luis, J. Rullamas, S. M. Luoh, W. C. Darbonne, D. S. Knutzon, R. Yen, and K. R. Chien. 1995. Expression cloning of cardiotrophin 1, a cytokine that induces cardiac myocyte hypertrophy. *Proc Natl Acad Sci U S A* 92:1142-1146.

209. Jin, H., R. Yang, G. A. Keller, A. Ryan, A. Ko, D. Finkle, T. A. Swanson, W. Li, D. Pennica, W. I. Wood, and N. F. Paoni. 1996. In vivo effects of cardiotrophin-1. *Cytokine* 8:920-926.

210. Jin, H., R. Yang, A. Ko, D. Pennica, W. I. Wood, and N. F. Paoni. 1998. Effects of cardiotrophin-1 on haemodynamics and cardiac function in conscious rats. *Cytokine* 10:19-25.

211. Parrillo, J. E., M. M. Parker, C. Natanson, A. F. Suffredini, R. L. Danner, R. E. Cunnion, and F. P. Ognibene. 1990. Septic shock in humans. Advances in the understanding of pathogenesis, cardiovascular dysfunction, and therapy. *Ann Intern Med* 113:227-242.

212. Vyas, D., P. Javadi, P. J. Dipasco, T. G. Buchman, R. S. Hotchkiss, and C. M. Coopersmith. 2005. Early antibiotic administration but not antibody therapy directed against IL-6 improves survival in septic mice predicted to die on basis of high IL-6 levels. *Am J Physiol Regul Integr Comp Physiol* 289:R1048-R1053.

213. Roth-Isigkeit, A., L. Hasselbach, E. Ocklitz, S. Bruckner, A. Ros, H. Gehring, P. Schmucker, L. Rink, and M. Seyfarth. 2001. Inter-individual differences in cytokine release in patients undergoing cardiac surgery with cardiopulmonary bypass. *Clin Exp Immunol* 125:80-88.

214. Millar, A. B., L. Armstrong, J. van der Linden, N. Moat, R. Ekroth, J. Westwick, M. Scallan, and C. Lincoln. 1993. Cytokine production and hemofiltration in children undergoing cardiopulmonary bypass. *Ann Thorac Surg* 56:1499-1502.

215. Lindsay, D. C., C. A. Lovegrove, M. J. Dunn, J. G. Bennett, J. R. Pepper, M. H. Yacoub, and P. A. Poole-Wilson. 1996. Histological abnormalities of muscle from limb, thorax and diaphragm in chronic heart failure. *Eur Heart J* 17:1239-1250.

216. McParland, C., E. F. Resch, B. Krishnan, Y. Wang, B. Cujec, and C. G. Gallagher. 1995. Inspiratory muscle weakness in chronic heart failure: role of nutrition and electrolyte status and systemic myopathy. *Am J Respir Crit Care Med* 151:1101-1107.

217. Hammond, M. D., K. A. Bauer, J. T. Sharp, and R. D. Rocha. 1990. Respiratory muscle strength in congestive heart failure. *Chest* 98:1091-1094.

218. Howell, S., J. M. Maarek, M. Fournier, K. Sullivan, W. Z. Zhan, and G. C. Sieck. 1995. Congestive heart failure: differential adaptation of the diaphragm and latissimus dorsi. *J Appl Physiol* 79:389-397.

219. Lipkin, D. P., D. A. Jones, J. M. Round, and P. A. Poole-Wilson. 1988. Abnormalities of skeletal muscle in patients with chronic heart failure. *Int J Cardiol* 18:187-195.

220. Hussain, S. N., C. Roussos, and S. Magder. 1989. Effects of tension, duty cycle, and arterial pressure on diaphragmatic blood flow in dogs. *J Appl Physiol* 66:968-976.

221. Flaim, S. F., W. J. Minteer, S. H. Nellis, and D. P. Clark. 1979. Chronic arteriovenous shunt: evaluation of a model for heart failure in rat. *Am J Physiol* 236:H698-H704.

222. Savage, M. T., C. J. Ferro, A. Sassano, and C. R. Tomson. 2002. The impact of arteriovenous fistula formation on central hemodynamic pressures in chronic renal failure patients: a prospective study. *Am J Kidney Dis* 40:753-759.

223. Nava, S., G. Gayan-Ramirez, H. Rollier, A. Bisschop, R. Dom, V. de Bock, and M. Decramer. 1996. Effects of acute steroid administration on ventilatory and peripheral muscles in rats. *Am J Respir Crit Care Med* 153:1888-1896.

224. Gobl, A. E., M. R. Huang, S. Wang, Y. Zhou, and K. Oberg. 1997. Molecular cloning and characterization of a cDNA encoding the rat interleukin-8 receptor. *Biochim Biophys Acta* 1326:171-177.

225. Goto, J., N. Kanayama, T. Asahina, Y. Okada, T. Kobayashi, and T. Terao. 1997. Induction of follicular growth by exogenous interleukin-8. *Hum Reprod* 12:2729-2734.

226. Laterveer, L., I. J. Lindley, M. S. Hamilton, R. Willemze, and W. E. Fibbe. 1995. Interleukin-8 induces rapid mobilization of hematopoietic stem cells with radioprotective capacity and long-term myelolymphoid repopulating ability. *Blood* 85:2269-2275.

227. Rot, A. 1991. Chemotactic potency of recombinant human neutrophil attractant/activation protein-1 (interleukin-8) for polymorphonuclear leukocytes of different species. *Cytokine* 3:21-27.

228. Gaudino, M., F. Andreotti, R. Zamparelli, A. Di Castelnuovo, G. Nasso, F. Burzotta, L. Iacoviello, M. B. Donati, R. Schiavello, A. Maseri, and G. Possati. 2003. The -174G/C interleukin-6 polymorphism influences postoperative interleukin-6 levels and postoperative atrial fibrillation. Is atrial fibrillation an inflammatory complication? *Circulation* 108 Suppl 1:II195-II199.

229. Lindholm, L., A. Bengtsson, V. Hansdottir, M. Lundqvist, L. Rosengren, and A. Jeppsson. 2003. Regional oxygenation and systemic inflammatory response during cardiopulmonary bypass: influence of temperature and blood flow variations. *J Cardiothorac Vasc Anesth* 17:182-187.

230. Wan, S., M. B. Izzat, T. W. Lee, I. Y. Wan, N. L. Tang, and A. P. Yim. 1999. Avoiding cardiopulmonary bypass in multivessel CABG reduces cytokine response and myocardial injury. *Ann Thorac Surg* 68:52-56.

231. Tayama, E., N. Hayashida, S. Fukunaga, K. Tayama, T. Takaseya, R. Hiratsuka, and S. Aoyagi. 2001. High-dose cimetidine reduces proinflammatory reaction after cardiac surgery with cardiopulmonary bypass. *Ann Thorac Surg* 72:1945-1949.

232. Boldt, J., C. Brosch, S. Suttner, S. N. Piper, A. Lehmann, and C. Werling. 2002. Prophylactic use of the phospodiesterase III inhibitor enoximone in elderly cardiac surgery patients: effect on hemodynamics, inflammation, and markers of organ function. *Intensive Care Med* 28:1462-1469.

233. Boldt, J., C. Brosch, A. Lehmann, G. Haisch, J. Lang, and F. Isgro. 2001. Prophylactic use of pentoxifylline on inflammation in elderly cardiac surgery patients. *Ann Thorac Surg* 71:1524-1529.

234. Bourbon, A., M. Vionnet, P. Leprince, E. Vaissier, J. Copeland, P. McDonagh, P. Debre, and I. Gandjbakhch. 2004. The effect of methylprednisolone treatment on the cardiopulmonary bypass-induced systemic inflammatory response. *Eur J Cardiothorac Surg* 26:932-938.

235. Schmartz, D., Y. Tabardel, J. C. Preiser, L. Barvais, A. d'Hollander, J. Duchateau, and J. L. Vincent. 2003. Does aprotinin influence the inflammatory response to cardiopulmonary bypass in patients? *J Thorac Cardiovasc Surg* 125:184-190.

236. Kwapisz, M. M., M. Muller, E. Schindler, S. Demir, M. Veit, P. Roth, and G. Hempelmann. 2004. The effect of intravenous quinaprilat on plasma cytokines and hemodynamic variables during cardiac surgery. *J Cardiothorac Vasc Anesth* 18:53-58.

237. Janssen, S. P., G. Gayan-Ramirez, A. Van den Bergh, P. Herijgers, K. Maes, E. Verbeken, and M. Decramer. 2005. Interleukin-6 causes myocardial failure and skeletal muscle atrophy in rats. *Circulation* 111:996-1005.

238. Xu, J., J. F. Ren, A. Mugelli, L. Belardinelli, J. J. Keith, Jr., and A. Pelleg. 2002. Age-dependent atrial remodeling induced by recombinant human interleukin-11: implications for atrial flutter/fibrillation. *J Cardiovasc Pharmacol* 39:435-440.

239. Vanaudenaerde, B. M., W. A. Wuyts, L. J. Dupont, D. E. Van Raemdonck, M. M. Demedts, and G. M. Verleden. 2003. Interleukin-17 stimulates release of interleukin-8 by human airway smooth muscle cells in vitro: a potential role for interleukin-17 and airway smooth muscle cells in bronchiolitis obliterans syndrome. *J Heart Lung Transplant* 22:1280-1283.

240. Fillinger, M. P., A. J. Rassias, P. M. Guyre, J. H. Sanders, M. Beach, J. Pahl, R. B. Watson, P. K. Whalen, K. T. Yeo, and M. P. Yeager. 2002. Glucocorticoid effects on the inflammatory and clinical responses to cardiac surgery. *J Cardiothorac Vasc Anesth* 16:163-169.

241. El Azab, S. R., P. M. Rosseel, J. J. de Lange, A. B. Groeneveld, R. van Strik, E. M. van Wijk, and G. J. Scheffer. 2002. Dexamethasone decreases the pro- to anti-inflammatory cytokine ratio during cardiac surgery. *Br J Anaesth* 88:496-501.

242. Royston, D., T. Kovesi, and N. Marczin. 2003. The unwanted response to cardiac surgery: time for a reappraisal? *J Thorac Cardiovasc Surg* 125:32-35.

SUMMARY

Chronic Obstructive Pulmonary Disease (COPD) is a major public health problem and its prevalence keeps increasing yearly. It is not only characterized by an abnormal pulmonary inflammatory process but also by several extra-pulmonary effects. Skeletal muscle dysfunction is thought to be one of the most important systemic consequences of this disease as it contributes to exercise intolerance, poor quality of life and mortality.

Recently, inverse correlations between circulating levels of IL-6 or IL-8 and skeletal muscle mass or peripheral muscle force have been observed in stable COPD patients. During exacerbations, when muscle force is further reduced and plasma pro-inflammatory cytokine levels are further increased, these correlations were found to be more significant. Therefore, these pro-inflammatory cytokines are thought to play a role in skeletal muscle dysfunction in COPD.

In the present study, the possible causal deleterious effects of IL-6 and IL-8 on respiratory and peripheral skeletal muscle function were therefore tested in rats. After 7 days of treatment with IL-6, skeletal muscle atrophy was observed as shown by decreases in weight and fiber type cross-sectional area of the diaphragm and gastrocnemius. The atrophy pattern, without any signs of myopathy, was found to be mainly caused by blood flow decreases which occurred as a consequence of high-output myocardial failure. All these findings were observed with clinically relevant IL-6 plasma levels in the range of those found in patients suffering from sepsis, pneumonia or acute respiratory distress syndrome, diseases in all of which skeletal muscle weakness is known to be present. In contrast, 7 days of IL-8 administration to rats gave rise to plasma levels in the range of those found in some COPD patients, but did not result in any skeletal muscle atrophy or weakness. This likely indicates

that the previously mentioned correlation in COPD patients was rather a coincidental finding.

In a last part of the present study, the potential for elevated circulating cytokines to induce a deleterious clinical outcome in patients was examined. Patients undergoing heart valve surgery with extracorporeal circulation were included as systemic cytokines are known to be induced in extremely high amounts by cardiopulmonary bypass. Highly significant correlations between IL-6, IL-10, or sTNF-Rs and haemodynamic variables have been found in these patients. When compared to the observed negative effect of IL-6 on myocardial function in rats, the correlations between IL-6 and haemodynamic parameters express a similar myocardial dysfunction pattern in patients, and therefore likely express a causal relation. This is further supported by similar IL-6 plasma levels in both patients and rats. From this point of view, anti-cytokine treatment might be useful to decrease the deleterious outcome in patients undergoing myocardial surgery.

SAMENVATTING

Chronisch Obstructieve Longziekte (COPD) is een enorm belangrijk volksgezondheidsprobleem waarvan het voorkomen jaarlijks blijft stijgen. Deze ziekte is niet enkel gekenmerkt door een abnormaal inflammatoir proces in de longen, maar eveneens door verscheidene systemische effecten. Een slechte skeletspierwerking wordt geacht één van de meest belangrijke systemische bijverschijnselen te zijn omdat deze verminderde spierfunctie bijdraagt tot een beperkt inspanningsvermogen, een slechte levenskwaliteit en een hoge mortaliteit.

Onlangs werden negatieve correlaties tussen circulerende IL-6 of IL-8 spiegels en skeletspiermassa of perifere spierkracht aangetoond in stabiele COPD patiënten. Tijdens exacerbaties, die gepaard gaan met een nog sterkere daling van de spierkracht en een verdere stijging van plasmaspiegels van pro-inflammatoire cytokines, waren deze correlaties meer significant. Omwille van deze bevindingen worden deze pro-inflammatoire cytokines dus geacht een rol te spelen in skeletspierdysfunctie in COPD.

In deze thesis werden daarom de eventuele schadelijke en oorzakelijke effecten van IL-6 en IL-8 getest op de functie van ademhalingspieren en perifere skeletspieren van ratten. Na een 7 dagen durende behandeling met IL-6 werd skeletspieratrofie waargenomen door middel van dalingen in het gewicht en in de cross-sectionele doorsnede van de verschillende spiervezeltypen in het diafragma en de gastrocnemius. Het atrofiepatroon, dat geen tekenen vertoonde van myopathie, werd hoofdzakelijk veroorzaakt door dalingen in bloedstroom die een gevolg waren van hartfalen met verhoogd hartdebiet. Dit alles werd verkregen met klinisch relevante IL-6 plasmaspiegels omdat ze van dezelfde grootteorde waren als deze bij patiënten die lijden aan sepsis, pneumonie, of acuut longfalen, ziektebeelden die

allemaal gekenmerkt zijn door enige vorm van skeletspierzwakte. Zeven dagen toediening van IL-8 aan ratten leidde daarentegen tot plasmaspiegels van dezelfde grootteorde als bij sommige COPD patiënten, maar veroorzaakte geen enkele skeletspieratrofie of zwakte. Dit wijst er waarschijnlijk op dat de eerder vermelde correlatie in COPD patiënten tussen IL-8 en skeletspierkracht waarschijnlijk een toevallige bevinding was.

In het laatste deel van deze thesis werd onderzocht of verhoogde circulerende cytokineconcentraties ook verantwoordelijk kunnen zijn voor een nadelige prognose in patiënten. Hiervoor werd een beroep gedaan op patiënten die hartklepchirurgie ondergingen met behulp van cardiopulmonaire bypass omdat dit type van operatie een enorm hoge systemische vrijzetting van cytokines teweeg brengt. Hoog significante correlaties tussen IL-6, IL-10 of beide TNF-Rs en haemodynamische variabelen werden in deze patiënten aangetoond. Wanneer de correlaties tussen IL-6 en haemodynamische variabelen in patiënten vergeleken werden met het patroon van hartfalen dat IL-6 veroorzaakte in ratten, blijkt dat IL-6 in patiënten gerelateerd is aan eenzelfde vorm van hartfalen, en dat er daardoor dus waarschijnlijk een causaal verband bestaat tussen beide factoren. De bevinding van dit causaal verband wordt nog verder gesterkt door gelijkaardige IL-6 plasmaspiegels in patiënten en ratten. Vanuit dit standpunt kan het daarom nuttig zijn om patiënten die myocard chirurgie ondergaan te behandelen met een anti-cytokine therapie om alzo een post-operatieve nadelige prognose te voorkomen.

CURRICULUM VITAE

Janssen Sofie was born in Herk-de-Stad, Belgium, on March 11th 1980. From 1992 on, she attended high school, Latin-Mathematics at the 'Humaniora Virga Jesse' in Hasselt. In 1998, she started her biology studies at the 'Limburgs Universitair Centrum' in Diepenbeek. Two years later, she went on with her studies at the 'Katholieke Universiteit Leuven' in Leuven where she graduated with honour in 2002. Since then, she worked on her PhD project, entitled 'Systemic inflammation in Chronic Obstructive Pulmonary Disease: effects of interleukin-6 and interleukin-8 on respiratory and peripheral skeletal muscle function' at the Respiratory Muscle Research Unit, Laboratory for Pneumology, Department of Internal Medicine at the Katholieke Universiteit Leuven, under supervision of Prof Dr Marc Decramer and Prof Dr Ghislaine Gayan-Ramirez.

LIST OF PUBLICATIONS

Articles

1. **Sofie P.M. Janssen**, Ghislaine Gayan-Ramirez, An Van Den Bergh, Paul Herijgers, Karen Maes, Erik Verbeken and Marc Decramer.
   Interleukin-6 causes myocardial failure and skeletal muscle atrophy in rats.
   Circulation 2005 March 1; 111 (8): 996-1005.

In preparation

1. Paul Herijgers, **Sofie P.M. Janssen**, Patrick Wouters, Ghislaine Gayan-Ramirez, Willem Flameng and Marc Decramer.
   Clinical relevance of peri-operative cytokine levels in heart valve surgery.
   Manuscript in preparation.

2. **Sofie P.M. Janssen**, Ghislaine Gayan-Ramirez and Marc Decramer.
   The effects of cytokines on respiratory and peripheral skeletal muscles.
   Manuscript in preparation.

3. **Sofie P.M. Janssen**, Ghislaine Gayan-Ramirez and Marc Decramer.
   IL-8 administration to rats does not affect skeletal muscle function or morphometry.
   Manuscript in preparation.

Abstracts and presentations for national congresses

1. **S. Janssen**, G. Gayan-Ramirez en M. Decramer.
   Effecten van inflammatoire cytokines op respiratoire en perifere spierfunctie in ratten.
   Oral presentation at the Glaxo Smithkline Award in Pneumology – Basic Science award (08/03/2003; Antwerp).
   Bloedvaten, Hart, Longen – vol 8, nr 3, 2003, p131.

2. **Sofie P.M. Janssen**, Ghislaine Gayan-Ramirez, An Van Den Bergh, Paul Herijgers, Karen Maes, Erik Verbeken en Marc Decramer.
IL-6 toediening veroorzaakt myocardiale dysfunctie en skeletspieratrofie in ratten.
Oral presentation at the Glaxo Smithkline Award in Pneumology – Basic Science award (27/03/2004; Charleroi).
Bloedvaten, Hart, Longen – vol 9, nr 4, 2004, p131.

3. **Sofie P.M. Janssen**, Ghislaine Gayan-Ramirez, An Van Den Bergh, Paul Herijgers, Karen Maes, Erik Verbeken en Marc Decramer.
IL-6 geïnduceerde myocard dysfunctie is verantwoordelijk voor skeletspieratrofie in ratten.
Oral presentation at the Glaxo Smithkline Award in Pneumology – Basic Science award (23/04/2005; Leuven).
Bloedvaten, Hart, Longen – vol 10, nr 6, 2005, p164.

Abstracts and presentations for international congresses

1. **S.P. Janssen**, G. Gayan-Ramirez , V. Reynders, K. Van Kuyck, M. Decramer.
IL-6 causes respiratory and peripheral skeletal muscle atrophy in rats.
Oral communication at the European Respiratory Society Annual Congress 2003 (27/09 – 01/10; Vienna, Austria).
European Respiratory Journal – Abstracts – 2003, vol 22, supp 45, 573s.

2. **S.P. Janssen**, G. Gayan-Ramirez, A. Van Den Bergh, P. Herijgers, K. Maes, E. Verbeken, M. Decramer.
IL-6 causes respiratory and peripheral skeletal muscle atrophy induced by myocardial failure.
Poster presentation at the American Thoracic Society Annual Congress 2004 (21/05 – 26/05; Orlando, Florida, USA).
American Journal of Respiratory and Critical Care Medicine – Abstracts – 2004, vol 169, number 7, A614.

3. **Sofie P. Janssen**, Ghislaine Gayan-Ramirez, An Van Den Bergh, Paul Herijgers, Karen Maes, Erik Verbeken, Marc Decramer.
IL-6 causes myocardial dysfunction in vivo.
Oral presentation at the European Respiratory Society Annual Congress 2004 (4/09 – 8/09; Glasgow, UK).
European Respiratory Journal – Abstracts – 2004, vol 24, supp 48, 233s.

4. **Sofie P.M. Janssen**, Ghislaine Gayan-Ramirez and Marc Decramer.
Effects of IL-8 on respiratory and peripheral skeletal muscles in rats.
Poster presentation at the European Respiratory Society Annual Congress 2005 (17/09 – 21/09; Copenhagen; Denmark).
European Respiratory Journal – Abstracts – 2005, vol 26, supp 49, 365s.

5. **S.P.M. Janssen**, G. Gayan-Ramirez, and M. Decramer.
IL-8 administration does not result in skeletal muscle wasting in rats.
Poster E-session at the American Thoracic Society Annual Congress 2006 (19/05 – 24/05; San Diego, California, USA).
Proceedings of the American Thoracic Society – Abstracts – 2006, vol 3, A256.

6. **Sofie P.M Janssen**, Paul Herijgers, Patrick F. Wouters, Ghislaine Gayan-Ramirez, Willem Flameng, and Marc Decramer.
Clinical relevance of peri-operative IL-6 plasma levels in heart valve surgery.
Poster presentation at the European Respiratory Society Annual Congress 2006 (02/09 – 06/09; Munich; Germany).
European Respiratory Journal – Abstracts – 2006, vol 28, supp 50, 60s.

ACTA BIOMEDICA LOVANIENSIA